Design of a Humanoid Robot for Disaster Response

Bryce Kenji Tim-Sung Lee

Thesis submitted to the faculty of the Virginia Polytechnic Institute and State University
in partial fulfillment of the requirements for the degree of

Master of Science
In
Mechanical Engineering

Dennis W. Hong, Chair
Brian Y. Lattimer
Craig A. Woolsey

March 27, 2014
Blacksburg, VA

Keywords: Humanoid robot, Range of motion, Joint torque, Series elastic actuator

Design of a Humanoid Robot for Disaster Response

Bryce Kenji Tim-Sung Lee

ABSTRACT

This study focuses on the design and implementation of a humanoid robot for disaster response. In particular, this thesis investigates the lower body design in detail with the upper body discussed at a higher level. The Tactical Hazardous Operations Robot (THOR) was designed to compete in the DARPA Robotics Challenge where it needs to complete tasks based on first-responder operations. These tasks, ranging from traversing rough terrain through driving a utility vehicle, suggest a versatile platform in a human sized form factor. A physical experiment of the proposed tasks generated a set of joint range of motions (RoM). Desired limb lengths were determined by comparing existing robots, the test subject in the experiment of proposed tasks, and an average human. Simulations using the desired RoM and limb lengths were used to calculate baseline joint torques.

Based on the generated design constraints, THOR is a 34 degree of freedom humanoid that stands 1.78 [m] tall and weighs 65 [kg]. The 12 lower body joints are driven by series elastic linear actuators with multiple joints actuated in parallel. The parallel actuation mimics the human body, where multiple muscles pull on the same joint cooperatively. The legs retain high joint torques throughout their large RoM with some joints achieving torques as high as 289 [Nm]. The upper body uses traditional rotary actuators to drive the waist, arms, and head. The proprioceptive sensor selection was influenced by past experience on humanoid platforms, and perception sensors were selected to match the competition.

Acknowledgements

Before all others, I would like to thank my parents for their support throughout this process. It has been a long and tiring journey, but your encouragement has propelled me through it. I would also like to thank my entire family for their continued support.

Thanks to my labmates of the past and present who have worked tirelessly with me on our various research projects. Working with you all has been a blast. I may be forgetting a couple names (and sorry if I do), but thanks to Derek, Viktor, Mike, Steve, Marbles, Jack, Paul, Ryan, Taylor, Eric, JK, Ping, Joe H., Joe H., Jake, Hunter, Semi, Jason, Johnson, Chris, minion Mike, Jordan, Nik, Hak, Panit, and Sebastien. Special thanks to Viktor for offering to write this acknowledgements section, I just couldn't live with the possible risks.

Thanks to my committee, Dr. Hong, Dr. Lattimer, and Dr. Woolsey, for their guidance through this process. I have learned invaluable amounts of knowledge, both technical and programmatic, from all of you.

I also need to thank the staff upstairs, especially Brandy and Kim, for all the things that you put up with from our lab. We came up with the most outrageous requests, and you never failed to deliver.

Finally, I'd like to thank my friends who have helped me through this process. Especially thanks to Avi for being the first to read and comment on this thesis (and for the stress-relieving introduction to Civ with Goo, Jenn, Jared, Luke, Beard, and Lorraine), to Adam, Bryan, Pete, and Matt for all the interesting and insightful lunch discussions, and to Becca for all the discussions to preserve my sanity.

And Stan…

All photos by the author unless otherwise noted. The test subject is the author, no other human subjects were used.

Table of Contents

List of Figures

List of Tables

List of Abbreviations

THOR: Tactical Hazardous Operations Robot
SAFFiR: Shipboard Autonomous Fire Fighting Robot
DRC: DARPA Robotics Challenge
RoM: Range of Motion
DoF: Degree of Freedom
SEA: Series Elastic Actuator
CoM: Center of Mass
COTS: Commercial-Off-The-Shelf
AHRS: Attitude and Heading Reference System

1. Introduction

Robots are suited to relieve people from dangerous, dull, and dirty jobs. With their similar morphology, humanoid robots are uniquely positioned to jump into any situation that a person could address. The myriad of tasks that people perform demands a large amount of versatility in the capabilities of the robot. Improvements in control theory, mechanical design, sensors, and computing have advanced humanoid robots from slowly walking on flat terrain to reliably walking over rough terrain with some amount of disturbance rejection. Though humanoid robots do not move as effectively as people, they are steadily advancing in their capabilities.

The DARPA Robotics Challenge (DRC) is a worldwide competition to develop robots for disaster response scenarios. It consists of eight individual tasks modeled after first responder activities. Included in the challenge are driving a utility vehicle, traversing a rough terrain field, removing debris blocking a doorway, and closing valves. This wide range of tasks demands a capable platform that can operate in human-structured environments. Though challenging to implement, a humanoid robot at average human size would be well suited for this competition.

The Tactical Hazardous Operations Robot (THOR) is a 1.78 [m] tall, 65 [kg] humanoid robot with a human-like range of motion (RoM). THOR has 34 degrees of freedom (DoF) with limbs proportioned similar to the average adult human. It carries onboard power and computing, making it capable of fully untethered operation. Shown in Figure 1-1, THOR is designed to compete in the DRC.

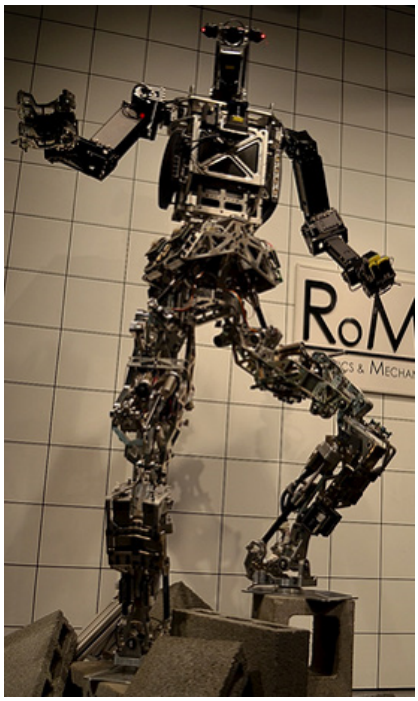

Figure 1-1: The Tactical Hazardous Operations Robot (THOR)

1.1. Summary of Chapters

Chapter 2 reviews the literature of previously designed humanoid robots and their designs. This section will also include a review of series elastic actuators which are integral components of the THOR lower body design.

Chapter 3 details the design specifications for THOR. There is a discussion about the proposed challenge tasks, the initial investigation performed to measure necessary joint angles, and the desired specifications for the robot.

Chapter 4 discusses the actuator placement throughout the legs of THOR. A brief description of the series elastic linear actuator is presented. The configurations of the parallel actuators around the hip and ankle joints are detailed. The four-bar linkage that drives the knee and hip pitch joints is also discussed.

Chapters 5 and 6 discuss the design of the lower body and upper body of THOR respectively. The lower body is broken down to its structural elements: torso, coxa, thigh, shin, and foot. The upper body design is separated into its functional parts: waist, chest, head, arm, and hand.

Chapter 7 presents a summary of the work and proposes some recommendations for future work related to the design of THOR.

Appendix A discusses the sensors and electronics used on THOR. The proprioceptive and perception sensors are presented. Some of the custom control electronics are briefly discussed.

2. Literature Review

Since the debut of WABOT by Waseda University in 1973, humanoid robots have evolved into highly-dynamic walking machines [1, 2]. Modern day humanoids are capable of walking over loose gravel, ascending and descending stairs, falling and getting back up, and manipulating power tools. These advances are all necessary for humanoids robots to be useful outside of the laboratory in real disaster scenarios.

2.1. Rotary Actuated Humanoids

The earliest humanoids were driven solely by rigid rotary actuators. These actuators allow for a high RoM in each joint while maintaining a constant amount of joint torque. Additionally, a rigid rotary actuator will provide exact joint angle measurements for the entire system without the need for extra calculations. Rotary actuated humanoid robots remain as some of the most advanced and capable in the world. Some of the more well-known fully rotary humanoids are described below.

- The latest in a long line of humanoids by Honda, ASIMO is one of the most advanced robots in the world. Since its unveiling, ASIMO has demonstrated numerous capabilities including climbing and descending stairs. Currently, ASIMO has demonstrated functionality beyond most other humanoid robots. It has 34 DoFs, all driven by rotary actuators [3, 4].

- The HPR-3 robot by Kawada Heavy Industries and the National Institute of Advanced Industrial Science and Technology (AIST) is a 42 DoF humanoid robot. The rotary actuators on HRP-3 allow for sealing around the covers of the individual joints [5]. This platform has demonstrated the ability to operate in wet and dusty environments, making it one of the most capable for potential field use. The DRC competitor from SCHAFT Inc. shown in Figure 2-1A is a variant of the HRP family of robots.

- The HUBO robot from the Korea Advanced Institute of Science and Technology (KAIST) is a 41 DoF humanoid. For several DoFs in the legs, the actuators are located away from the joint and are connected through a pulley system [6]. This design allows the larger actuator components to be packaged within the robot away from the intricate joint, and it gives the ability to rapidly change gearing ratios for those joints if needed. An image of HUBO can be seen in Figure 2-1B.

The humanoids outlined above are only a few of the full-sized platforms being researched today. Waseda University has advanced their work on the WABOT and WABIAN platforms [2, 7]. Reem-B from Pal Robotics is capable of walking up small steps and sitting in a chair [8].

Virginia Tech has created a lightweight humanoid CHARLI that can stabilize against upper body impacts [9].

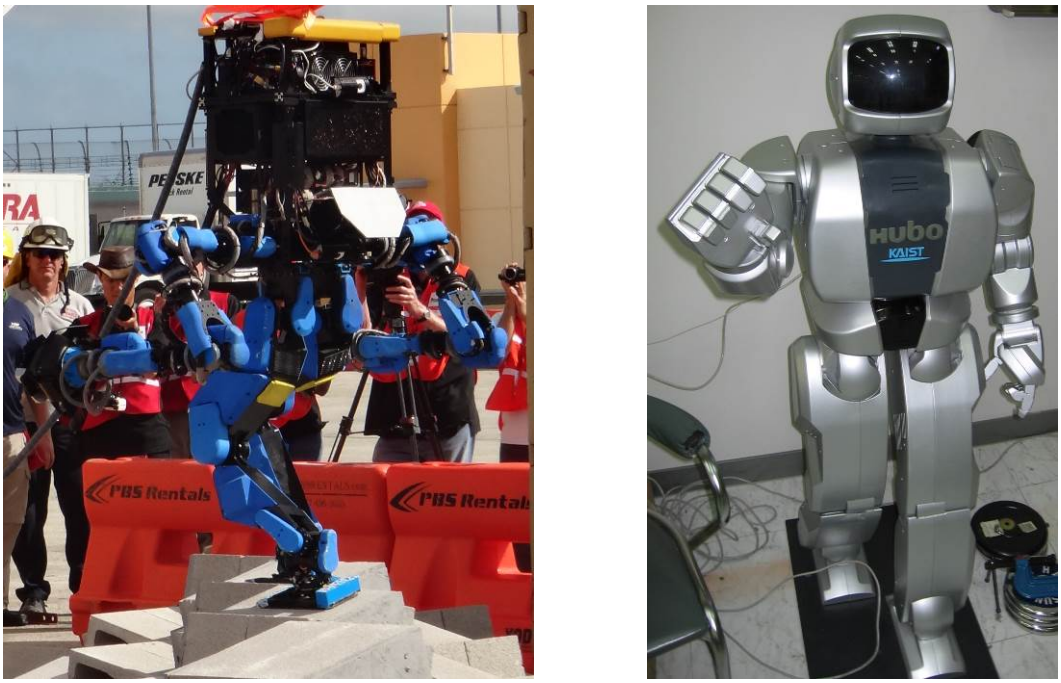

(A) (B)

Figure 2-1: Images of the (A) HRP-2 based biped from SCHAFT Inc. and (B) HUBO from KAIST.

2.2. Hybrid Linear-Rotary Actuated Humanoids

More recently, humanoid robots have started using linear actuators in tandem with rotary actuators to drive leg joints. Simpler joints with smaller RoM, such as the ankle, are ideal targets for linear actuation. When used in parallel, a set of linear actuators can control the same number of DoF. Acting together, these multiple actuators increase the number of motors acting on the same DoF, effectively increasing the potential torque output while maintaining the same relative size of actuator. This scheme is simplified from the human musculoskeletal system, where numerous muscles span a single joint and work cooperatively to drive limb movement. However, linear actuators limit the RoM by introducing additional physical interference constraints. Several groups have tried to reduce the cost to RoM by introducing additional gearing elements. A few of the linear actuated humanoids are presented below.

- Though not a true humanoid robot, spring flamingo from the Massachusetts Institute of Technology was one of the first successful walking robots to use series elastic linear actuators to drive its joints. Six actuators housed in the torso transmitted power to the joints through a series of cables running down each leg [10, 11]. This allowed spring flamingo to achieve a large enough RoM to climb and descend slopes.

- The successors to spring flamingo, M2 and M2V2 exclusively use linear actuators to drive all the joints in their legs [12, 13]. In order to mitigate the RoM challenge for the spherical hip joint, the designers coupled the linear actuator with a cable system for the pitch DoF. This moved one of the actuators away from the spherical joint to make its design simpler. Both robots also used parallel linear actuators at the ankle joint to cooperatively drive both pitch and roll.

- LOLA is a 25 DoF humanoid robot from the Technical University Munich. The ankles in LOLA use a long gear train to connect motors in the thighs to ball screws on the shin that push on the foot [14, 15]. This set of belts, gears, and ball screws allow for the mass of the motors to be moved higher up the legs. This helps decrease the inertia of the legs relative to the hip. The knee of LOLA is also driven by a linear actuator. However, its mechanical advantage will change over the RoM of the knee joint.

- Deviating slightly from its predecessor, HRP-4 uses a linear actuator to drive its ankle pitch joint [16]. The linear actuator helps to move the motors and transmission components into a smaller package inside the shin. It also slims down the size and weight of the ankle by removing an actuator from the foot. The roll joint is still driven by a rotary actuator.

- One of the most advanced robots in the world, Boston Dynamics' PETMAN platform is a hydraulic-powered humanoid that uses a mixture of linear and rotary actuators [17]. The hydraulic actuators provide large amounts of force, allowing the linear actuators to be placed closer to the joints. The large force output also allows PETMAN to have a high RoM at most of its joints because it does not need a high mechanical advantage to move.

- The successor to PETMAN is Boston Dynamics' Atlas robot. It is a hydraulic-powered humanoid with parallel linear actuated ankle joints. Though Atlas is a new robot, it is the selected Government Furnished Equipment (GFE) for seven teams in the DRC. One of the primary objectives when designing THOR was to compete in the challenge, so it must be able to perform similar tasks to Atlas. An image of Atlas can be seen in Figure 2-2A. Atlas was under development at the same time as THOR.

- The Virginia Tech Shipboard Autonomous Fire Fighting Robot (SAFFiR) is the predecessor to THOR. The legs of SAFFiR have 12 DoFs, including 10 series elastic linear actuators [18]. It is one of the first humanoid robots to use parallel actuation at both the ankles and hips. An image of SAFFiR can be seen in Figure 2-2B.

Similar to the rotary actuated humanoids, these hybrid linear-rotary actuated robots are only a portion of those in operation. The Waseda WABIAN-2RIII uses parallel linear actuators at the

ankles [19]. TUlip from the Technical Universities of Twente, Delft, and Eindhoven uses a cable system to translate motor rotation to linear cable motion to actuate its ankles [20, 21].

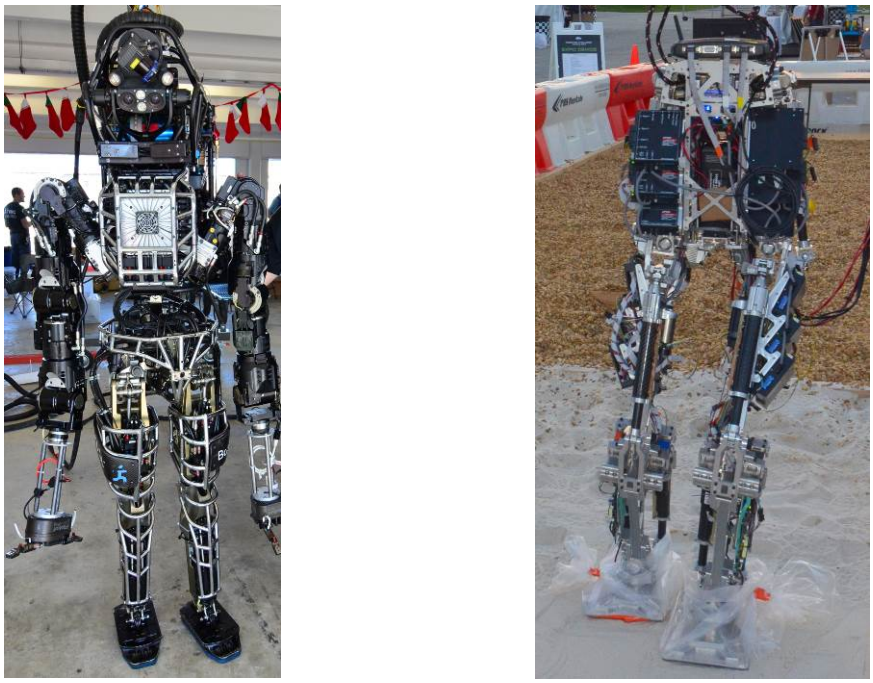

(A) (B)

Figure 2-2: Images of (A) Atlas from Boston Dynamics and (B) SAFFiR from Virginia Tech.

2.3. Series Elastic Actuators

Series Elastic Actuators (SEAs) are one of the primary technologies used in THOR. They provide the ability to perform high-bandwidth force control by placing an elastic component in series with the output of a rigid actuator [22-25]. Since their introduction by Pratt, SEAs have been frequently used in legged robotic applications because they mimic the biomechanical structure of legged animals [10-13, 18]. Force control allows a humanoid robot to better respond to the unexpected disturbances it will encounter in unstructured environments. The spring gives the actuator time to move out of the way and react to disturbances, making SEAs safer for operating around people. The spring can also be used to absorb impacts and store energy, reducing external loads on the actuator. A good force-controlled actuator has low friction so that it can command small forces. Using a low-impedance SEA allows the actuator to emulate a virtual mass-spring-damper system [26]. Numerous other research groups have created SEAs for various applications [27-31].

2.3.1. SAFFiR SEA

The Virginia Tech SAFFiR platform uses custom designed linear SEAs to drive the majority of its joints [18, 31]. This actuator serves as the basis for THOR's SEAs. The SAFFiR actuator has a few design features that differentiate it from other linear SEAs being used. A rendering of the

SAFFiR actuator can be seen in Figure 2-3. The SEA is comprised of two stand-alone components: a linear actuator with an integrated load cell and a configurable compliant spring.

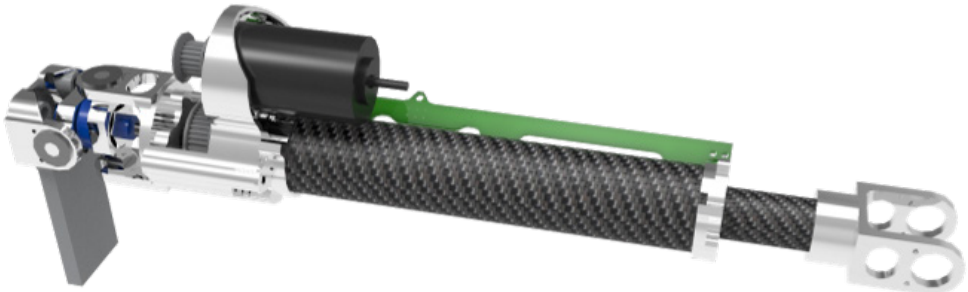

Figure 2-3: Series elastic actuator for SAFFiR

Two actuators cooperatively control two degrees of freedom at each of the hip and ankle joints, as seen in Figure 2-4. This parallel actuation scheme requires that one end of the actuator is a universal joint and the other is a spherical joint to prevent the actuators from binding as the leg rotates. In order to make the spherical joint, the actuator could have a traditional ball joint with a linear guide on the ball screw, or it could have a universal joint with no linear guide.

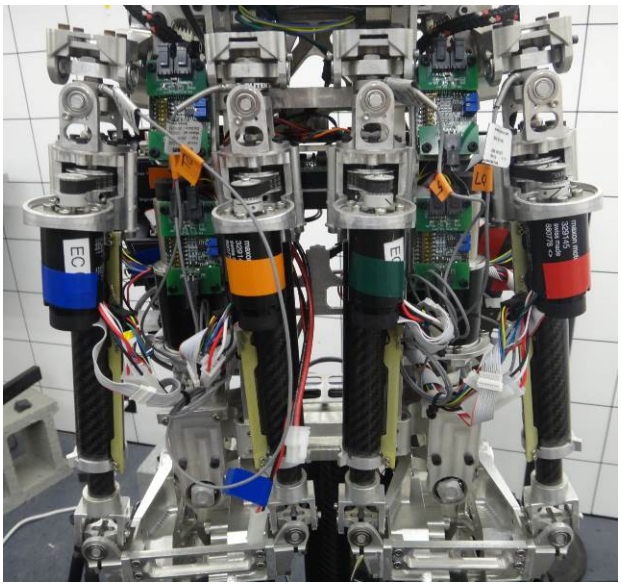

Figure 2-4: Two sets of parallel actuators spanning the hip joint of SAFFiR

A linear guide would add weight and friction to the actuator. However, it would allow for a simple measurement of the length of the actuator. Using a universal joint without a linear guide simplifies the design, reduces its weight, and reduces the overall friction in the actuator. But, the third degree of freedom in the spherical joint is achieved by allowing the ball nut to rotate, and not just translate, about the ball screw axis. This rotation will result in an error in the length calculated from the quadrature encoder on the motor. It was shown that the length errors were

acceptable over the RoM of SAFFiR's ankle joint, so the actuator was designed without a linear guide [31].

The actuator was designed to bolt onto a configurable compliance spring. To compensate for the spring constant uncertainty, it has a proprioceptive tension and compression load cell for direct force measurements. This load cell will measure up to 1100 [N] in tension or compression. Building the load cell into the actuator allows for adjusting the compliance while minimally altering any of the control code.

The second main component of the SAFFiR SEA is the configurable compliant spring located perpendicular to the primary axis of the actuator [31, 32]. The configurable compliance allows for tuning the springs to the walking of the robot. With the same mechanism, it is easy to test different stiffness settings at each leg joint. Additionally, the ankles can have looser compliance than the knees and hips which will aid the walking performance. The length of the spring cantilever is set before operating the robot and cannot be changed during use. The configurable compliant mechanism is shown in Figure 2-5.

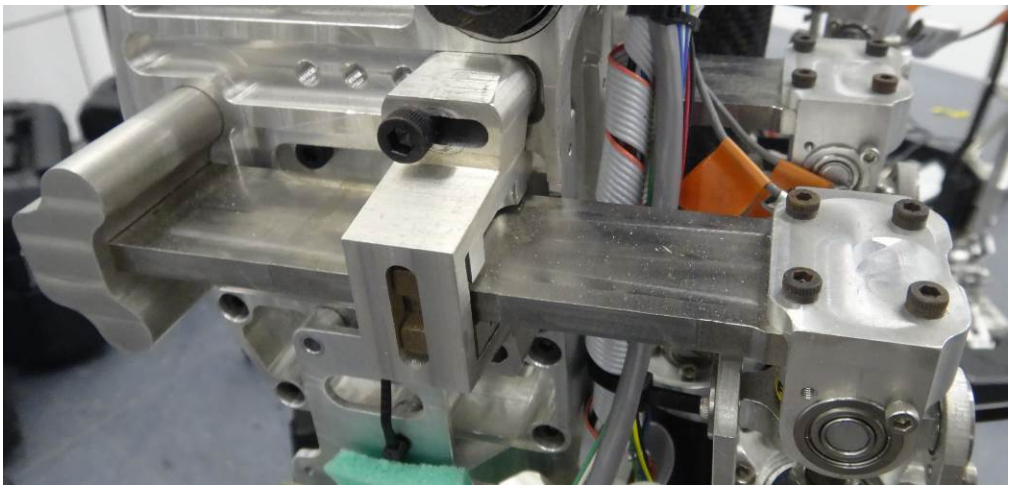

Figure 2-5: Configurable compliant spring for SAFFiR

These main features differentiate the SAFFiR SEA from most other research SEAs. The THOR SEAs integrate the same highlighted features with improvements over the original design.

3. Design Specifications

For THOR to be an effective disaster response robot, it must have the capability to perform similar motions to humans. The DRC is set-up to test robots in situations emulating disaster scenarios to see how close robots can perform to people. The competition has laid out a series of tasks to stretch the capabilities of robotics in locomotion, manipulation, and control. Several of these challenges push the limits on what is possible mechanically with a humanoid robot. Even though the specific details of each task were not released until after THOR was designed, their broad descriptions drove the design process.

3.1. DARPA Robotics Challenge Tasks

The DAPRA Robotics Challenge is broken down into eight individual events, each simulating a different aspect of first-responder disaster relief efforts. The competition will focus on human-designed environments. Though each task is independent, there are many shared traits between all of them. Based on different rules releases, the tasks have been moving targets throughout the entire process. Below is a description of each task and the desired qualitative specifications to complete that task. Details regarding each task were released in the initial task description documents from DARPA [33, 34].

3.1.1. Driving a Vehicle

When THOR was being designed, the driving task included vehicle ingress, driving, and egress. The vehicle selected for the task was the Polaris Ranger XP900 with the roll cage. Getting into a vehicle, while seemingly easy for a human, is a very difficult task. People have very advanced control systems that govern balance and coordination while performing difficult tasks. The robot would need enough RoM to stand next to the vehicle and get its leg into the car. It would then need enough torque in its joints to lift its body into the vehicle. Grasping the roll cage could decrease the necessary torque in the lower body, but it would also present a much more challenging whole-body control problem. A Polaris Ranger stands approximately 0.3 [m] off the ground, which is a tall height to lift a robotic leg. Once inside the vehicle, the robot would need to operate in a confined space, pressing the pedals and turning the steering wheel without interference between the arms and the body. Egress should have similar requirements to ingress.

After positioning itself in the vehicle, the robot needs to operate the car. Initially, this was described as turning on the Ranger, shifting it into gear, and steering and operating the pedals to make it move. In a confined space, this presents many manipulation challenges. Turning a key requires the ability to grasp the key as well as turn it. That same manipulator needs to grab and operate the shifter. Another large challenge is the perception of the environment. Because of the steering wheel and the dashboard of the vehicle, the robot needs to be able to perceive everything for driving using only its head sensors.

3.1.2. Traversing Rough Terrain

The second challenge task, the rough terrain course, presented the largest number of design specifications for the lower body. Originally, there was no description for the actual task, so THOR was designed to have the ability to walk, high step, kneel, and crawl. Even though the functionality would not be used until the second year of the competition, THOR was also designed with the RoM to stand up from a lying position.

Towards the end of the design process, the initial task description for the rough terrain course was released. Separated into increasingly difficult sections, the course tests a robot's mobility over a range of obstacles. Several of these obstacles can be seen in Figure 3-1.

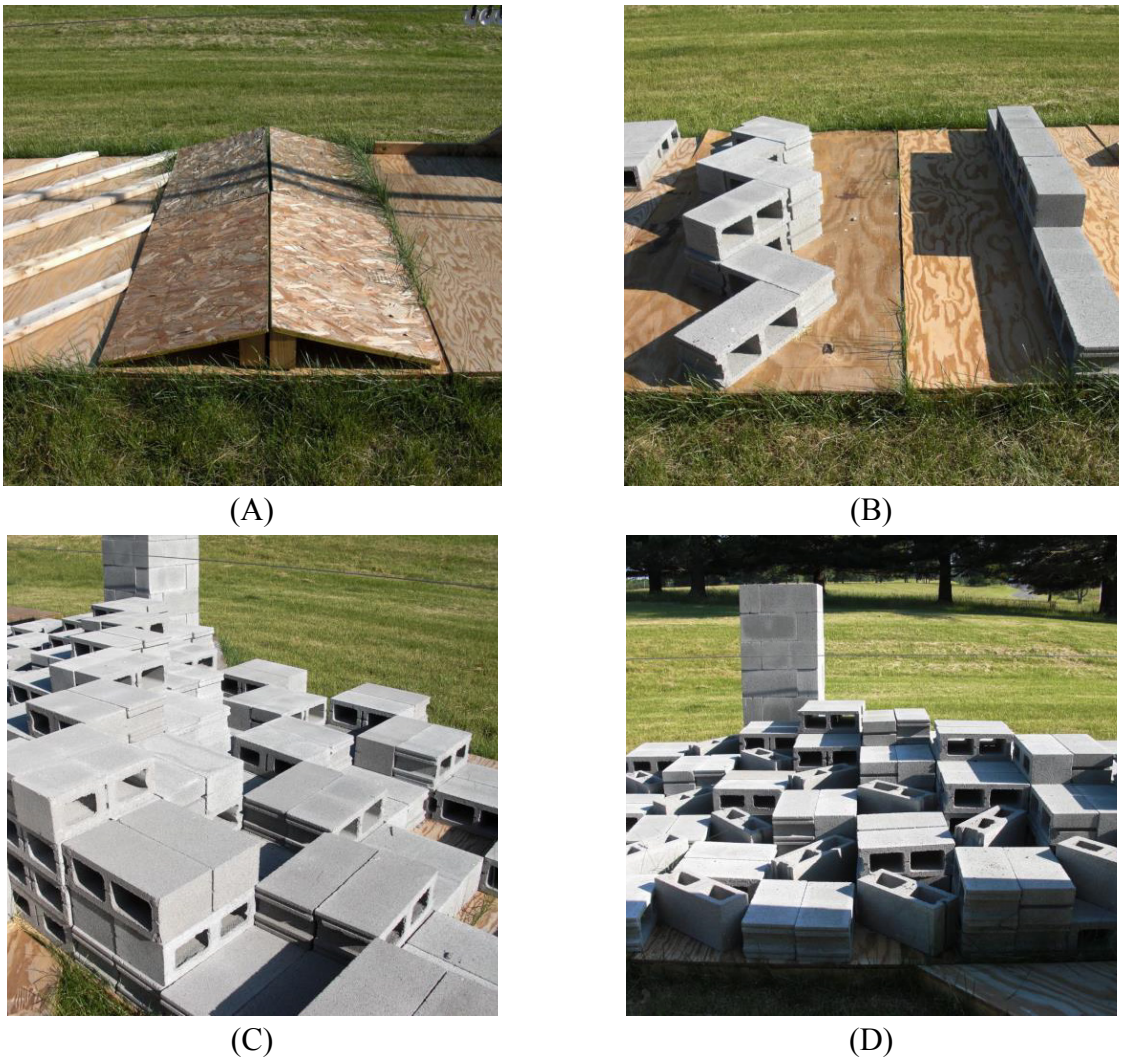

(A) (B)

(C) (D)

Figure 3-1: Various obstacles in the rough terrain walking challenge. These obstacles only represent a subset of the whole task. Obstacles include (A) 15° slopes followed by tripping hazards, (B) step-over sets of cinder blocks, (C) ascending diagonal hill, and (D) descending diagonal hill. Images used with permission from DARPA, http://www.darpa.mil/NewsEvents/Usage.aspx, 2013.

The cinder blocks used in the challenge are 8x6x16 [in]. Based on the layout of the obstacles, the tallest step necessary is two cinder blocks or 1 [ft]. With careful planning for the ascending and descending hills, it is possible for the robot to take each step with a maximum height change of one block. One other consequence of the course design is that a flat foot is capable of completing the task. There is no need to design a jointed foot to handle rough terrain.

3.1.3. Debris Clearing

The debris clearing task requires a mix of lower body movement with upper body manipulation. The pieces of debris all weigh 2.2-4.4 [kg] but may be up to 1.5 [m] long. These objects will be located close to the ground in a configuration similar to Figure 3-2. The objects include 2"x4" and 4"x4" pieces of lumber, metal pipes, and a girder section. The ultimate goal of the task is to walk through the doorway behind the debris.

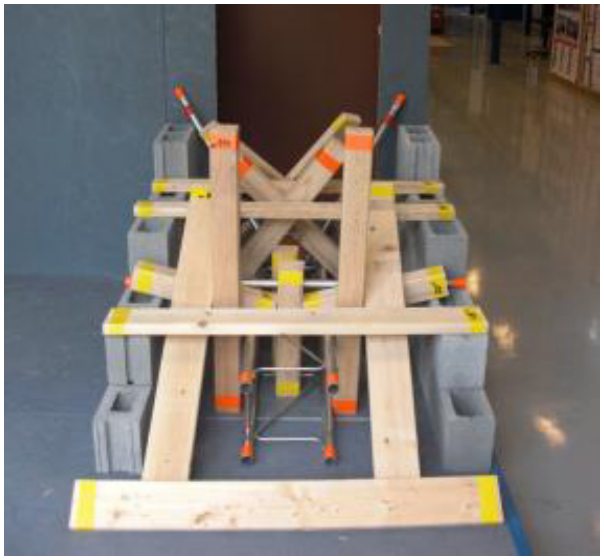

Figure 3-2: Debris clearing task proposed layout. Image used with permission from DARPA, http://www.darpa.mil/NewsEvents/Usage.aspx, 2013.

In order to reach some parts in the debris task, the robot must be able to reach down and touch the ground in front of it. This must result from a combination of THOR crouching with its lower body and having long-enough arms to touch the ground. Each arm should have enough strength to lift a 4.4 [kg] object because bi-manual manipulation on some objects may not be easy within the robot's workspace. Because of the varying sizes of the objects, the robot must have a dexterous manipulator that can grab both large and small objects.

3.1.4. Passing Through a Door

The door challenge consists of opening and passing through three doors: a push door with no resistance, a pull door with no resistance, and a pull door with a weighted closure. The three doors will be placed in succession, as seen in Figure 3-3. The doors are arranged in this configuration so that they are in order of increasing difficulty. The doors will have lever handles.

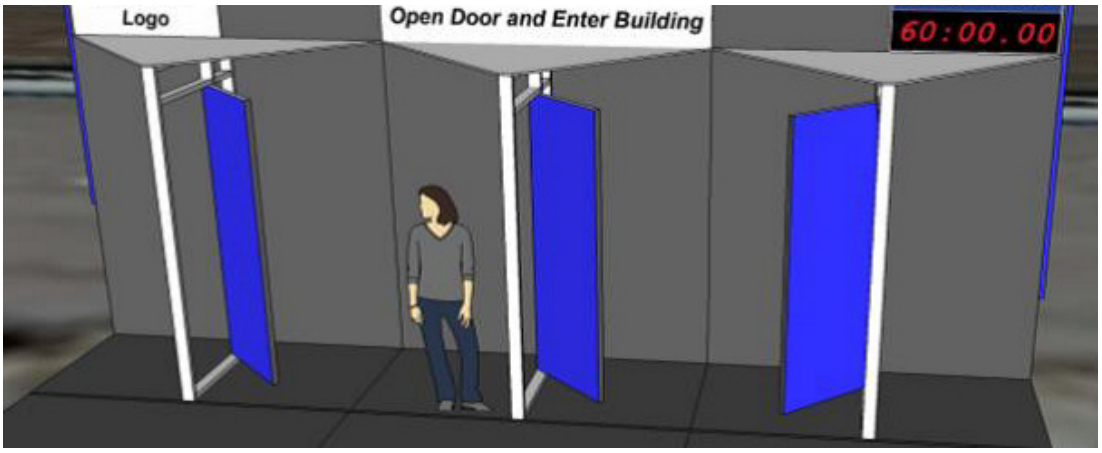

Figure 3-3: The three doors for the fourth challenge. The robot is expected to move from right to left. Image used with permission from DARPA, http://www.darpa.mil/NewsEvents/Usage.aspx, 2013.

This task presents numerous challenges. Because the door handles will be at a normal door height, the arms should not have difficulty reaching them. On the pull door, the robot must be close enough to open the door, but far enough away to dodge that same door. This may require repositioning the robot while it is still grasping the door. Though this is mostly a control problem, the arms need enough DoFs to allow THOR to move while it is still holding a constrained object. This challenge becomes harder when THOR is holding the weighted door, as the door will be pulling against the robot.

3.1.5. Climbing a Ladder

The ladder climbing task challenges THOR to ascend a 60° incline ladder. This task is modeled after shipboard and non-vertical industrial ladders. This is modified from the original task description, which used a vertical ladder. An example of the ladder is shown in Figure 3-4. This ladder has flat steps which will make balancing easier than round rungs.

Figure 3-4: Inclined ladder for the competition. Image used with permission from DARPA, http://www.darpa.mil/NewsEvents/Usage.aspx, 2013.

The steps are vertically separated by 0.3 [m], much like the step-over obstacles in the rough terrain course, so the robot must be able to lift its leg that height. However, unlike for those step-over obstacles, the robot does not need to take a step longer than the length of the foot to clear this obstacle. One of the main locomotion challenges is not running the foot or any other part of the shin into the step on the ladder. The steps on the ladder are 0.8 [m] wide, so the robot needs to be thinner than that in whatever profile it climbs up the ladder.

3.1.6. Breaking Through a Wall

Using a two-handed drill, the robot must cut through a section of cement board. From the start of the task, THOR needs to pick up the drill from a table, turn on the drill, and cut a triangular section between two specified sets of lines. An image of the drill and challenge can be seen in Figure 3-5. This task introduces dust and vibrations which are not as prevalent in the other tasks.

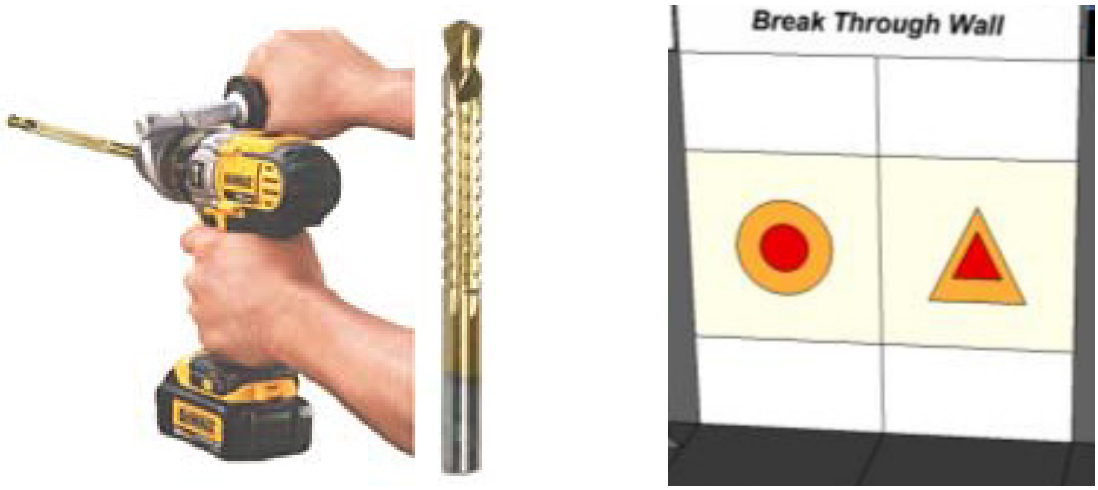

(A) (B)

Figure 3-5: Images of (A) the proposed cutting tool with side cutting bit and (B) representative task walls with the cut region in orange. Images used with permission from DARPA, http://www.darpa.mil/NewsEvents/Usage.aspx, 2013.

The main design challenges for this task are related to manipulation and arm movement. The hands must be small enough to grasp a drill handle, but large enough to wrap around the grip to press the trigger. Coupling this with the size required to grasp 4”x4” pieces of lumber for the debris task, the hand has a tight window for size to be effective at all the tasks. Additionally, the arms need to be longer to support moving the drill to cut through the wall. The triangular section is listed at about 0.6 [m] per side, so the arms need a large RoM. It is likely that the cutting will need to happen with both hands on the drill, further limiting the manipulation workspace. Lastly, the dust created from the cutting can cause problems for the robot. The robot will need to be designed with sealed bearings, and some form of dust shield to prevent unwanted particulates from entering the more delicate sections of THOR.

3.1.7. Closing Valves

The valve closing task requires the robot to close a set of three valves placed 3-5 [ft] above the ground. These valves are variable in size and shape. Several examples of test valve handles are seen in Figure 3-6. These handles include large wheels, garden hose valves, and 90° turn levers.

Figure 3-6: Example valves including large wheels, 90° turn levers, and hand knobs. Image used with permission from DARPA, http://www.darpa.mil/NewsEvents/Usage.aspx, 2013.

The designated valves will be determined at the competition, so the robot needs the ability to grasp various sized handles. Most of the smaller handles will be operated using one hand, so it needs enough dexterity to grasp various shapes. As seen in Figure 3-6, the smaller handles are both circular and square. Grasping the larger wheels will be similar to the steering wheel in the utility vehicle.

3.1.8. Installing a Fire Hose

The final task in the DRC is to install a fire hose in a fire hydrant. There were no specifications about the initial location of the fire hose, so it could be located on the floor, on a table, or attached to the wall. The hydrant will be located away from the hose, so the hose must be dragged to the hydrant. An image of the task setup can be seen in Figure 3-7.

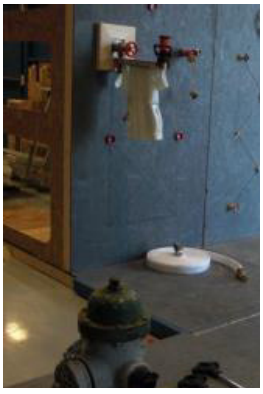

Figure 3-7: Firehose task setup with multiple possible starting locations for the firehose. Image used with permission from DARPA, http://www.darpa.mil/NewsEvents/Usage.aspx, 2013.

Though an extremely difficult task, this challenge does not present new design requirements beyond the other tasks. To reach a fire hose on the ground, the robot needs to touch the ground similar to the debris clearing task. Likewise, it will need to get low to the ground to install the hose in the hydrant. The main manipulation challenge is grabbing the fire hose, but if THOR can hold the pieces of debris and valve handles, it should be able to grab the end of the fire hose.

3.2. Study to Simulate Task Motions

At the beginning of THOR's design, the detailed task descriptions were not available from DARPA. This information did not become available until midway through the design process. The only available information for the task was their broad descriptions: drive a utility vehicle, traverse a rough terrain course, etc. Based on the broad task descriptions, the team identified a core set of motions that would provide enough RoM to accomplish the challenge. These core functions included:

- Walking
- Climbing into a golf cart
- Kneeling
- Crawling
- Climbing an A-frame ladder
- Standing from the prone position
- Standing from the supine position

Because these functions could represent a very large RoM for each joint, it was decided to test out the motions to measure what a person actually uses. The test subject chosen was the closest in size to the proposed THOR in the lab. Even if THOR is larger than the subject, it should be able to complete the challenge with the same joint RoM. Since the robot will not have the exact same DoFs as the subject, the test subject was told to try to perform motions using only the robot's DoFs. The DoFs for the legs are highlighted in Figure 3-8. Additionally, humans tend to move with very dynamic motions which are difficult to replicate with a robot. The subject was asked to try doing motions as statically as possible so that they could be replicated by the robot.

Based on the proposed design, the THOR arms had a large RoM exceeding that of a human. If the test subject could complete a task, then the arms would have enough RoM to complete it as well. The tests were used to look at the arm length and which functions involved the arms. The test subject does not have long arms, so the results were influenced by their shortened reach while attempting to manipulate objects.

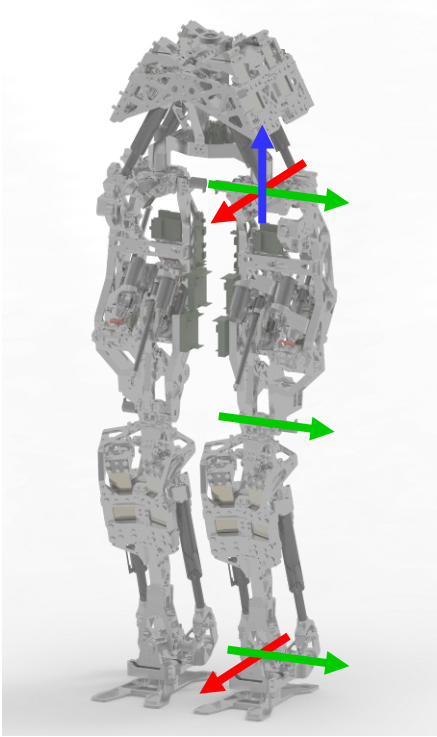

Figure 3-8: Depiction of THOR's legs with the axes for the DoFs highlighted for left leg. Each leg has a 3 DoF hip (yaw, roll, and pitch), 1 DoF knee (pitch), and 2 DoF ankle (pitch and roll). The yaw axis is in blue, roll axes are in red, and pitch axes are in green.

This quick study was performed to measure rough RoM requirements for THOR's joints, not to create motion primitives for advanced tasks. Therefore, there was no need for accurate motion tracking. Instead, the test subject was dressed in black clothing with bright electrical tape lines drawing connections between the various body joints. Videos were recorded from both the side and front to allow measurement of most of the body angles. The videos were analyzed using a protractor to get approximate joint angle measurements. Barring an unexpectedly difficult task in the competition, this data provided a set of joint angles that would allow THOR to complete the challenge.

Even though walking is one of the primary tasks associated with the competition, it does not have a large RoM requirement compared to the other proposed functions. Ladder climbing encompasses the RoM needed for a tall step. Based on the walking of SAFFiR, the legs do not use a large RoM while performing a regular step.

3.2.1. Climbing into a Golf Cart

Climbing into a utility vehicle is one of the most challenging RoM tasks. As stated in Section 3.1.1, the floor of a Polaris Ranger stands roughly 0.3 [m] above the ground. In addition to the high step height, the legroom area in the utility vehicle is limited. Beyond finding the gas pedal, the robot needs to avoid hitting the steering wheel as it moves around the utility vehicle.

Because a Polaris Ranger was not available for testing, this task was simulated using an off-road golf cart. The floor of the golf cart used for testing is 0.45 [m] from the ground. This requires a much larger step than a stock Ranger, making the recorded task more difficult. On many of the ingress attempts, the test subject used their jointed foot to help move their body higher. This particular movement could be mitigated by designing THOR's limbs to be longer than the test subject. An image of the test subject entering the golf cart is seen in Figure 3-9.

Figure 3-9: Test subject climbing into the golf cart

The RoM required to lift a leg to the necessary height is large. In particular, the hip, knee, and ankle pitches experience a large amount of movement. Depending on the ingress strategy, hip and ankle roll could both be important too. Table 3-1 shows the minimum and maximum measured joint angles for the attempts at vehicle ingress. Hip yaw did not have any large values so it is omitted from this table. Because the legs are designed to be symmetric, the joint angles are presented for a left leg in all subsequent results.

Table 3-1: Measured joint angles for golf cart ingress

Joint DoF	Minimum Angle [deg]	Maximum Angle [deg]
Hip Roll	-25	35
Hip Pitch	-110	0
Knee Pitch	0	130
Ankle Pitch	-35	45
Ankle Roll	-35	25

3.2.2. Kneeling

Unlike golf cart ingress, kneeling is a motion that can be used in multiple events. After looking at the challenge tasks, it was determined that kneeling could be beneficial for debris clearing, breaking through a wall, valve closing, and installing a fire hose. These tasks presented the possibility of manipulating objects close to the ground. Figure 3-10 shows the test subject midway through a kneeling trial.

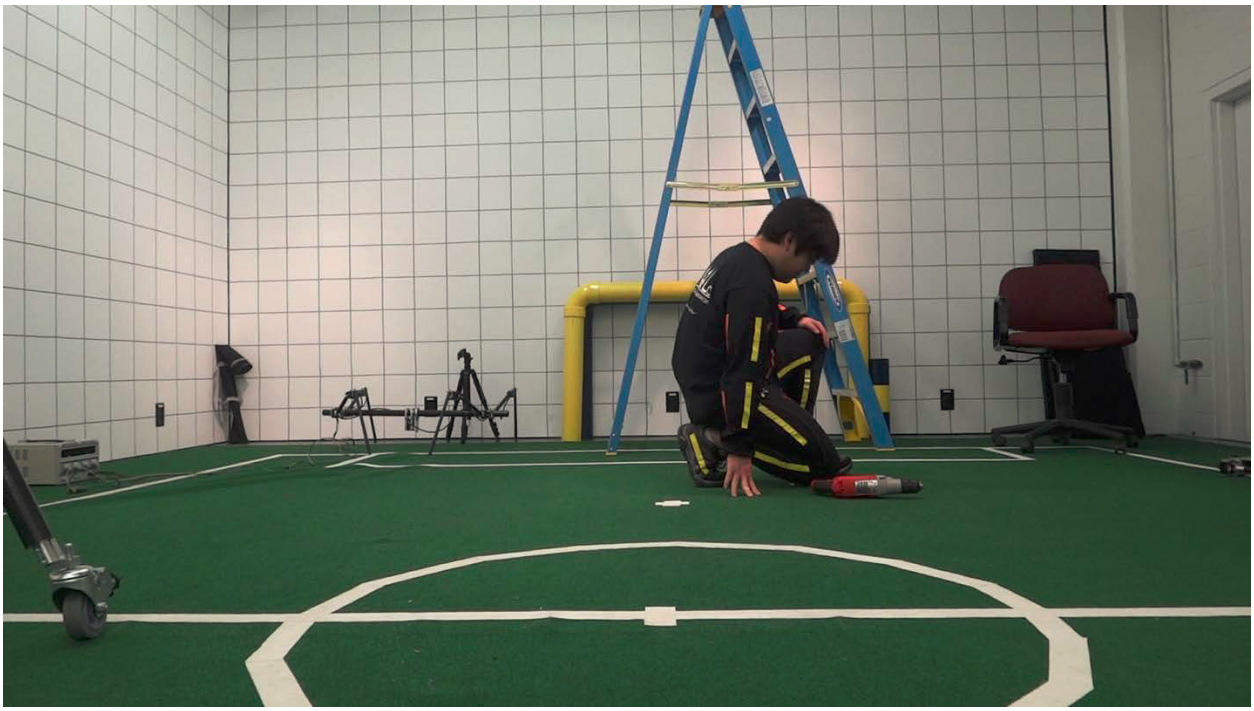

Figure 3-10: Test subject kneeling

Similar to the vehicle ingress, not all of the leg DoFs saw major movement. As expected, the majority of the motion was in pitch for all leg joints. This test resulted in a several important observations. The RoM results from this test can be found in Table 3-2.

- It is important that the knee can make contact with the ground for stability. When the knee is in contact with the ground, the support polygon beneath the test subject grows significantly compared to only feet in contact.
- A toe eases the transition between squatting and kneeling. When lowering the knee towards the ground, the ankle does not have enough RoM to allow the knee to reach the ground. Instead, the back of the foot lifts off the ground leaving the front still in contact. The toe joint allows a wide portion of the foot to remain in contact with the ground, helping to prevent the subject from rolling to the side. If the subject had a flat front edge on their foot, instead of the rounded edge of a shoe, the toe would not be necessary.

- The arms can stabilize the robot as it starts to kneel. Similar to a sprinter, the robot can use its arms to create a larger support polygon as it adjusts its legs into the kneeling position.
- Once kneeling, it is difficult for the subject to move their legs. In order to shift the manipulation space for the arms, a waist joint is needed. The manipulation space moves the most during yaw motions of the waist.

Table 3-2: Measured joint angles for kneeling

Joint Axis	Minimum angle [deg]	Maximum angle [deg]
Hip Yaw	0	25
Hip Pitch	-125	0
Knee Pitch	150	0
Ankle Pitch	-50	0
Waist Yaw	-45	45
Waist Pitch	0	30
Waist Roll	-20	20

3.2.3. Crawling

Crawling is not an explicitly required motion for the competition, but similar to kneeling, it could be useful to complete certain tasks. Because the layout of the rough terrain course was not known at the beginning of the design process, crawling was a possibility to traverse that course. Having the RoM to crawl would also provide most of the necessary RoM to scramble over smaller obstacles. An image of the test subject crawling can be seen in Figure 3-11.

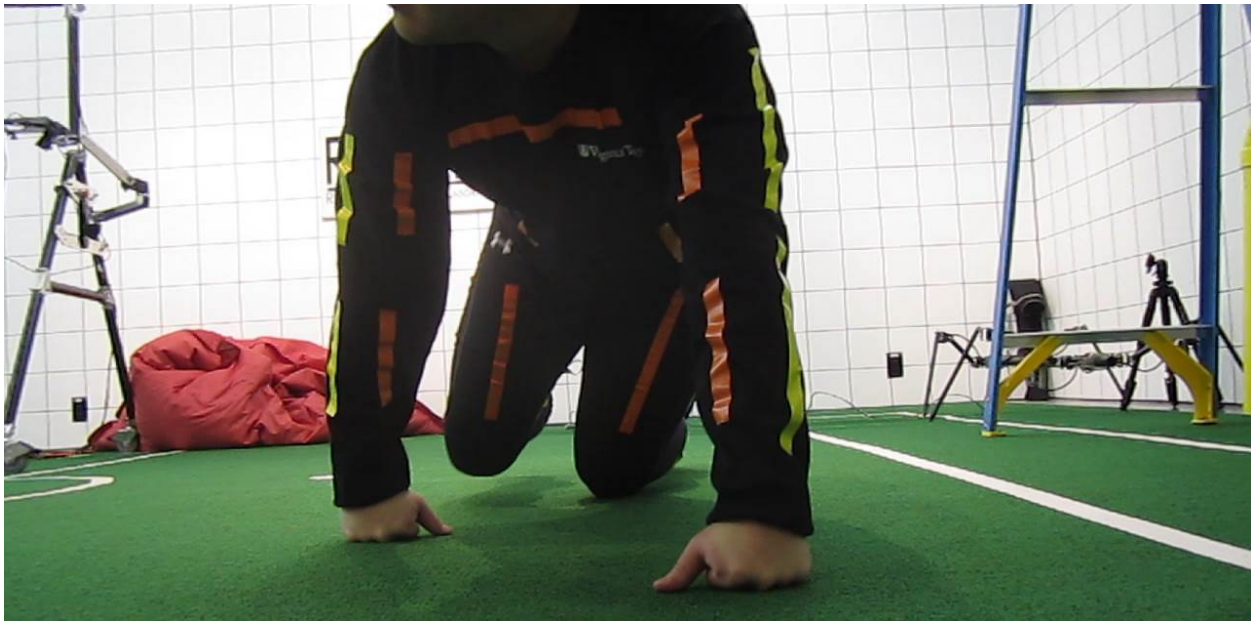

Figure 3-11: Test subject crawling

The most important DoF for crawling is the waist yaw. In order to keep the subject's center of mass (CoM) above the support polygon formed by the knee and hands, the support leg must have an inward yaw. In all the testing, crawling was the only function that required inward yaw. Finally, crawling was the first task that constantly required the use of the arms. The arms are used for both balancing and locomotion. Because THOR's proposed arms are more flexible than the test subject, the RoM was not measured during the test. The leg RoM results from the crawling test can be seen in Table 3-3.

Table 3-3: Measured joint angles for crawling

Joint Axis	Minimum angle [deg]	Maximum angle [deg]
Hip Yaw	-25	20
Hip Pitch	-100	0
Knee Pitch	0	130
Ankle Pitch	-35	40

3.2.4. Climbing an A-Frame Ladder

The effect of THOR being able to climb a ladder extends beyond the ladder climbing task. If THOR has the RoM to climb the A-frame ladder, it would be able to step over larger obstacles. However, one advantage a person has when climbing a ladder, the ability to use their hands for both stability and lifting, is not used when they try to step over large obstacles. Figure 3-12 shows the test subject climbing the ladder from above.

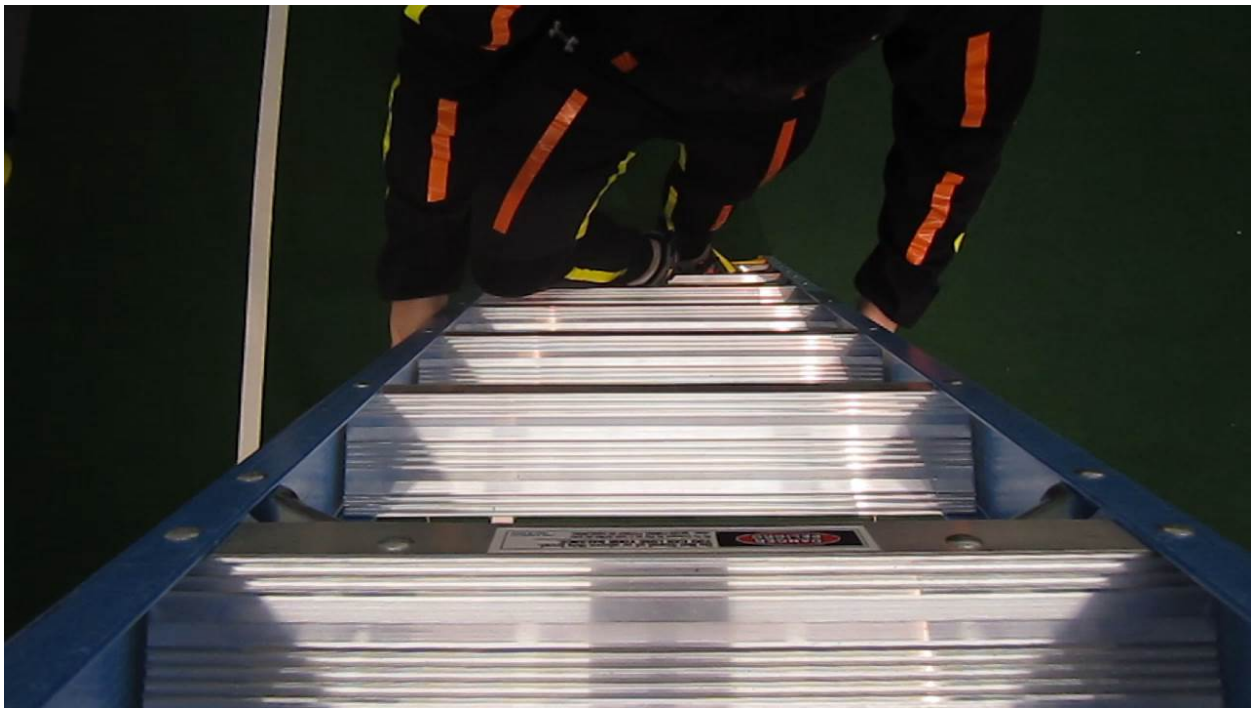

Figure 3-12: Test subject climbing an A-frame ladder

The test subject found that the largest challenge associated with climbing the ladder was the ability to lift their leg from one step to the next. Not only is each step roughly 0.3 [m] above the last, the steps also act as obstacles for the foot. The robot will need to move its foot clear of the steps, lift its foot high enough to get to the next step, and then reinsert its foot before lowering it to make contact with the step. This is a challenging problem because the robot will need to use its arms for stabilization while it moves each leg. Based on the test subject, there are multiple possible strategies for moving its feet while climbing a ladder.

- The robot can approach the ladder straight-on and pull its leg far backwards to clear the rungs. This is the simplest method involving only the pitch DoFs in the legs but would require the arms to stabilize the robot as it climbs.
- The robot can climb the ladder with both legs at a large outwards yaw angle. This strategy allows the robot to keep its body closer to the ladder, decreasing the amount of work that its arms must perform for stabilization. The motion to raise one leg to the next rung is more complicated and involves a combination of yaw, roll, and pitch. Additionally, based on the foot placement, the leg may need to rise by two rungs each time. As shown in Figure 3-12, the right heel of the test subject is located where the left would need to land on that step.
- The robot can use a hybrid approach with one leg completely straight and the other turned outwards. If the outward facing leg is the first leg to rise each step. The robot can still keep its body close to the ladder while climbing. This strategy would involve both feet landing on the same step before proceeding to the next.

The various attempts at climbing a ladder showed the importance of yaw in the legs. Climbing is the first tested function that required any significant outward yaw. Additionally, the arms were used in every trial for stability. Similar to crawling, climbing will be a full-body locomotion task. The relevant RoM results from ladder climbing can be found in Table 3-4.

Table 3-4: Measured joint angles for ladder climbing

Joint Axis	Minimum Angle [deg]	Maximum Angle [deg]
Hip Yaw	0	45
Hip Pitch	-100	10
Knee Pitch	0	120

3.2.5. Standing From the Prone and Supine Positions

While common to small-sized humanoid robots, only a couple adult-sized humanoids have the ability to stand from a lying position [35, 36]. This function is limited by several factors. First, standing requires a very large RoM and high joint torques. It is a whole-body task requiring coordination between the arms and legs. It is also helpful to have a waist joint to help shift

around the upper body mass. Finally, standing is typically paired with falling. During a fall, any part of the robot is liable to break. Mitigating falls involves a combination of protective covers and smart impact-reducing strategies [35, 37].

The two standing functions had the largest amount of variability in the methods that the test subject used for completion. Unlike the previous functions, there is no apparent method to complete this task. Standing is an extremely dynamic motion that is difficult to replicate using static motions. The numerous trials involved the test subject standing by using mainly pitch motions, spreading their legs and rocking their body forward, and rolling their body onto their feet. There was no one method that worked better than the others. Because of the numerous methods to stand, the RoM measurements were extremely varied. Table 3-5 lists the joint angle measurements for standing from lying in the prone position and Table 3-6 lists the results for standing from lying in the supine position.

Table 3-5: Measured joint angles for standing from the prone position

Joint Axis	Minimum Angle [deg]	Maximum Angle [deg]
Hip Yaw	0	60
Hip Roll	-10	10
Hip Pitch	-125	35
Knee Pitch	0	120
Ankle Pitch	-35	35
Ankle Roll	-35	10

Table 3-6: Measured joint angles for standing from the supine position

Joint Axis	Minimum Angle [deg]	Maximum Angle [deg]
Hip Yaw	0	55
Hip Roll	-15	45
Hip Pitch	-105	10
Knee Pitch	0	150
Ankle Pitch	-10	45
Waist Yaw	-45	45

3.3. Desired THOR Range of Motion

The simulation of the proposed task motions provided a set of RoM angles that a human needed to complete the tasks. This was just one of a few important sets of RoM data used in the design of THOR. As stated in Section 2.2, the Atlas robot is the chosen standard platform for the DRC. This means that Atlas needs to be able to complete every task in the competition. The joint angle capabilities of Atlas were proposed by Boston Dynamics early in the design process, so they were factored into THOR's design. The third set of data points used to design THOR was the

joint RoM of the average human [38-40]. The DRC is designed to mimic human-engineered environments, so the average person should be able to operate in that environment. A human does not have the exact same joints as THOR and Atlas, so the human RoM was approximated to match the robot DoFs. Another data set used was the joint RoM of the test subject. Because the test subject is less flexible than the average human, their joint angle RoM data is not presented. Finally, the RoM of Virginia Tech's SAFFiR platform was used. The design of THOR is inspired by the design of SAFFiR, so it was natural to compare the two. The compiled RoM data for the lower body and upper body are presented in Table 3-7 and Table 3-8 respectively. The joint angles are presented for a left leg and left arm.

Table 3-7: Range of motion data for the lower body

Joint Axis		Average Human	SAFFiR	Atlas	RoM Videos	Desired THOR
Hip Yaw	Min [deg]	-30	-10	-10	-25	-20
	Max [deg]	60	25	70	60	60
Hip Roll	Min [deg]	-30	-23	-30	-25	-30
	Max [deg]	45	23	30	45	45
Hip Pitch	Min [deg]	-135	-45	-100	-125	-120
	Max [deg]	20	45	20	35	30
Knee Pitch	Min [deg]	0	0	0	0	0
	Max [deg]	135	90	135	150	150
Ankle Pitch	Min [deg]	-20	-40	-40	-50	-45
	Max [deg]	50	50	40	45	45
Ankle Roll	Min [deg]	-35	-20	Unk	-35	-30
	Max [deg]	15	20	Unk	25	30

The desired THOR lower body joint angles do not match those from the RoM testing. With the exception of hip roll, the desired ranges are decreased compared to the test subject videos. Most of these design decisions were based on simplifying the potential design, especially given the tight timetable to develop THOR. The test subject used an extremely large RoM in both hip and knee pitch, which would be difficult to replicate while maintaining a high achievable torque throughout that range. The desired yaw RoM is less than an average human. This is partially due to the difficulty of designing a hip joint with a large RoM while preventing limb interferences. This is also due to the test subject not needing to use large amounts of yaw while performing the tasks. The test subject also used a large amount of ankle pitch, exceeding that of an average human. The main reason for this measurement is the subject's foot slipping inside their shoe, allowing their shin to move closer to the shoe as the subject bent their toe.

As stated in Section 3.2, the proposed arms for THOR have a greater RoM than a human. These arms are also the arms of SAFFiR. Because the arms are the same, they will have the same RoM

in Table 3-8. These arms should have enough RoM to complete the DRC. For similar reasons, the RoM of the test subject's head was not measured. Though SAFFiR's head is different from THOR's head, the design concepts would be similar enough to need a new range.

Table 3-8: Range of motion data for the upper body with the waist pitch estimated from the test subject

Joint Axis		Average Human	SAFFiR	Atlas	RoM Videos	Desired THOR
Waist Yaw	Min [deg]	-45	-90	-45	-45	-45
	Max [deg]	45	90	45	45	45
Waist Roll	Min [deg]	-35	N/A	-40	-20	N/A
	Max [deg]	35	N/A	40	20	N/A
Waist Pitch	Min [deg]	-30	N/A	-35	-30	-30
	Max [deg]	10	N/A	25	0	0
Shoulder Pitch	Min [deg]	-180	-180	-90	N/A	-180
	Max [deg]	60	180	50	N/A	180
Shoulder Roll	Min [deg]	-75	-20	0	N/A	-20
	Max [deg]	180	180	115	N/A	180
Shoulder Yaw	Min [deg]	-70	-180	-40	N/A	-180
	Max [deg]	45	180	100	N/A	180
Elbow Pitch	Min [deg]	-150	-160	-135	N/A	-160
	Max [deg]	0	0	0	N/A	0
Wrist Yaw	Min [deg]	-80	-180	-85	N/A	-180
	Max [deg]	80	180	85	N/A	180
Wrist Roll	Min [deg]	-80	-90	-30	N/A	-90
	Max [deg]	70	90	60	N/A	90
Neck Yaw	Min [deg]	-60	-90	N/A	N/A	-90
	Max [deg]	60	90	N/A	N/A	90
Neck Pitch	Min [deg]	-45	-60	-45	N/A	-60
	Max [deg]	45	60	45	N/A	60

The most noticeable exclusion from the proposed THOR RoM data in Table 3-8 is the waist roll joint. This joint was excluded for design simplicity. Even though it was used in the test subject trials, its effectiveness could be replaced through a combination of waist yaw and pitch motions. This reduced the complexity of the waist, and also increased its strength by removing an actuator that would be likely to break.

The leg, waist, and neck joint angles in Table 3-7 and Table 3-8 are the desired RoM values for THOR, not the actual RoM values. These numbers were used as guidelines to drive the design.

The layout of the actuators in the legs limited the actual RoM. The achievable RoM will be discussed in Chapter 4.

3.4. Body Dimensions

The second main aspect to THOR's design is the length of its respective body segments. Similar to the RoM, the desired body segment lengths were determined by looking at the average person, SAFFiR, Atlas and the test subject. The body dimensions of the average person were found by looking at the GM-ATD 502 crash test dummy, which was later released as the Hybrid III [41]. The Hybrid III was developed to closely mimic the anthropometric makeup of the 50th percentile male of the early 1970's. This is one of the industry standard crash test dummies because it accurately replicates the human form. SAFFiR and Atlas are included for similar reasons to the RoM comparisons. The dimensions for Atlas were measured from the first Gazebo simulator model provided by DARPA, but they are not necessarily final design numbers for that robot. Unlike for the RoM analysis, it was necessary to look at the test subject's body dimensions. The test subject's ability to complete the trial tasks is directly coupled to both their RoM and body dimensions. The test subject body dimensions were approximated with a tape measure.

To simplify the design of THOR, all the body joints were placed on the same coronal plane. Additionally, joints on the same limb were all assumed to be vertically aligned. For example, on the left leg, the hip joint is directly above the ankle and knee joints. This simplified the body dimension measurements to those in the cardinal directions. The leg was split into three primary bodies: the thigh, shin, and foot. Connecting the legs to the upper body, the torso was modeled as a single piece. There was no waist joint in this initial investigation because its location would be driven by the packaging of THOR's lower body actuators and electronics. The vertical dimensions associated with THOR's design are in Table 3-9.

Table 3-9: Vertical body segment lengths

Link All dims. in [m]	Hybrid III	SAFFiR	Proposed Atlas	Test Subject	Proposed THOR
Foot	0.0787	0.049	0.081	0.10 (with shoes)	0.055
Shin	0.414	0.379	0.4288	0.36	0.41
Thigh	0.399	0.379	0.38	0.42	0.41
Torso to Shoulder	0.455	0.517	0.5557	0.43	0.53
Shoulder to Eye	0.272	0.214	0.1694	0.24	0.23
Total Height	1.6187	1.538	1.6149	1.54	1.635

These lengths only rise to eye level or camera level for a robot. The cameras on the Atlas sensor head are very low, so it will be taller than THOR when measured to the top of the head. There is

approximately 0.1 [m] between the eyes on Hybrid III and the top of its head, making its listed total height shorter than reality.

The shoulder joint connects the arms to the torso. Each arm was broken into two segments: the (upper) arm and forearm. These body segments directly match-up with parts of the human body. The overall arm length is an important factor because it determines THOR's manipulation workspace. Arms that are too short reduce the work area while those that are too long decrease the lifting capabilities. The arm lengths were initially designed to be close to the test subject. It is simple to increase the lengths of the arms because of their design. The arm length specifications are in Table 3-10.

Table 3-10: Body segment lengths associated with wingspan

Link All dims. in [m]	Hybrid III	SAFFiR	Proposed Atlas	Test Subject	Proposed THOR
Shoulder Width	0.346 (from [39])	0.438	0.5943	0.36	0.44
Arm	0.262	0.24	0.3088	0.24	0.25
Forearm	0.249	0.226	0.2498	0.24	0.24
Wingspan w/o Hands	1.368	1.37	1.7115	1.32	1.42

There are a few other important length specifications. The width of the hips determines how close the legs are to each other. The width needs to be large enough to prevent collisions between the legs. However, increasing the width increases the torque demand for the hip and ankle roll joints. The size of the foot is also very important. The foot is the only body that regularly interfaces between the robot and the world. The size and shape of the foot determines the support polygon of the robot during locomotion. These dimensions are in Table 3-11.

Table 3-11: Hip width and foot dimensions

Length All dims. in [m]	Hybrid III	SAFFiR	Proposed Atlas	Test Subject	Proposed THOR
Hip Width	0.164 (from [39])	0.194	0.178	0.165	0.18
Foot Length	0.264	0.23	0.262	0.28 (with shoes)	0.25
Foot Width	0.102	0.125		0.09 (with shoes)	0.135

Just like the RoM, these are only proposed lengths for THOR. The lengths were modified in the design process to fit the actual robot. For example, the arms are longer than the proposed to

simplify reaching the ground. Additionally, the waist location was never proposed because it depends on the parallel actuator configuration for the hips.

3.5. Leg Joint Torques

A basic investigation on leg joint torques was performed to determine ballpark values to surpass. The ideal scenario is to provide as much joint torque as possible at each joint, but this is not always possible. There will be limitations on THOR's joint torque based on the nominal configuration of the actuators and the changes to the mechanical advantage over the full RoM.

The investigation used the model of SAFFiR to calculate the ballpark joint torque estimates. Even though THOR will be taller and heavier than SAFFiR, it will not be significantly different. At most, the calculated joint torques would need to be doubled. The model of SAFFiR was posed in three poses to calculate the maximum joint torques required to maintain static poses. Because these were static poses, the center of mass (CoM) of the model needed to remain above the area of the foot on the ground.

- A full squat pose was used to test the knee torque requirement. When stepping up to higher levels, the knee is the joint that requires the largest amounts of torque. In a static scenario, a squat uses a large amount of knee torque. This pose is seen in Figure 3-13A.
- The second pose was the robot kicking its leg out to the side. This pose tested the roll torques necessary in the hips and ankle. This pose is seen in Figure 3-13B.
- To test the pitch torque requirements, the robot was posed with its leg fully extended behind. The upper body was leaning forward to keep the model balanced. This pose is seen in Figure 3-13C.

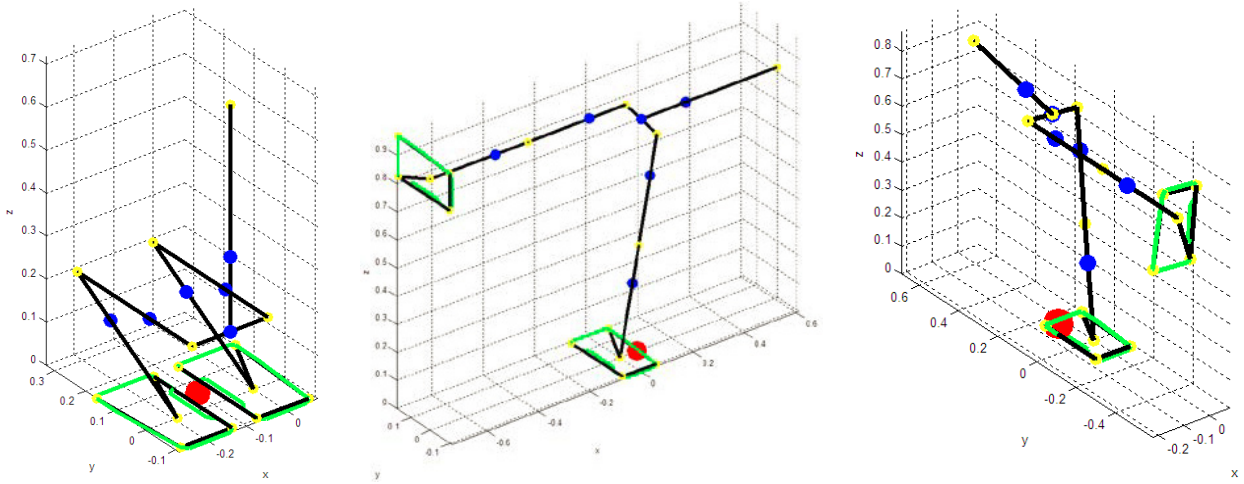

(A) (B) (C)

Figure 3-13: Three static poses to calculate ballpark joint torque requirements. The poses are (A) squatting, (B) kicking its leg to the side, and (C) kicking its leg backwards.

In Figure 3-13, the robot model is shown in black. Its joints are highlighted in yellow, and the body segment CoMs are in blue. The large red marker is the overall robot CoM projected to the plane of the foot. This point must always remain in the boundary of the foot touching the ground. The joint torque magnitude estimates are presented in Table 3-12. The empty cells represent small torque values. The largest torque estimate is bolded for each joint axis.

Table 3-12: Joint torque estimates for static poses

Joint Axis Torque	Squat	Leg Sideways	Leg Backwards
Hip Roll [Nm]		17.5	16.8
Hip Pitch [Nm]			17.5
Knee Pitch [Nm]	25.3		14.2
Ankle Pitch [Nm]	5.8		31.1
Ankle Roll [Nm]		14.0	4.9

These torque estimates are only for the robot posing in static positions. The torque requirements will be larger for dynamic motions. The most concerning joint axis is the knee pitch because it requires a high torque over a large proposed RoM.

4. Lower Body Actuation

The lower body of THOR has 12 DoF (2x 3 DoF hip, 2x 1 DoF knee, and 2x 2 DoF ankle) all driven by linear SEAs. The layout of these actuators determines both the achievable RoM and joint torques. Two of the joints, the hip and ankle, use parallel SEAs to drive their motions. These joints use two actuators working cooperatively to drive 2 DoFs, but also have a more limited RoM due to physical interferences between the actuators and structure. The knee and hip use an inverted straight-line mechanism to achieve large RoMs with consistently high torques possible. The configurations of the actuators were determined using preliminary designs for the structural bodies. This chapter will discuss the design of the THOR linear SEA and its placement throughout the legs to achieve close to the proposed RoM and large joint torques.

4.1. THOR Linear SEA Design

The THOR SEA is fundamentally based on the SAFFiR SEA, but contains many design improvements to increase the output force while decreasing the overall size [31, 32, 42]. The SEA still consists of a stand-alone actuator paired with a titanium compliant spring. A rendering of the hip SEA can be seen in Figure 4-1.

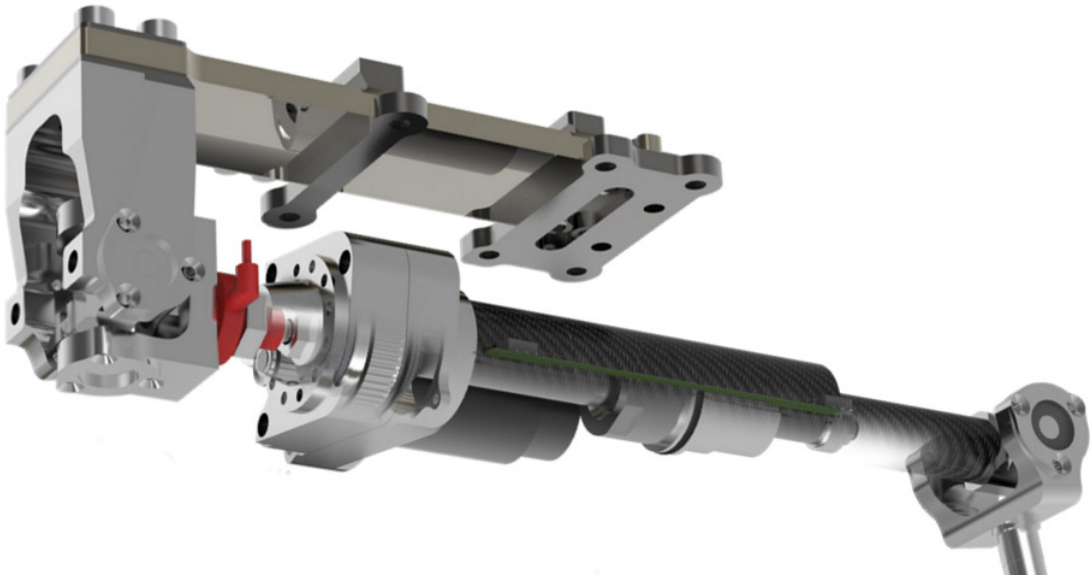

Figure 4-1: THOR series elastic actuator for the hip

The fundamental elements of the stand-alone actuator are still the same. A brushless DC motor rotates a ball screw through a belt drive. There is no linear guide on the ball nut, allowing for free rotation between the ends of the actuator. Instead, the structure of the robot restricts the rotation about the primary axis of the actuator. There are universal joints at both ends of the actuator and a uni-directional load cell measures the actuator force. A comparison of the SAFFiR and THOR actuator parameters is in Table 4-1.

Table 4-1: Comparison of 100W actuators for SAFFiR and THOR

Actuator	SAFFiR Hip	THOR Hip	THOR Ankle
Mass (Actuator Only) [kg]	0.653	0.725	0.792
Mass (Full SEA) [kg]	0.816	0.937	1.004
Fixed Length [m]	0.153	0.111	0.133
Stroke [m]	0.11	0.085	0.142
Continuous Force [N]	300	640	
Peak Force [N]	1,000	2,740	
Maximum Speed [m/s]	0.35	0.198	

The housing of the THOR actuator is shorter than the SAFFiR actuator. The two deep-groove ball bearings are replaced by smaller deep-groove bearings and a pair of needle thrust bearings. The thrust bearings press on the pulley, forcing the actuator loads through the pulley. The small deep-groove bearings align the ball screw radially. This new bearing configuration decreases the overall length of the actuator while allowing for higher loads.

One of the known errors of the SAFFiR actuator was the force measurement. The SAFFiR actuator incorporated the load cell into the cross gimbal of the universal joint, often misaligning the load cell from the actuator axis. This was done to reduce the fixed length of the actuator. The load cells were moved to the end of the housing in the THOR actuator to eliminate that measurement error. Though this added to the fixed length of the actuator, the other design changes accommodated this length increase.

The universal joints on the THOR actuator are designed to match their respective RoMs. The SAFFiR actuators use universal joints that have an exceedingly large RoM to prevent any possible mechanical interference. This design decision made the actuators longer than necessary. The universal joints on THOR were designed to have a RoM that is slightly larger than required to move the leg joint through its RoM. This created shorter universal joints at both ends of the actuators. Additionally, the universal joints for the hip and ankle actuators are not identical. The hip and ankle actuator configurations presented different interference constraints, forcing the different universal joint designs.

The configurable compliant spring also changed from the SAFFiR design. The THOR spring no longer has a continuous range of spring constants, but instead has three defined settings for stiffness. The beam is placed parallel to the actuator axis and is connected through a rigid lever arm. This configuration places the entire beam in uniform bending when the actuator applies forces to the lever. It allows a thinner beam to store larger amounts of energy from the THOR actuators. Finally, the parallel configuration of the compliant spring decreased the packaging

volume of the SEA, simplifying the design of the leg structure. Because THOR has a large RoM in its legs, it was important to use components that were easier to package.

4.2. Ankle Parallel Actuator Configuration

The ankle connects the shin and foot through a 2 DoF (pitch and roll) joint. Because the ankle is at the bottom of the leg, it is important to reduce its weight. This will reduce the overall inertia of the leg relative to the hip, making it easier to swing during walking. Additionally, the ankle actuators should not require a large footprint because they are the most likely components to collide between the legs. The ankle actuation style was chosen from three configurations.

- Parallel actuation with linear SEAs: This configuration is similar to the ankle on SAFFiR [18]. The potential joint torques are larger due to two actuators cooperatively pushing on the same DoF, but the overall RoM could be smaller. Additionally, the mechanical advantage will decrease at the ends of the RoM. The majority of the weight of the linear SEAs is towards the top of the shin, moving mass away from the foot.
- Series actuation with an actuator in the ankle gimbal: This configuration is similar to the ankle on CHARLI [9]. A rotary SEA would be incorporated into the cross gimbal of the ankle to directly drive the final DoF of the leg, making each DoF in the ankle independent. While the RoM could increase, it would also decrease the maximum joint torque for each DoF when compared against the parallel actuation. This configuration would also require designing a new rotary SEA with similar features to the linear SEA.
- Series actuation using a Clemens joint: Similar to the option above, the ankle would be driven using a pair of rotary SEAs. Instead of incorporating one actuator into the cross gimbal, both actuators would be placed on the shin. This would move the mass higher on the leg. One of the SEAs would connect to the ankle roll joint through a Clemens linkage [43]. The Clemens linkage is a constant velocity linkage that transmits torque well. This configuration would require designing both the rotary SEA and the Clemens linkage.

Because of the success using parallel actuation on SAFFiR, THOR was designed with parallel linear SEAs in its ankle. The ankle actuator decision was coupled with the designs of the hip and knee joints. Both the hip and ankle have parallel linear actuators, so there would be fewer unique components to design and fabricate if both used the same type of actuators.

The large RoM requirement of the knee and ankle pitch decided the locations of the ankle actuators. In order to accommodate large knee bends, the shin actuator attachments could not be on the back of the shin. That would cause an interference with the thigh as the knee bends. Similarly, placing the foot actuator attachment towards the front of the foot would have created interference problems when the ankle pitched in the negative direction. The initial layout of the linear actuators in the ankle can be seen in Figure 4-2.

Stepping up to taller objects and kneeling both require a large amount of negative ankle pitch. Because people have toes and are good at controlling their own bodies, they are able to perform these tasks with relative ease. However, a robot is not as capable as the average person. Having a larger amount of negative pitch at the ankle would allow the robot to shift its weight around easier while high stepping and kneeling. The RoM videos used a larger amount of positive pitch than negative pitch, however this happened during less critical motions. The ankle pitch RoM limits were biased from -45° and 45° to -55° and 35° to help the more-difficult walking motions.

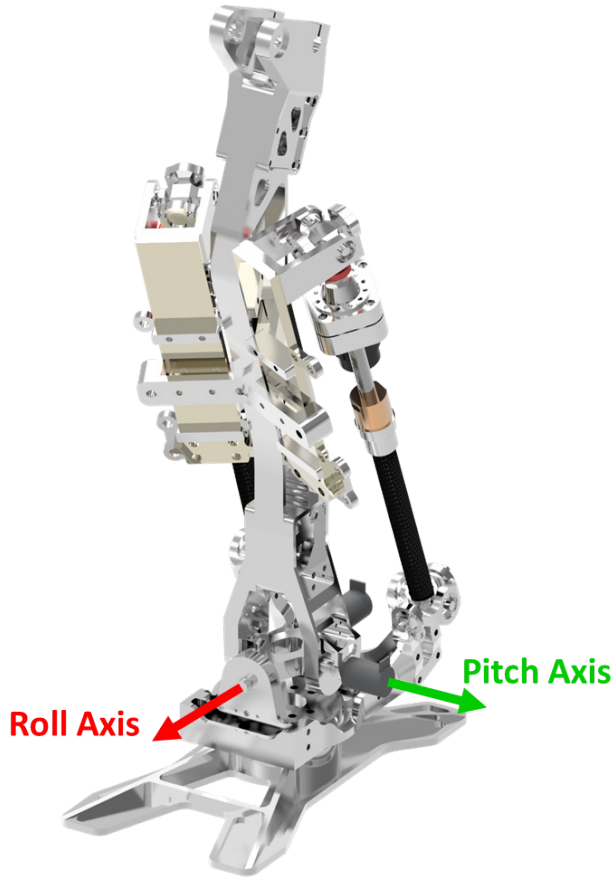

Figure 4-2: Initial ankle actuator placement

With the general ankle actuator configuration determined, the exact location of each actuator end needed to be calculated. Rough models of the shin and foot were used to check for interferences throughout the RoM. Several factors were used to determine the end locations.

- The joint torques needed to be high throughout the RoM, especially about the pitch axis. A static model of SAFFiR would have needed 32 [Nm] to kick its leg backwards. THOR is larger and heavier than SAFFiR so it will need more torque to hold the same pose.
- There needed to be clearance for the shin, actuator, and foot parts to not intersect as the robot moved. If the parts interfered somewhere in the ankle RoM, then it would not a feasible set of actuator end locations. Additionally, there needed to be some extra space

between parts for wires. The wire routing for THOR was not determined until a physical robot was built.

- The universal joint angles needed to be attainable. Traditional universal joints are capable of very large RoMs, but can grow large when a high RoM is needed. The universal joints on THOR are designed to achieve the necessary RoM and not much more, reducing their length and size [42].
- The outside profile of the shin actuators determines how far inward a leg may swing while walking. The SEAs are the first components to collide when the legs come together. Even if the design and manufacture of the associated parts was difficult, it was important to place the actuators closer to the center of the shin.

With these criteria in mind, the ends of the actuator were iteratively placed on the shin and foot. The main concern with the foot end of the actuator was interference between the shin and the actuator universal joint as the ankle moved through its RoM. Because the shin attachment was far away from the ankle, interference with that universal joint was not a concern. The most important factor in the shin attachment placement was the outer profile of the shin. Even though the design was complicated, the shin attachments were moved closer to the middle of the shin than the foot attachments to the center of the foot. The final ankle actuator configuration is seen in Figure 4-3. Even though it is subtle, the actuators are not vertical when viewed from the back.

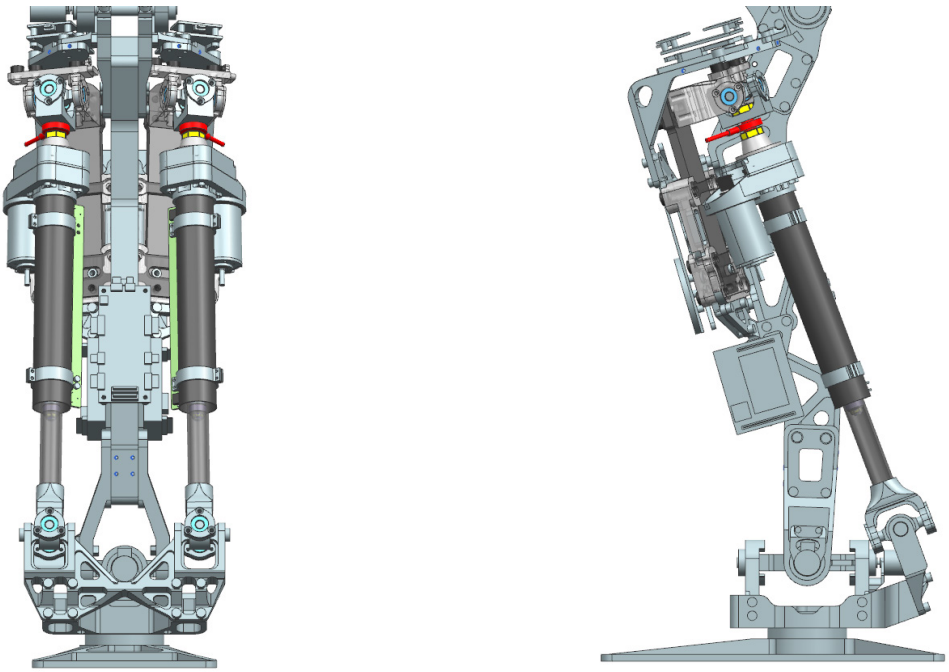

(A) (B)

Figure 4-3: Views of the final ankle actuators from the (A) back and (B) side

The actuators are capable of producing large amounts of joint torque in their nominal configurations. As the joint moves, the mechanical advantage for each actuator changes from the

nominal positions. Figure 4-4 shows the maximum possible torques for pitch and roll over the ankle RoM using a pair of 2000 [N] actuators. The torques are calculated using actuators at peak force output: both pushing to produce a pitch torque, or one pushing and the other pulling for roll torque. It is not possible to simultaneously produce the maximum pitch and roll torques.

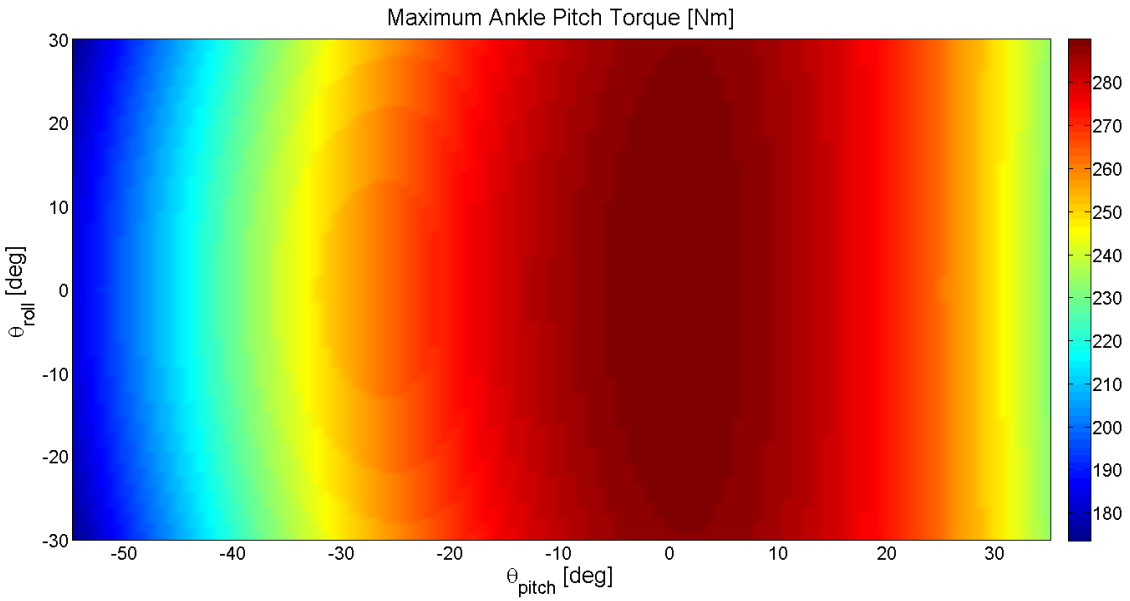

(A)

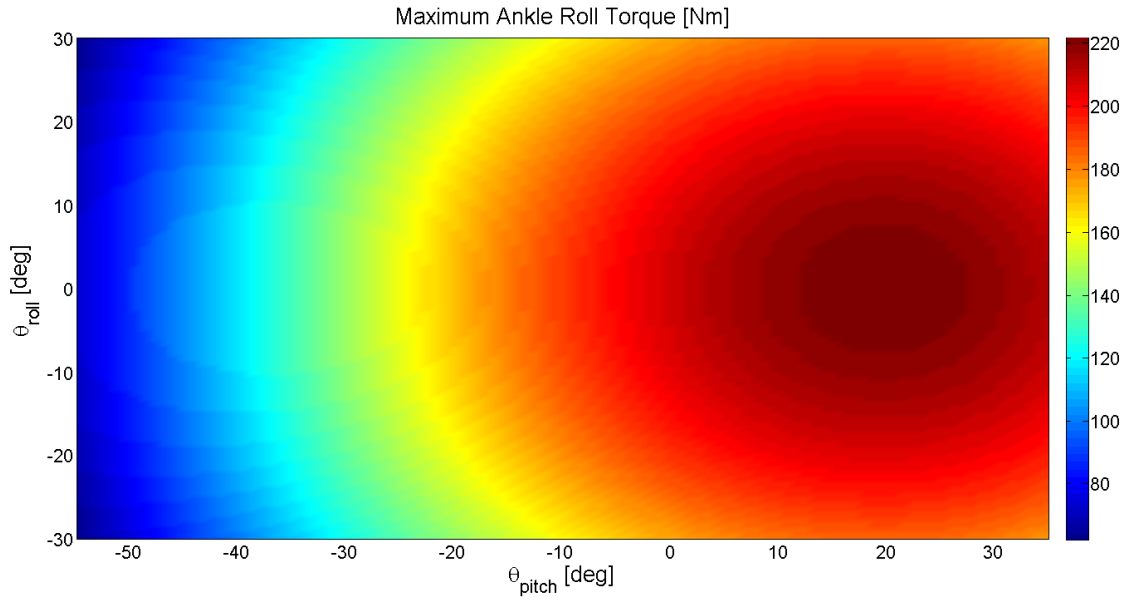

(B)

Figure 4-4: Maximum possible ankle torques for both (A) pitch and (B) roll

The torque outputs of the ankle are mostly affected by pitch motions. A pitch motion of the ankle induces a large change to the mechanical advantage. Though roll motions affect the maximum

possible torque, they do not change the mechanical advantage as much as a pitch motion. Due to symmetry in the ankle design, the maximum pitch and roll torques are the same for a positive and negative roll motion of the same magnitude. Table 4-2 lists the largest and smallest maximum possible torques for both pitch and roll.

Table 4-2: Summary of the maximum torque range for the ankle joints

Joint Axis	Smallest Max Torque [Nm]	Largest Max Torque [Nm]
Ankle Pitch	173.47	289.96
Ankle Roll	62.21	221.53

The ankle pitch is capable of large torques throughout its RoM. Compared against the estimated torques from Table 3-12, the smallest maximum torque in the ankle pitch is six times larger. Likewise, the smallest maximum torque is five times larger for ankle roll. The smallest maximum torques occur at extreme pitch and roll position of the ankle joint, which does not correspond to the worst static positions from the joint torque calculations from Section 3.5. This ankle actuator configuration should provide enough joint torque for both pitch and roll.

The actuator placement is a compromise between torque, length, and interference over the RoM. Moving the foot actuator attachments farther from the ankle joint would increase the possible torques throughout the RoM, but it would increase the necessary actuator length range and introduce more part interferences at the ends of the RoM. Though the part interferences drove the foot actuator attachment locations, the actuator length range was still investigated. The necessary length of the outside ankle actuator over the ankle RoM is shown in Figure 4-5.

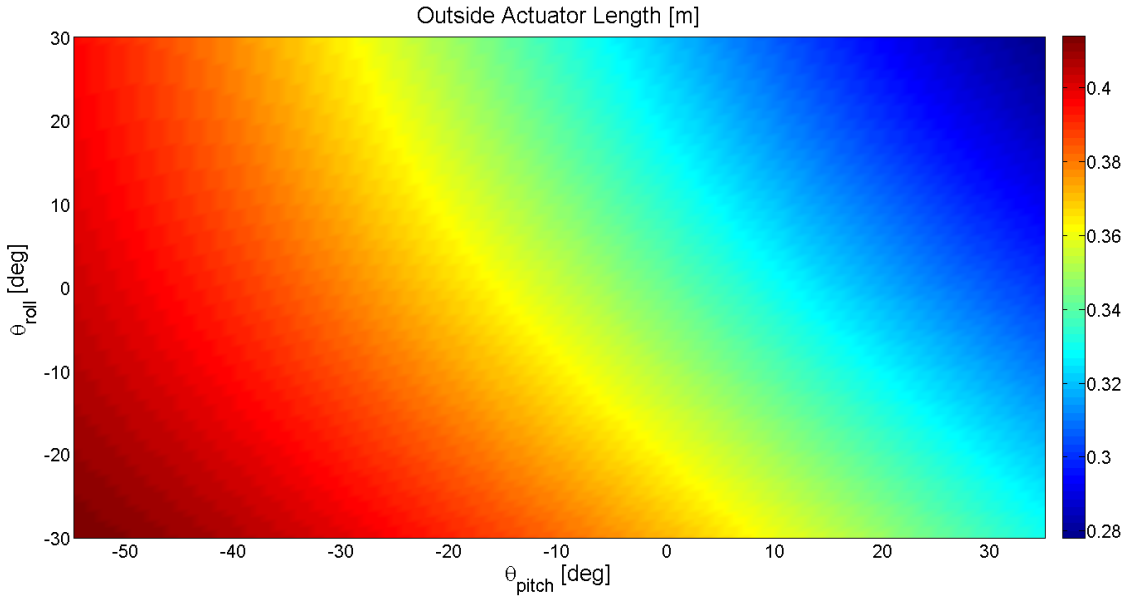

Figure 4-5: Length of the outside ankle actuator in [m] over the full RoM

Because of the symmetric design of the ankle, the outside and inside actuators have the same length ranges. The inside actuator lengths over the ankle RoM can be found by negating the roll angle axis of Figure 4-5. The actuator length range can be found in Table 4-3 .

Table 4-3: Lengths for the outside ankle actuator

Length Range [m]	0.2780 to 0.4136
Minimum Stroke [m]	0.1356
Maximum Fixed Length [m]	0.1423

The two other lengths presented in Table 4-3, the minimum stroke and maximum fixed length, are more important than the length range. The minimum stroke, the difference between the ends of the length range, dictated the length of ball screw needed to achieve the full RoM. The fixed length is the length of an actuator with no stroke, representing the length of the universal joints, load cell, and transmission elements. The SAFFiR actuators have a fixed length of 0.153 [m] which would not fit in THOR.

The THOR actuators have universal joints on both ends. These joints help to reduce backlash and friction in the SEAs, but they increase the fixed length of the actuators if improperly designed. The SEAs on SAFFiR were designed with universal joints that had an exceedingly large RoM. The universal joints on both ends of the actuator were capable of reaching ±90° of motion without mechanical interferences. This added unnecessary length to the joints to accommodate that RoM. The THOR SEAs were designed to match the necessary RoM at each joint [42]. The universal joint RoM for the shin outside actuator attachment is shown in Figure 4-6. These rotation angles were calculated using the same method as the SAFFiR universal joint angles [31].

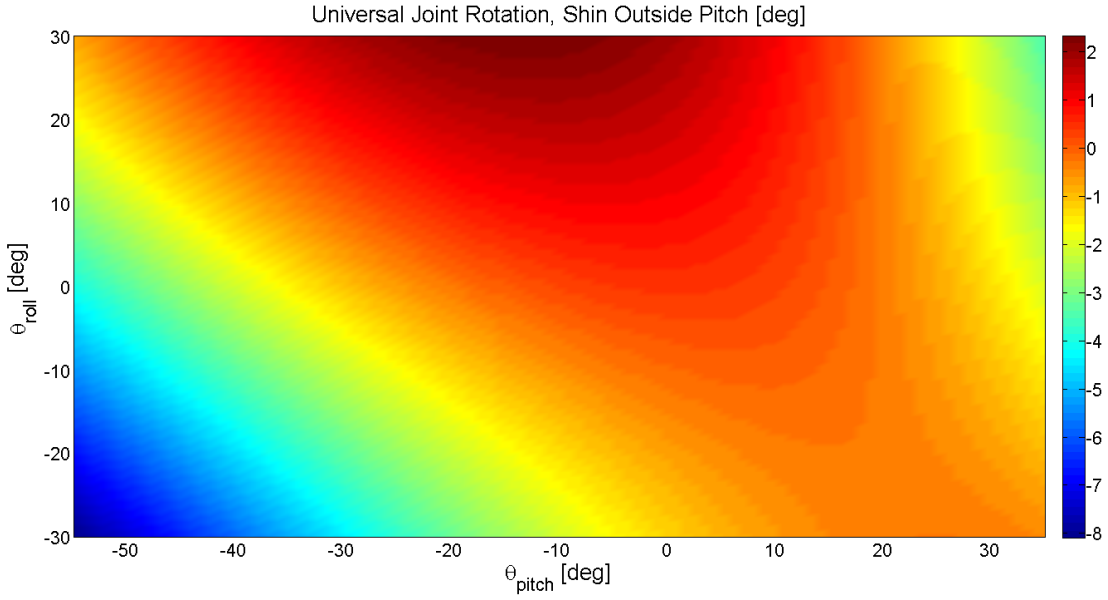

(A)

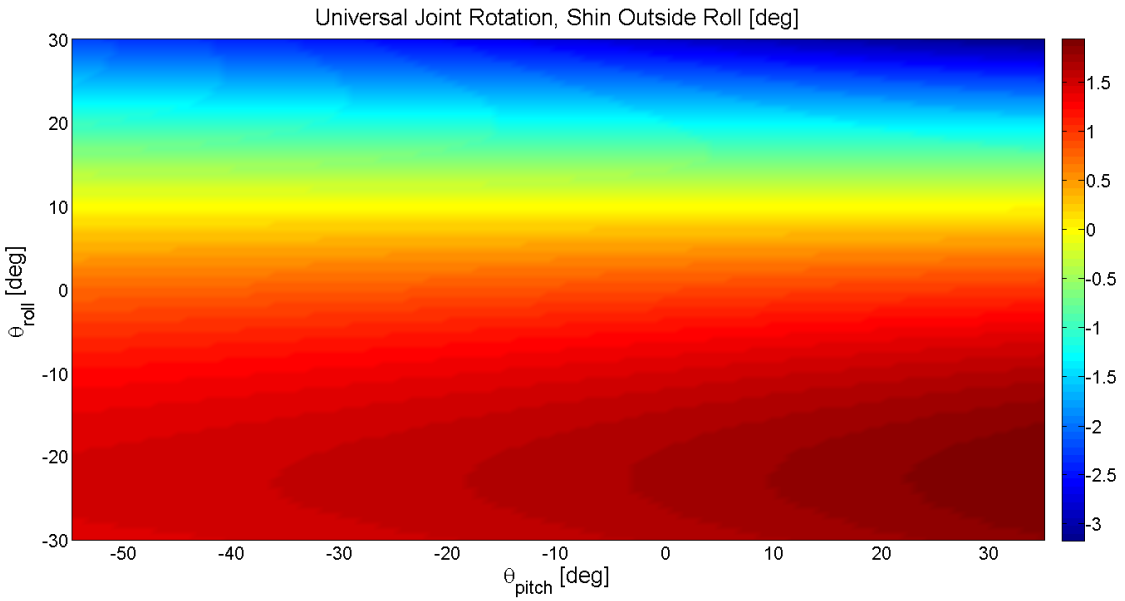

(B)

Figure 4-6: Universal joint rotations of the outside actuator at the shin for (A) pitch and (B) roll. The pitch axis is attached to the shin of the robot, and the roll axis is attached to the actuator.

The shin attachment universal joints are connected to the configurable compliant spring. This interface, shown in Figure 4-7, is identical for every compliant spring in the lower body. The pitch axis is embedded in the part attached to the configurable spring and the roll axis is attached to the actuator. The universal joint RoM necessary for the ankle actuators is smaller than for the hip actuators, which will be discussed in Section 4.3.

Figure 4-7: Universal joint attaching to the configurable compliant spring

The foot attachment universal joints are not identical to other universal joints on THOR. As seen in Figure 4-8, the foot universal joints require a much larger RoM than the shin universal joints. In addition to a larger RoM, the foot universal joint needed to fit in a small package that would not interfere with the shin over the ankle RoM.

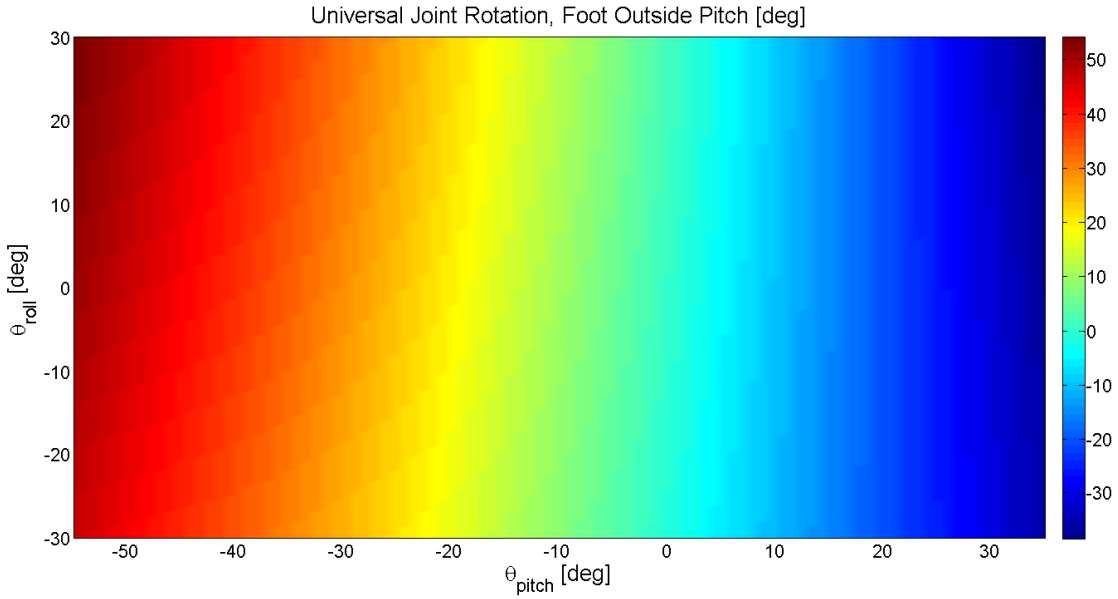

(A)

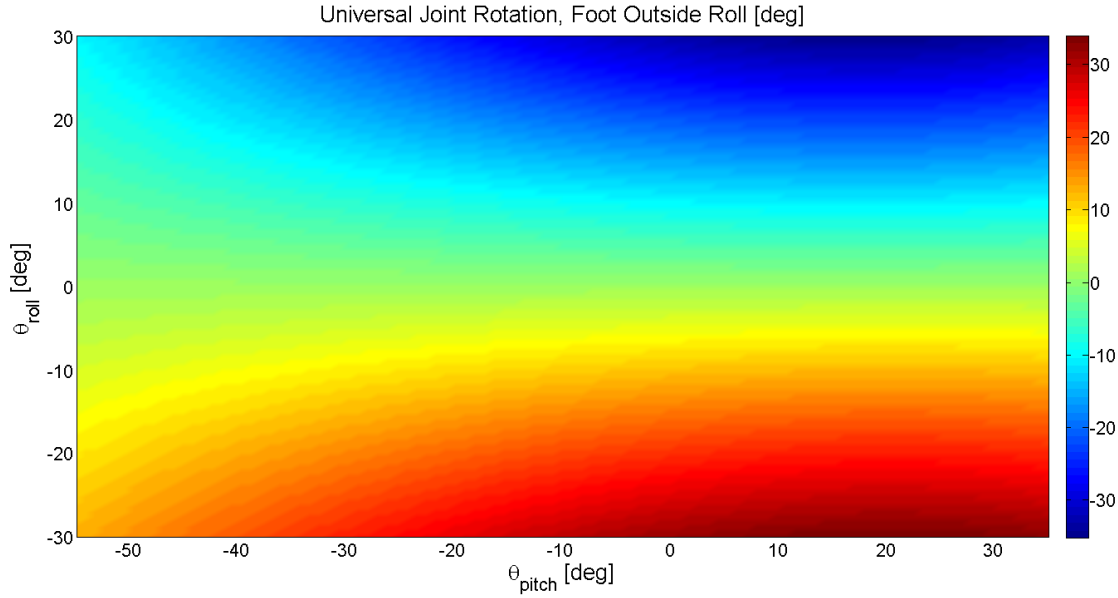

(B)

Figure 4-8: Universal joint rotations of the outside actuator at the foot for (A) pitch and (B) roll. The pitch axis is attached to the foot of the robot, and the roll axis is attached to the actuator.

Because it requires a larger RoM, the pitch axis of the foot universal joint is attached to the foot, while the roll axis is attached to the actuator. Treating the foot as a fixed body, it is easier to avoid interferences with the cross gimbal than the other side of the universal joint. An image of the foot actuator universal joint can be seen in Figure 4-9. A summary of the necessary universal joint RoM for the ankle actuators can be found in Table 4-4.

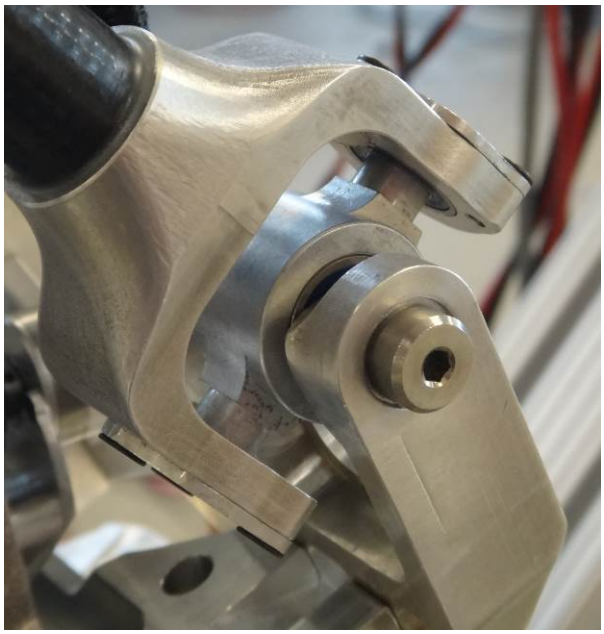

Figure 4-9: Universal joint attaching to the foot

This universal joint was designed to specifically meet the RoM requirements of the foot universal joint while not interfering with the shin at the extreme ends of the ankle RoM. For example, the universal joint requires 54.2° of pitch motion. The foot universal joint is designed to have 56° of motion before its two ends collide with one another.

Table 4-4: Universal joint RoMs for the outside ankle actuator

Shin Universal Joint Pitch [deg]	-8.1 to 2.4
Shin Universal Joint Roll [deg]	-2.0 to 3.2
Foot Universal Joint Pitch [deg]	-38.5 to 54.2
Foot Universal Joint Roll [deg]	-33.9 to 35.3

4.3. Hip Parallel Actuator Configuration

Connecting the torso to the thigh, the hip is the most complicated joint on THOR. The hip is a 3 DoF joint that requires that the yaw, roll, and pitch axes all intersect at the same location. This joint also has a large desired RoM, especially for the pitch DoF. The desired RoM for hip pitch could not be designed quickly with a large amount of torque throughout the motion, so the hip was split into two independent joints with the pitch isolated from the yaw and roll. Because it is

the last DoF in the hip joint, the hip pitch was designed as a part of the thigh. All 3 DoFs still intersect at the same point, but only the yaw and roll use parallel linear SEAs [44].

The intermediate body between the torso and thigh, the coxa is designed to align the three hip axes and to isolate the pitch mechanism from the yaw and roll actuators. This body is part of the cross gimbal for the spherical hip joint. All three hip actuators act on the coxa to drive their respective DoFs. Several possible SEA configurations were preliminarily designed to connect the torso to the coxa. These preliminary designs were weighed based on their size, torque potential, RoM achievable, design difficulty, and manufacturability. Unlike the other leg segments, four actuators needed to be placed in the torso to drive both the left and right hip joints.

- Fully symmetric actuators: This design would use two actuators that do not cross the mid-sagittal plane of the robot and are equally spaced from the hip joint. This is the easiest configuration to design and implement, but it is also the tallest and most intertwined with the final design of the stand-alone actuator. The vertical angle of the actuators depends on the fixed length. A steeper vertical angle would reduce the amount of yaw torque achievable. A concept of this design is in Figure 4-10A with the red lines representing the actuators.
- Slightly crossing actuators: This design would place all four actuators slightly crossing the mid-sagittal plane at their universal joints. Doing this would decrease the overall package size of the torso while increasing the design and manufacture difficulty. The inverse kinematics and statics of the right and left hips would no longer be the same. Because this configuration is nearly symmetric, the two hips could have the same RoM.
- Majorly crossing actuators: This design would have all four actuators crossing significantly with the torso-end of the left hip actuators on the right side of THOR, and vice versa. This configuration would have the smallest overall profile, but it would require the most complicated design and manufacture to execute. The crossing portions of the actuators would be the carbon fiber tubes, which are the narrowest parts of the actuators. This configuration would not guarantee the same RoM for both legs due to interference constraints, but the flatter actuators would increase the potential yaw torques. A concept of this design is in Figure 4-10B.
- Rotary actuation: This design would use at least one rotary actuator to drive the two hip DoFs. Similar to robots like SAFFiR, the yaw joint would use a rotary actuator to achieve the full desired RoM with a constant torque output. The roll joint would use either a linear or rotary actuator. This would lose the benefits of parallel actuation for a simpler packaging. This design would also require the design of a torque-sensing rotary SEA, which, as discussed in Section 4.2, eliminated this design.

Each of the potential designs had both benefits and drawbacks. On top of placing the actuators in each design, the configurable compliant spring also needed to be packaged alongside each

actuator. This challenge would add much larger complications to the two crossing configurations, especially because many of the compliant interfaces would be complicated, non-orthogonal parts. The fully symmetric design was chosen because it was the fastest to design and manufacture with a symmetric RoM for the two legs.

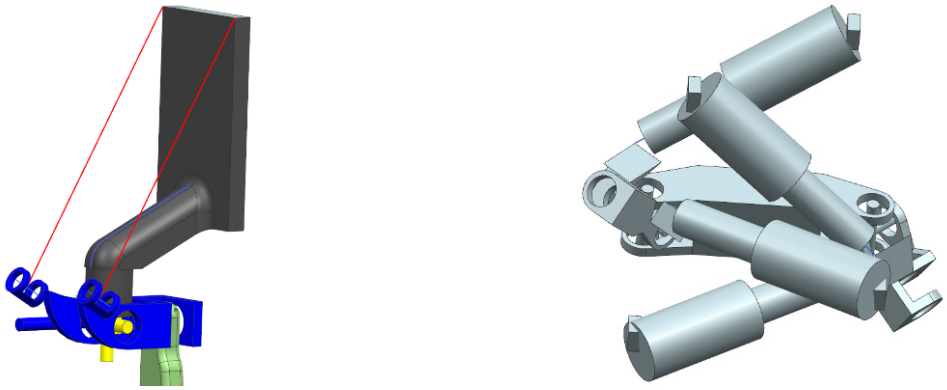

(A) (B)

Figure 4-10: Initial concepts for the (A) fully symmetric and (B) majorly crossing actuators

The fully symmetric design has two main drawbacks. First, this design requires a large amount of vertical space to successfully implement. Second, the yaw torque produced is low compared to the roll torque. In an ideal situation, the actuators would be horizontal to maximize the torque produced in both roll and yaw. However, this would require actuators with extremely small fixed lengths and short strokes or wide hips. To make the actuators fit within the design, the actuators need to be angled above the transverse plane of the robot. This will reduce the yaw torque, but will allow for actuators with longer fixed lengths. Widening the hips with angled actuators could create larger yaw torque outputs, but it would also increase the roll torque demand. Additionally, wider hips would increase the difficulty of climbing into a vehicle, walking through a doorway, and ascending a ladder.

The placement of the actuator ends was an iterative process for the hip as the design of the joint was done in conjunction with the design of the actuator. The maximum fixed length and universal joint rotations change as the ends of the actuators are moved around the torso and coxa. For each configuration iteration, the fixed lengths and universal joint rotations were compared against the actuator design to determine if a design was feasible. Using this criterion as well as the joint torques, the ends of the actuators were placed. A rendering of the final actuator placement is in Figure 4-11.

The largest challenge in placing the actuators was achieving the large yaw RoM while remaining within the fixed length constraint of the actuator. The desired yaw RoM is skewed heavily in the outward direction. With both actuators symmetrically placed around the joint, the actuators had largely different needs for stroke. Reducing the yaw RoM from the desired -20° and 60° to -20°

and 45° mitigated some of the concerns for the stroke differences. The 60° in the desired RoM was only found in standing from a lying position, which is not explicitly required for the challenge tasks.

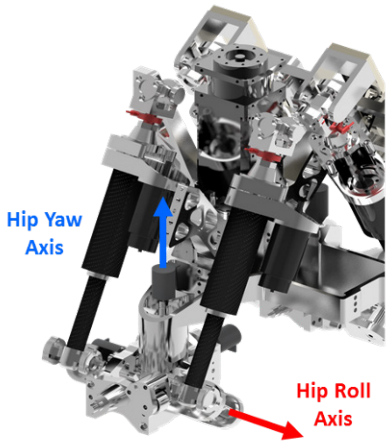

Figure 4-11: Actuator placement for the hip yaw and roll

Based on the joint architectures, the hip roll is analogous to the ankle pitch. Likewise, the hip yaw is analogous to the ankle roll. THOR is not able to produce as much torque at the hip as it can at the ankle. The hip actuators push on a shorter lever arm when driving the coxa than the lever for the ankle actuators. As stated earlier, the actuators are angled relative to the transversal plane, decreasing the potential yaw torque. The initial torque investigation showed that THOR requires less torque for the hips than ankles, as seen in Table 3-12. The maximum possible torques for both hip yaw and roll can be seen in Figure 4-12.

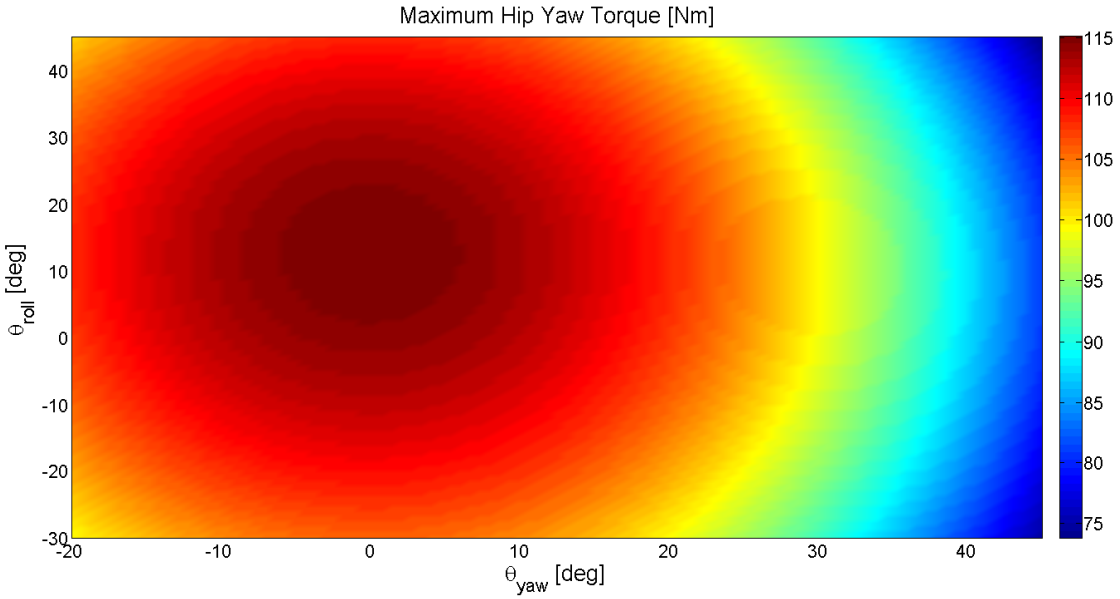

(A)

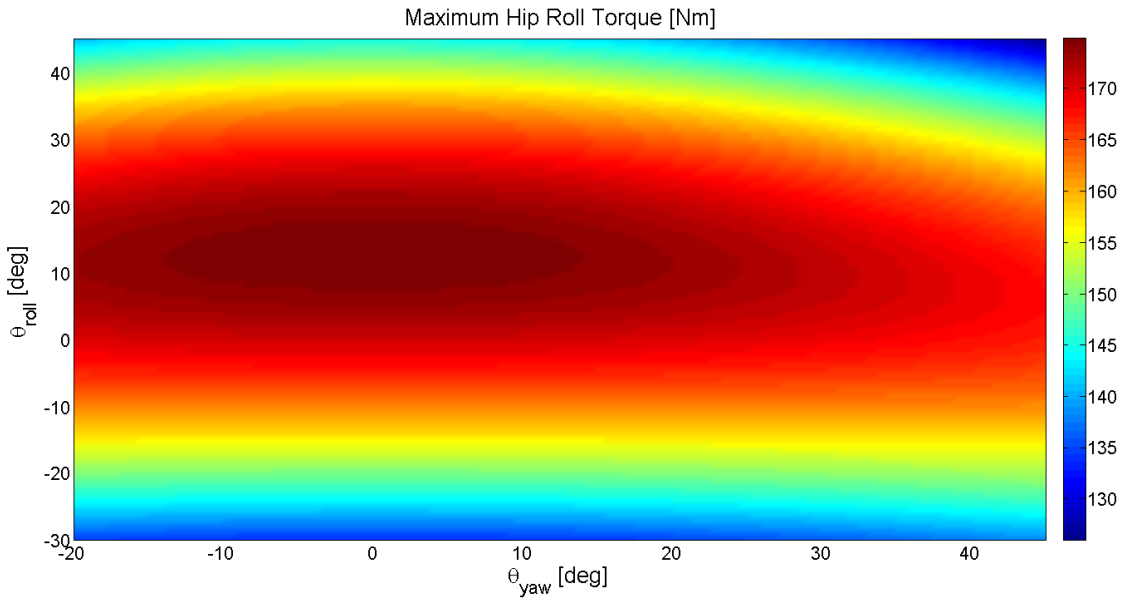

(B)

Figure 4-12: Maximum possible hip torques for both (A) yaw and (B) roll

Based on the design of the joint, the yaw and roll torques are symmetric about 0° of yaw rotation. While the maximum yaw torque varies with both yaw and roll, the maximum possible roll torque is relatively independent from the joint yaw angle. Both maximum torques occur at 12.5° of hip roll. This is due to the layout of the actuators while trying to keep the overall profile of the torso as low as possible. A table of the maximum torque range can be found in Table 4-5.

Table 4-5: Summary of the maximum torque range for the hip yaw and roll

Joint Axis	Smallest Max Torque [Nm]	Largest Max Torque [Nm]
Hip Yaw	73.74	115.02
Hip Roll	125.94	174.72

Compared against the calculated torque estimate from Table 3-12, THOR should have sufficient amounts of roll torque to hold the static poses. Of all the joint axes, the hip roll is one of the most likely to need extra torque during dynamic motions. One feature of the SAFFiR actuators was that the 100 [W] motors could be replaced with 200 [W] motors for increased peak and continuous forces [31]. This feature is still present in the THOR actuators [42]. Replacing the motors with 200 [W] versions would increase the torque output of the joint by approximately 1.5 times, making the smallest maximum roll torque 188.91 [Nm].

The biggest limiting factor in the hip actuator placement is the lengths of the two actuators. The actuator placement in the hip was closely coupled with the design of the actuator. This was due to the customized universal joints designed for each joint. The actuator lengths in the final placement are shown in Figure 4-13, and a summary of the lengths can be found in Table 4-6.

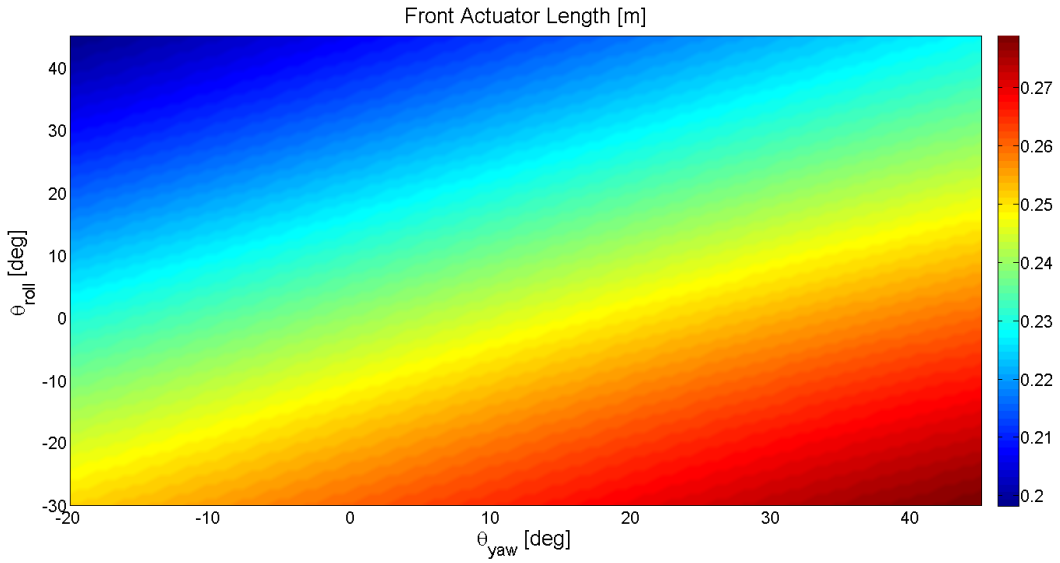

(A)

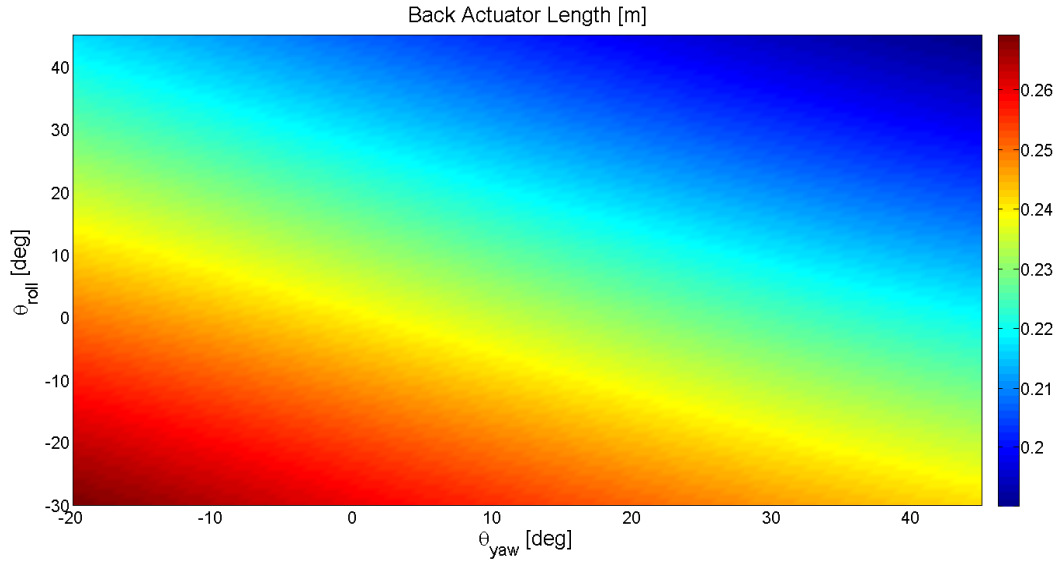

(B)

Figure 4-13: Lengths of the (A) front and (B) back actuators

Table 4-6: Lengths for the hip actuators

Hip Actuator	Front Actuator	Back Actuator
Length Range [m]	0.1982 to 0.2787	0.1901 to 0.2691
Minimum Stroke [m]	0.0805	0.079
Maximum Fixed Length [m]	0.1176	0.1112

As shown in Table 4-6 and Table 4-3, the hip actuators required a shorter fixed length than the ankle actuators. Shifting the ends of the actuators around a local area did not change the necessary RoM of the universal joints significantly, so the universal joints were not redesigned

for each configuration iteration. The initial design of the actuators had a fixed length of 0.107 [m] with reduced RoM universal joints. This would allow both actuators to use the same ball screw with a 2.0 [mm] buffer at both ends of the actuator travel for safety purposes.

The compliant spring attachments on the torso are identical to those on the shin. This universal joint, seen in Figure 4-7, was designed from the necessary RoM for the hip. Because of the asymmetric design, the universal joints of the front and back actuators had different RoM requirements. The pitch and roll requirements for these universal joints are shown in Figure 4-14.

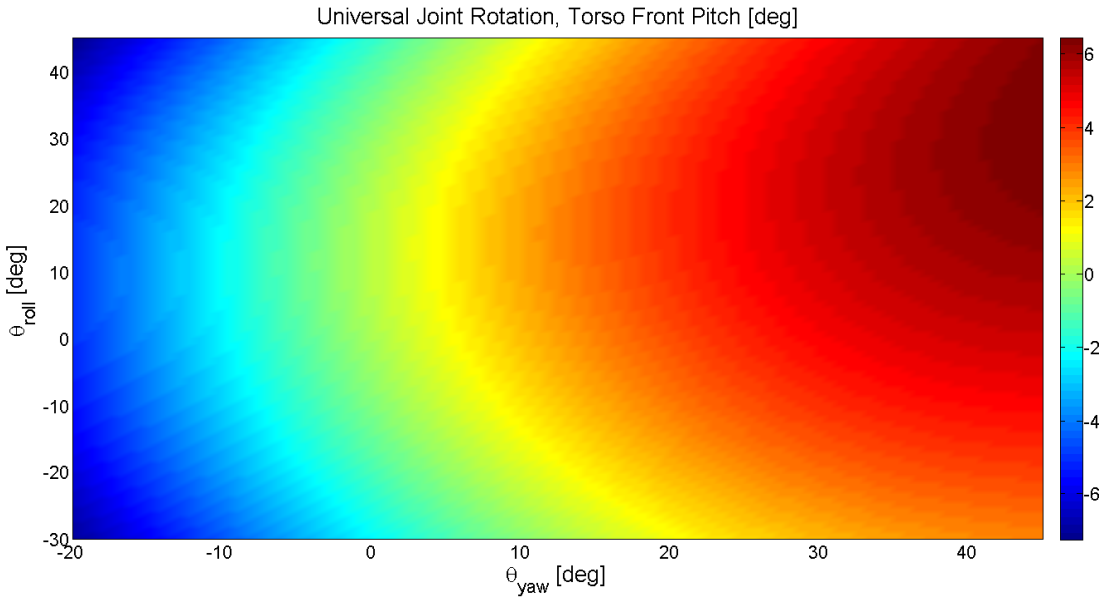

(A)

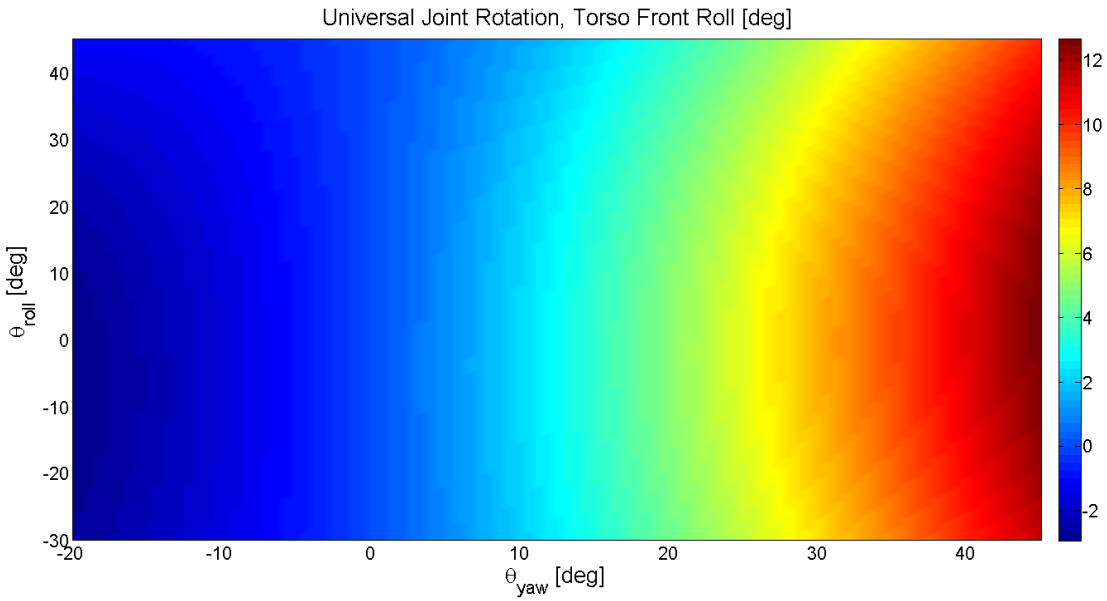

(B)

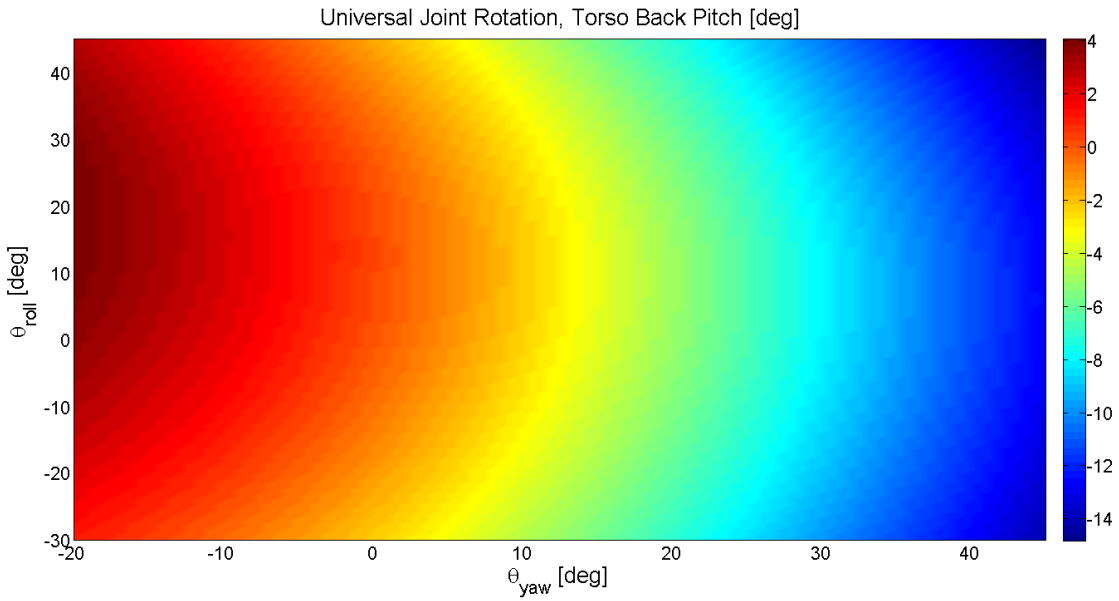

(C)

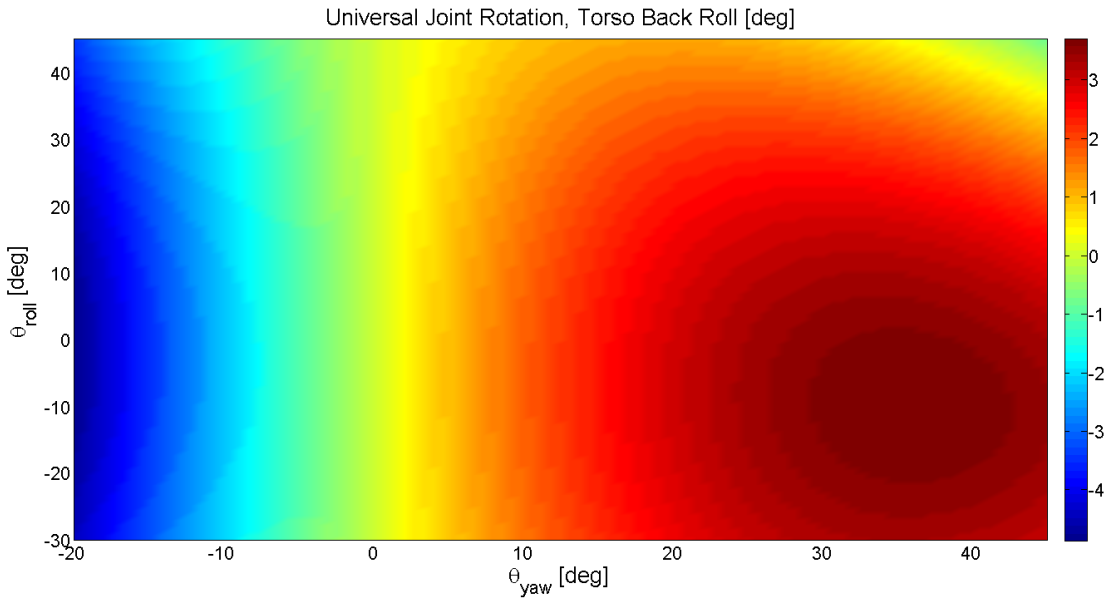

(D)

Figure 4-14: Universal joint rotations for the torso side of the hip actuators. The (A) front pitch and (C) back pitch axes are connected to the torso while the (B) front roll and (D) back roll axes are attached to the actuators.

The pitch and roll axes are defined the same as the pitch and roll axes from the shin universal joints. Both torso universal joints require a larger RoM than the shin universal joints. Because the front universal joint needs to reach the ends of its RoM nearly simultaneously, it was easiest to design the joints to achieve maximum roll and pitch without interferences. Additionally, the joints were designed to be symmetric so that they could be used for both right and left legs [42]. Even though this universal joint was designed for the torso, it is used throughout the robot at

every compliant beam interface to reduce the number of unique parts on THOR. The required RoM for the torso universal joints can be found in Table 4-7.

The universal joints on the coxa need a much larger RoM to accommodate the full actuator movement. Their rotations are larger than the torso universal joints because they are much closer to the hip joint. Graphs of the RoM requirements for the coxa universal joints are in Figure 4-15.

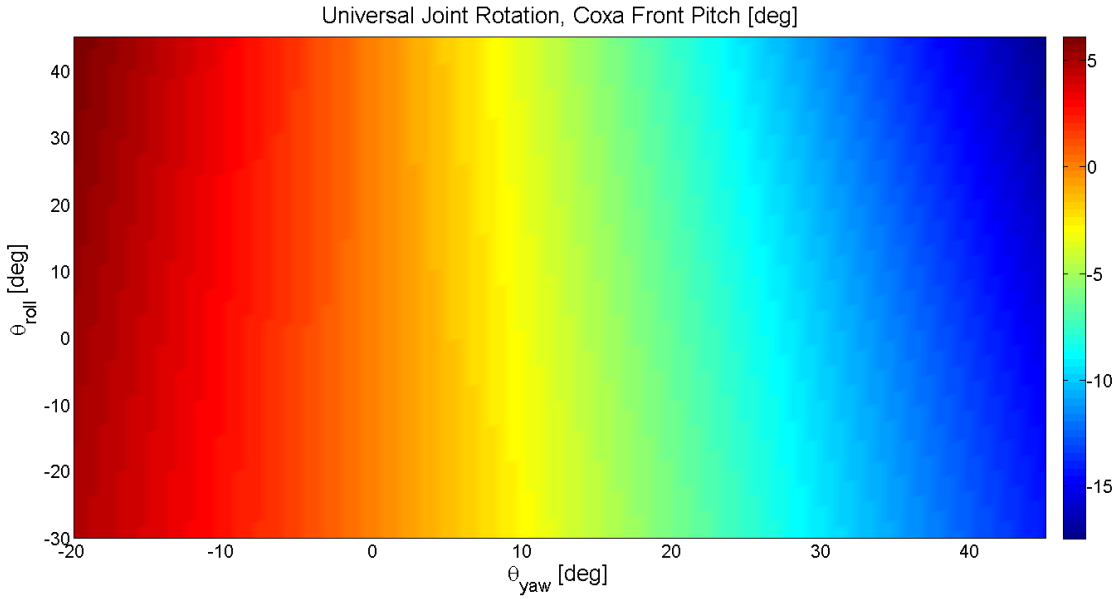

(A)

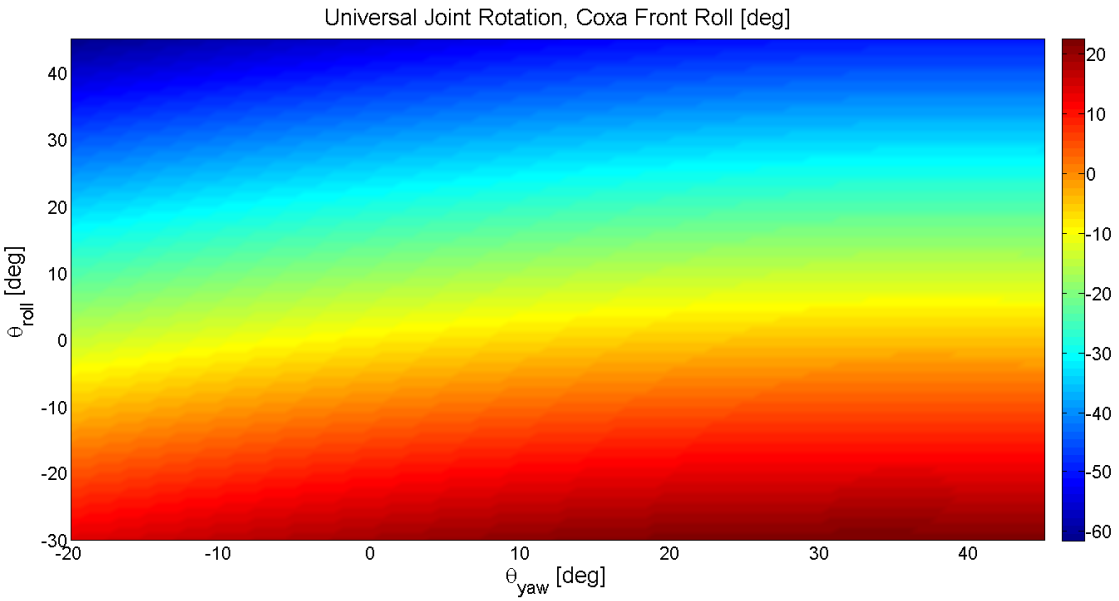

(B)

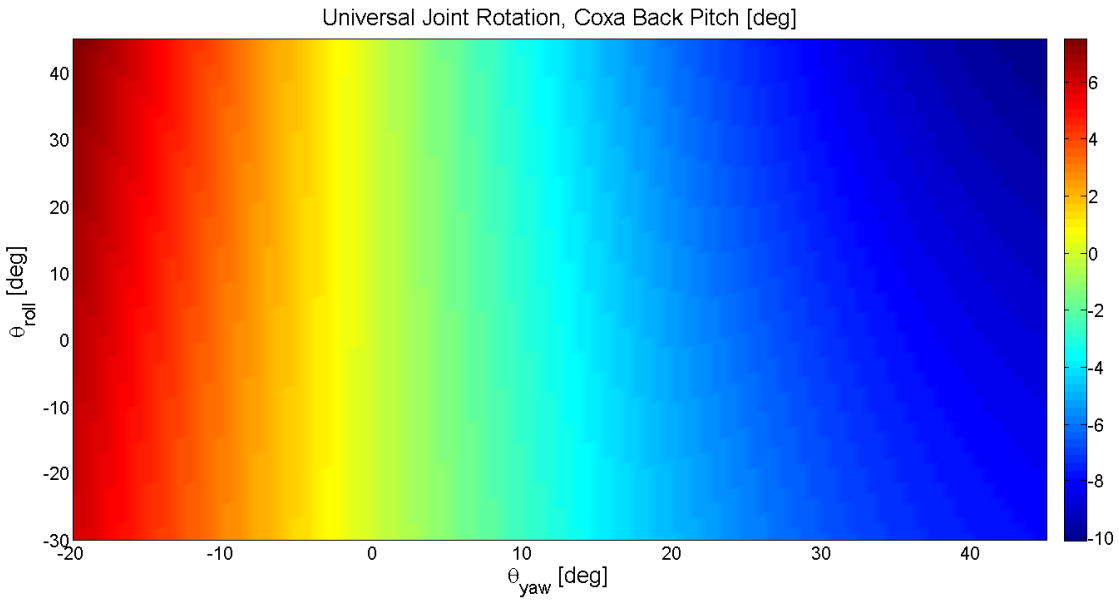

(C)

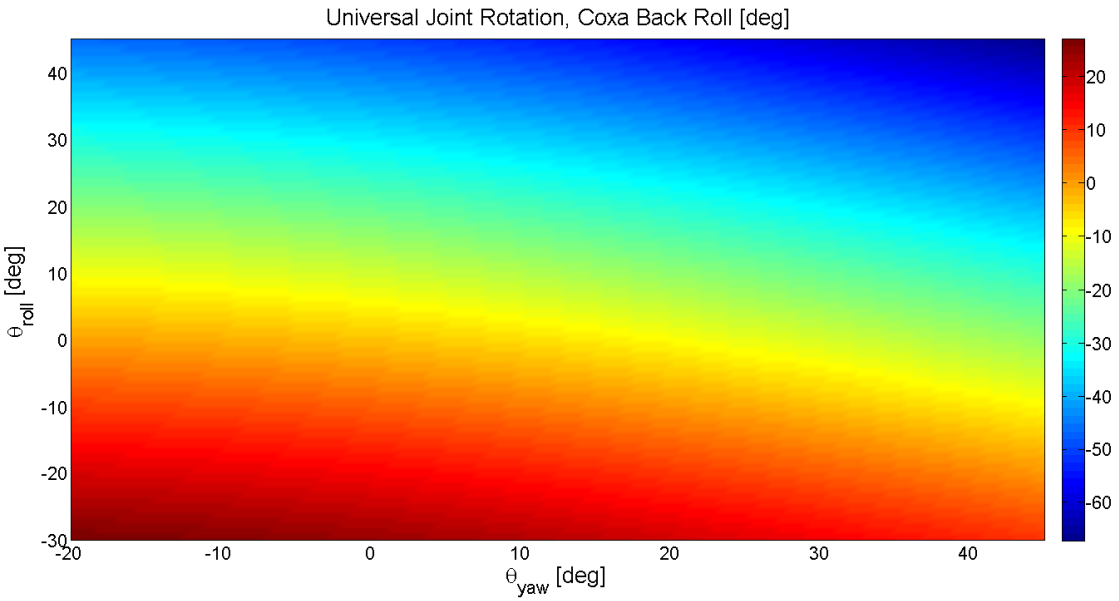

(D)

Figure 4-15: Universal joint rotations for the coxa side of the hip actuators. The (A) front pitch and (C) back pitch axes are connected to the coxa while the (B) front roll and (D) back roll axes are attached to the actuators.

Both of the coxa universal joints should be able to reach any combination of their maximum and minimum pitch and roll angles simultaneously. Due to the large RoM, the cross gimbal of the universal joint is shaped like a capital "Y" to prevent interference between the two ends of the joint. This design can be seen in Figure 4-16. By placing one of the axes of the cross gimbal in single support, this joint can achieve greater than its necessary RoM without any part interferences. Additionally, this design decreases the outer profile of THOR by not placing

bearings and supports farther from the sagittal plane. This configuration for the cross gimbal presents a new failure mode that is not possible with traditional universal joints. If the portion of the cross gimbal in single support axially aligns with the ball screw axis, the actuator would lose command authority over the joint. The motor would freely spin as the arm of the joint rotated in its bearings. One critical design consideration was that the single support portion of the cross gimbal could not align with the ball screw axis over the full RoM of the hip joint.

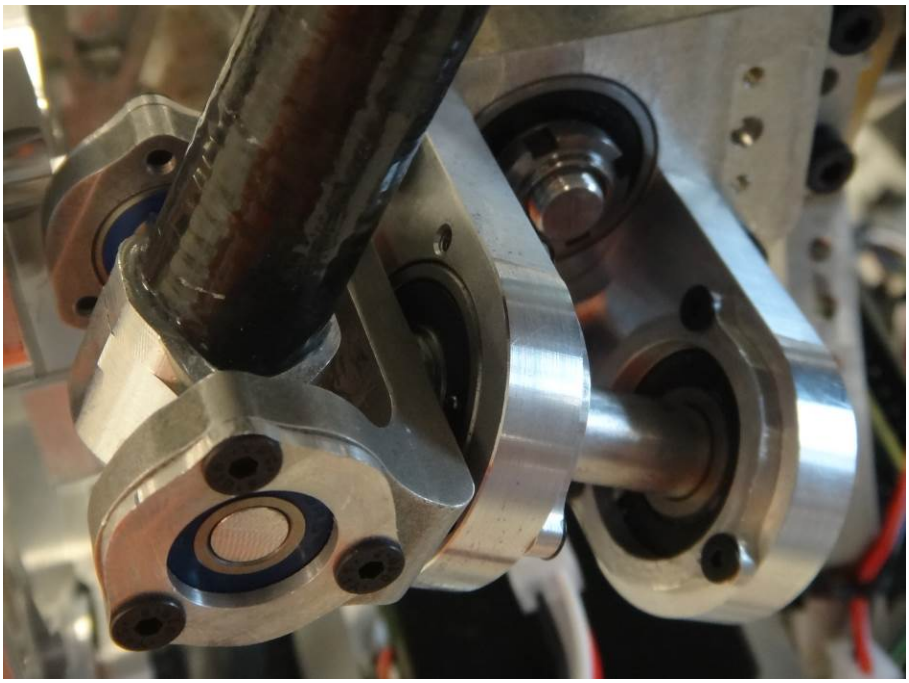

Figure 4-16: Universal joint on the coxa for the back hip actuator

As shown in Table 4-7, the coxa universal joints require a skewed amount of roll RoM. The pitch axis of the joint could not be parallel to the transversal plane because of part interferences, but it needed to be as close as possible to horizontal to still accommodate the RoM. This was especially important for the back actuator universal joint, since it needs a larger RoM than the front actuator. The pitch axis of the universal joint is mounted at a nominal angle of 93.5° between the actuator and cross gimbal. This would leave a 160.8° angle between the ball screw and cross gimbal when the universal joint is at the end of its RoM.

Table 4-7: Universal Joint RoMs necessary for the hip actuators

Hip Actuator	Front Actuator	Back Actuator
Torso Universal Joint Pitch [deg]	-7.3 to 6.5	-14.9 to 4.1
Torso Universal Joint Roll [deg]	-3.0 to 12.7	-4.9 to 3.7
Coxa Universal Joint Pitch [deg]	-17.5 to 6.1	-10.1 to 7.5
Coxa Universal Joint Roll [deg]	-61.6 to 22.5	-67.3 to 27.0

4.4. Thigh Actuator Configurations

Two of the leg DoFs, the hip pitch and knee pitch, require a RoM in excess of 135°. Achieving this large RoM with constant high torque is not feasible using a linear actuator in a similar configuration to the other leg joints. As shown in Figure 4-4 and Figure 4-12, the joint torques decrease significantly over the actuator RoM. To mitigate this problem, an inverted straight-line linkage was used to provide nearly constant torque over the whole joint RoM [45]. Though this linkage is too large to fit at the other joints of THOR, it uses the same linear actuators.

4.4.1. Hoeken's Linkage

The Hoeken's linkage is a planar, four-bar mechanism that converts rotary motion to nearly-linear motion. This linkage can be configured to produce a nearly-linear output through upwards of 180° of input rotation. A schematic of a Hoeken's linkage is in Figure 4-17.

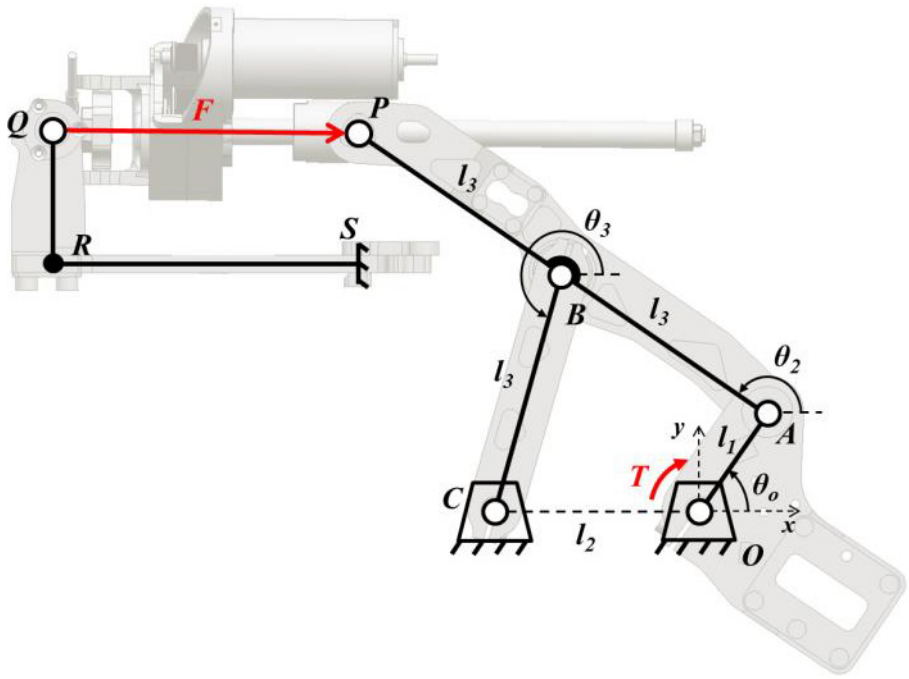

Figure 4-17: General schematic of Hoeken's linkage [45]. Image used with permission from C. Knabe, Lee, B., and Hong, D., "An Inverted Straight Line Mechanism for Augmenting Joint Range of Motion in a Humanoid Robot." Submitted to the *ASME International Design Engineering Technical Conferences & Computers and Information Engineering Conference*, Accepted, 2014.

Traditionally, a Hoeken's linkage is used to convert rotation to linear motion. Conversely, the linkages in THOR are used to convert linear motion to rotation [45]. This allows THOR to use the same actuators throughout the legs while producing a large RoM for the knee and hip pitches and accurate force control through each linkage.

The THOR Hoeken's linkage has three primary non-linearities: the mechanical advantage over the joint rotation, the required linear displacement for a given joint rotation, and the nearly-linear

input motion [45]. Each of these non-linearities can be made more linear by slightly varying the ratios of the lengths in the linkage, reducing the joint rotation range. Because the knee and hip pitch only required 150° of RoM, the linkages in THOR were optimized to be linear over only that amount of rotation [46].

The first non-linearity associated with the linkage is the mechanical advantage. As shown in Figure 4-18, the linkage does not produce a constant mechanical advantage, the joint torque in [Nm] over the actuator force in [N], over the full joint rotation. The mechanical advantage is nearly constant, and is large enough so that THOR can produce peak torques of 140 [Nm] and 150 [Nm] from a 100 [W] and 200 [W] actuator respectively at any joint angle. A look-up table of mechanical advantages is stored in the motor controllers to calculate the joint torque.

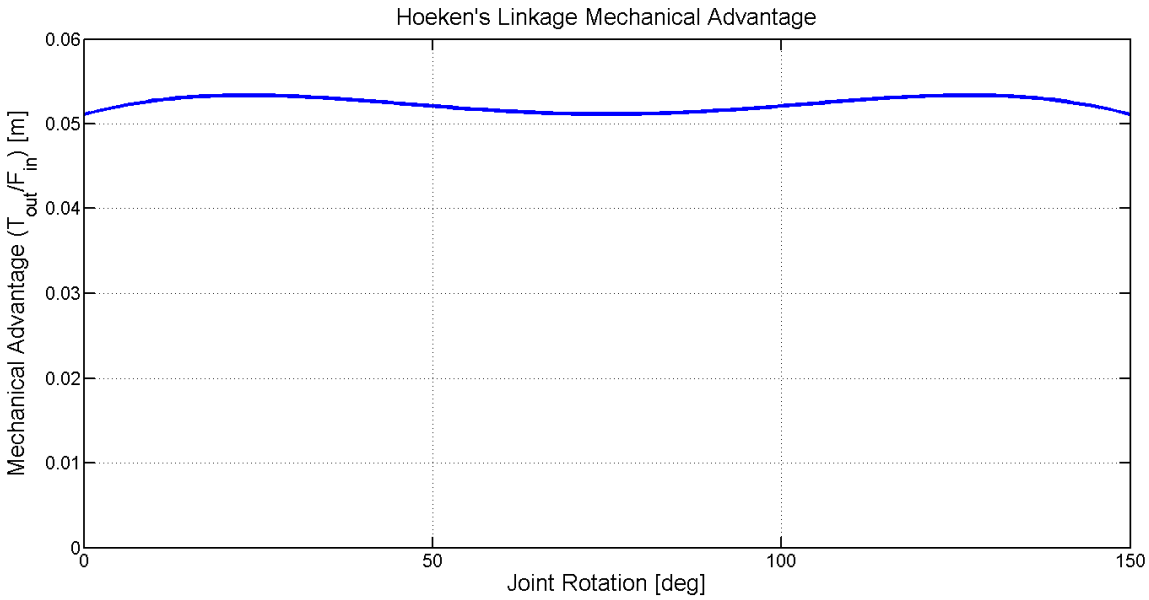

Figure 4-18: Hoeken's linkage mechanical advantage over the joint rotation

An important thing to note is that the mechanical advantage is measured relative to the joint rotation. There are absolute encoders located on the axis of each joint in the lower body to directly measure the joint angles. Even though the input to the linkage is the actuator stroke, the walking controller uses the joint angle measurement as the primary input.

The second non-linearity of the linkage is the linear actuator displacement needed to produce a given joint rotation. Shown in Figure 4-19, the actuator displacement deviation from a least-squares linear relationship between the actuator displacement and joint angle is small. The actuator displacement is used to calculate the joint velocity, so it is important to know this relationship. Similar to the mechanical advantage, a look-up table of actuator displacements is stored in the motor controllers for the walking algorithm.

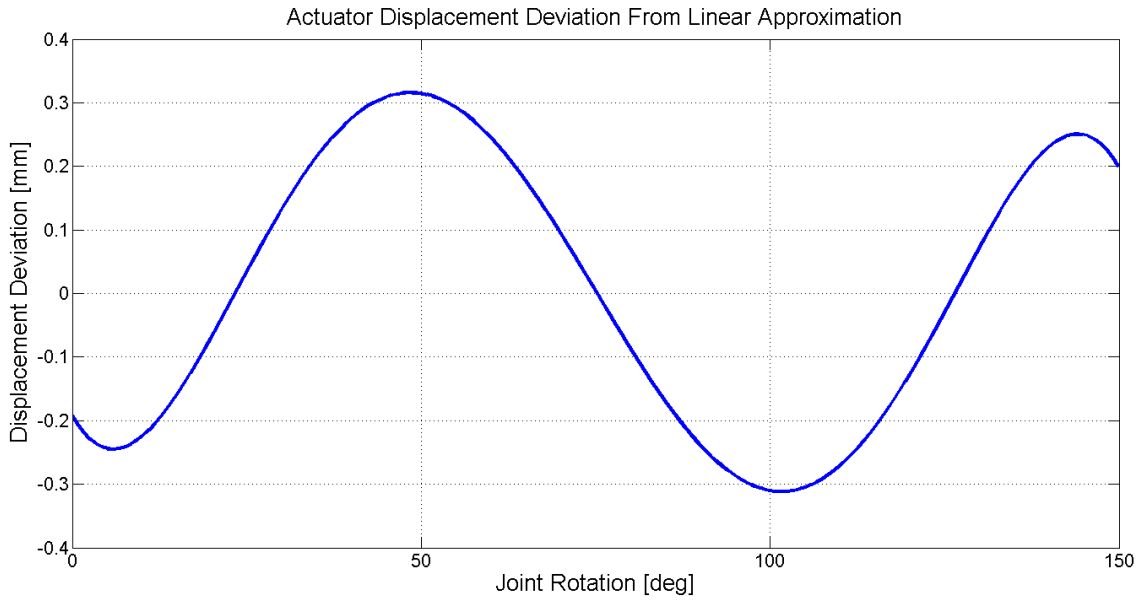

Figure 4-19: Output joint angle over the joint rotation

The final non-linearity is the shape of the input motion. The midpoint of the actuator travel lies about 1 [mm] above a line connecting the two ends of the travel. Though this is a small offset, it would cause a major binding issue if both ends of the actuator were attached to the robot structure. Therefore, the actuator is only attached to the compliant spring through an identical interface to the other actuators in the legs. The output of the actuator is attached to the linkage itself. The actuator is allowed to rotate about the axis connecting it to the compliant spring. Because this rotation is small, the actuator is always assumed to be parallel to the compliant spring.

There are many methods to design parts for a planar linkage like the Hoeken's linkage with each pin joint in double shear. One is to place pairs of components on different physical planes so that they cannot intersect. This method requires more space for the entire linkage. Another method is to place the majority of each link on the same physical plane and have the bodies split apart close to the joints. This split is shaped similar to a "Y", where most of the link is a singular part like the base of the "Y", and the joint is divided like the top of the "Y". This design method can be more compact than completely separating the linkage parts. The two Hoeken's linkages in THOR use these design strategies.

4.4.2. Hip Linkage Placement and Design

As stated earlier, the hip joint is divided into two independent joints that intersect at the same point. The first joint is driven by parallel actuators that control both yaw and roll. Because the pitch motion required a significantly larger RoM than the yaw and roll, it was designed using a Hoeken's linkage. The main challenge in designing the hip linkage was to have its joint axis

intersect the yaw and roll axes while keeping the thighs thin. The general linkage placement is shown in Figure 4-20A and B.

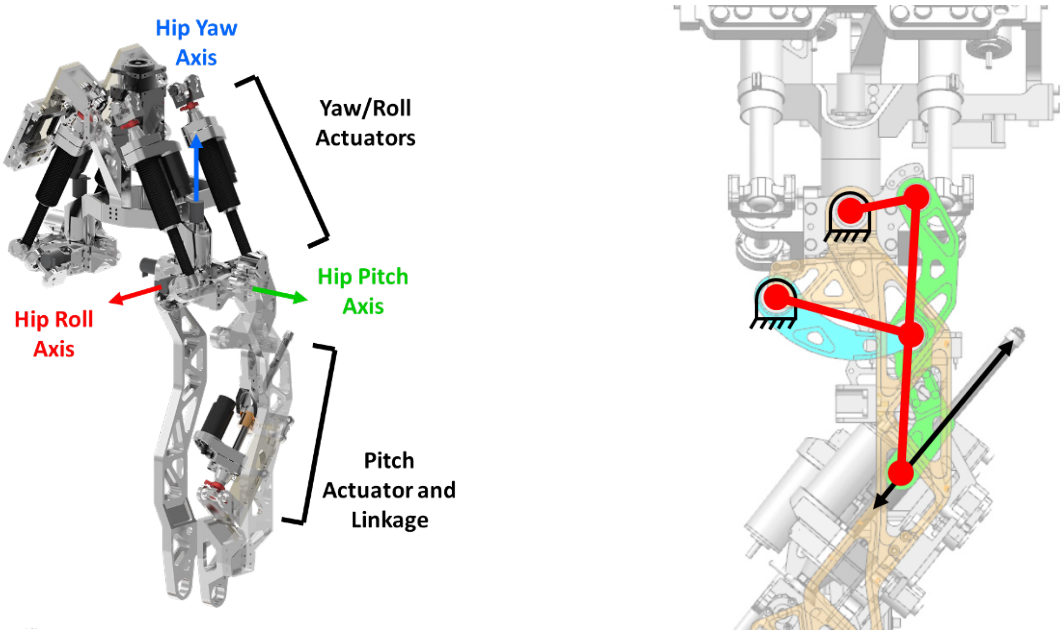

Figure 4-20: Hip actuator placement for (A) all the hip actuators and (B) the Hoeken's linkage in the thigh

The hip pitch linkage is located outside of the coxa. This placement best avoids interference with the torso as the hip goes through yaw and roll motions. The linkage was designed to be thin while still placing each axle in double shear by using the "Y" splitting method. Making the linkage thin increased the difficulty for any repairs, essentially requiring a full disassembly of the thigh to replace any linkage part. This is because the outside thigh and coxa are both members of the linkage that block access to the other links. A front view of the hip linkage can be seen in Figure 4-21.

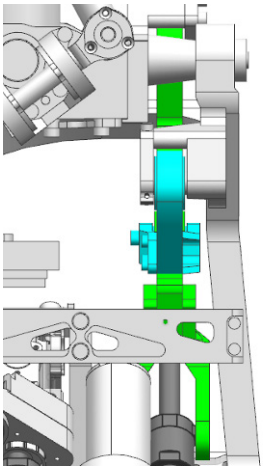

Figure 4-21: Hip Hoeken's from the front

In order to avoid interferences over the whole range of motion, the linkage pieces were designed with a non-linear shape. The three bearing part shown in Figure 4-22A is shaped like a "W" to avoid intersecting the main pitch axis of the hip and the actuator motor at -120° and at 30° of rotation respectively. The split at the bottom of the part is designed to fit around the ball screw of the actuator. The two bearing part shown in Figure 4-22B is curved to avoid interference with the coxa. Its split fits around the middle bearing in the three bearing link.

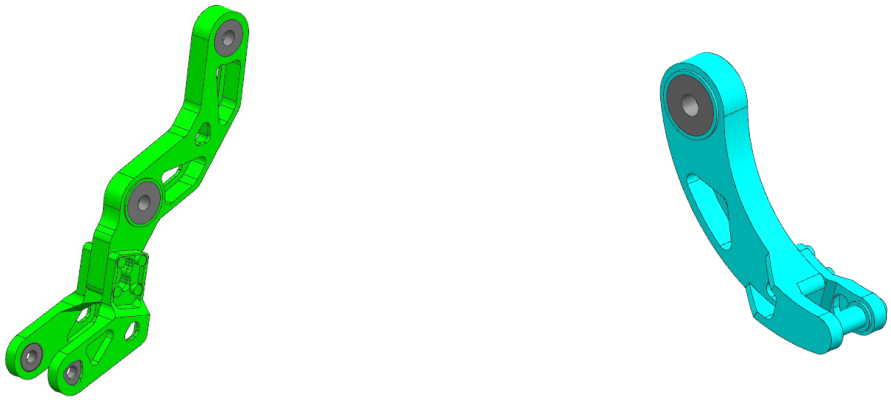

(A) (B)

Figure 4-22: (A) Three bearing Hoeken's linkage piece and (B) two bearing linkage piece for the hip

The hip pitch joint produces motion in both the positive and negative direction, though it is heavily biased in the negative direction. To produce this motion, the actuator is partway through its travel when the leg is in a vertical position. The motion of the linkage over the hip RoM can be seen in Figure 4-23.

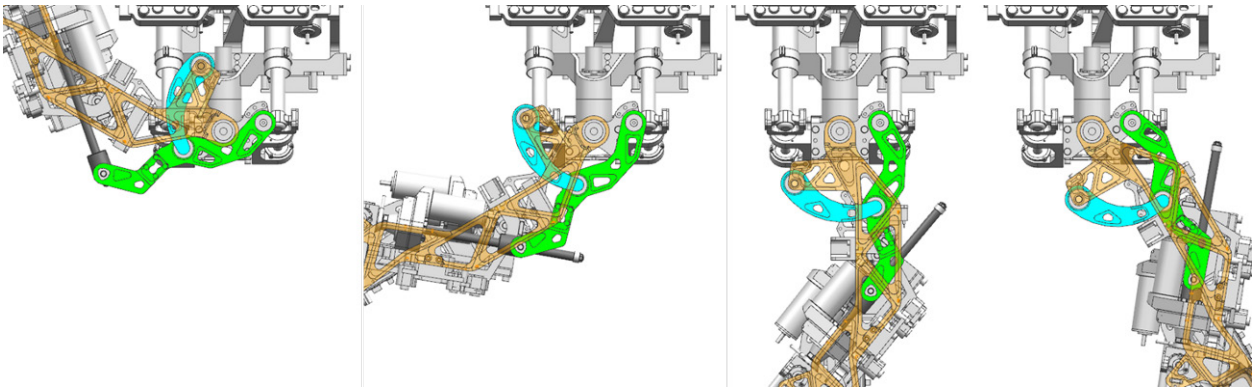

Figure 4-23: Hip Hoeken's linkage at -120°, -60°, 0°, and 30°

4.4.3. Knee Linkage Placement and Design

The Hoeken's linkage for the knee was simpler to design than the hip. The knee is a single DoF joint, so the linkage does not have the same tight packaging constraints of the hip. Additionally, it was designed with most parts on their own planes to prevent part intersections. The knee linkage can be seen in Figure 4-24.

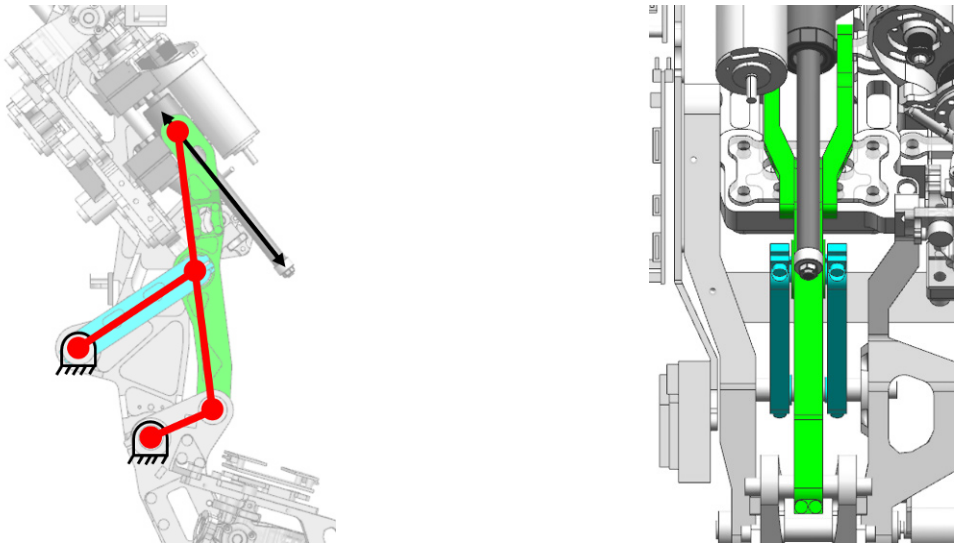

(A) (B)

Figure 4-24: Knee Hoeken's linkage seen from the (A) side and (B) front

Splitting the linkage pieces onto different physical planes simplified many portions of the design. Assembly and disassembly can occur when the rest of THOR is already assembled. This also means that this linkage will be easier to modify in the future. This design does use more width, but there is more than enough space available in the knee portion of the thigh.

The three bearing linkage piece for the knee, shown in Figure 4-25A is shaped similar to its counterpart in the hip linkage, but the valleys are less drastic. This part needs to avoid intersection with both the compliant spring mount and the knee axis shaft. The split at the top of the part is to fit around the actuator ball screw. The two bearing linkage parts, shown in Figure 4-25B, are two identical parts that assemble around the three bearing piece. These parts being separable makes the linkage easy to assemble and disassemble.

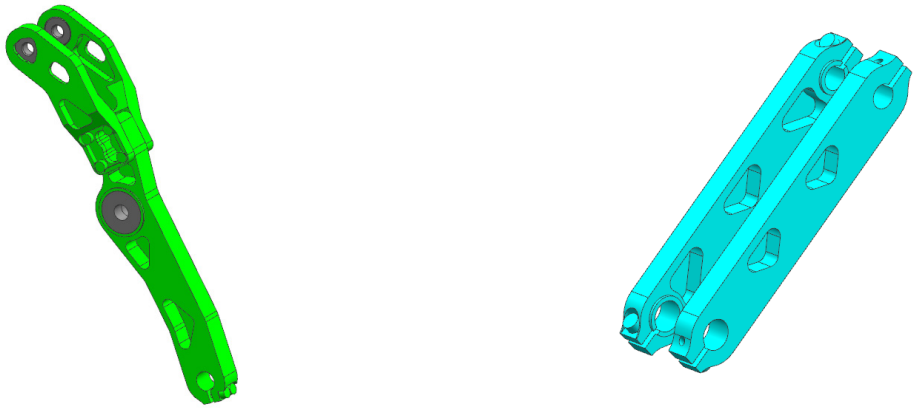

(A) (B)

Figure 4-25: (A) Three bearing Hoeken's linkage piece and (B) two bearing linkage pieces for the knee

The knee linkage is at the end of its rotation when the leg is in a vertical position. Therefore, the actuator is at the end of its travel in the neutral position. Even though the RoM investigation found that the human subject used 150° of knee rotation, structural interferences restricted the THOR knee rotation to only 135°. The 150° knee rotations occurred when the subject kneeled and stood up from the ground. The test subject was also able to complete these tasks without bending their knee past 135°, so the reduced amount of rotation was deemed acceptable. The full rotation of the knee linkage can be seen in Figure 4-26.

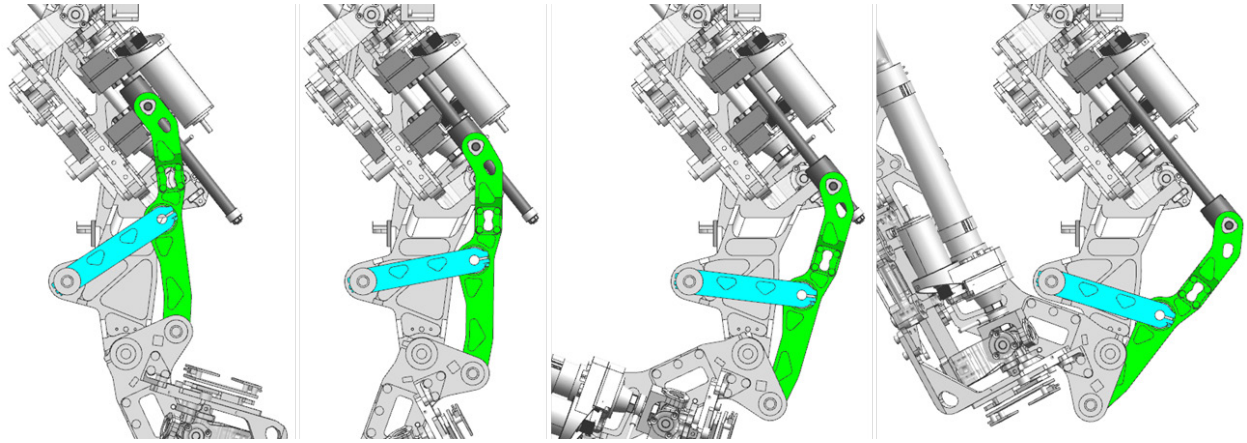

Figure 4-26: Knee Hoeken's linkage at 0°, 45°, 90°, and 135°

4.5. Final Leg Range of Motion

Several factors discussed throughout this chapter forced a reduced the actual THOR RoM from to the desired values. The hip yaw RoM was reduced to make the actuators easier to place with large torques possible. The knee pitch RoM was reduced to prevent physical interferences between the thigh and shin. Though not a reduction, the ankle pitch RoM was skewed to make it easier to step up to higher levels. Each of the changes to the RoM was considered against the tasks in the motion simulation to ensure that there would not be too severe of effects. The final RoM specifications for the changed joints can be found in Table 4-8. The DoFs not listed in Table 4-8 achieve the RoM desired in Table 3-7.

Table 4-8: Final RoM specifications for THOR

Joint Axis		Average Human	RoM Videos	Desired THOR	Actual THOR
Hip Yaw	Min [deg]	-30	-25	-20	-20
	Max [deg]	60	60	60	45
Knee Pitch	Min [deg]	0	0	0	0
	Max [deg]	135	150	150	135
Ankle Pitch	Min [deg]	-20	-50	-45	-55
	Max [deg]	50	45	45	35

5. Lower Body Structure

As detailed in the previous chapter, the actuators in the legs of THOR span the hip, knee, and ankle joints. In between each joint is a structural body that gives THOR a similar morphology to a human. The torso connects both hip joints and the waist. Each hip joint has an intermediate body, the coxa, which separates the spherical joint into a universal joint and a pin joint. Finally, each leg has a thigh, shin, and foot. These structural bodies house the configurable compliant springs for the SEAs, proprioceptive sensors, and support electronics. This chapter will discuss the design of the structure of THOR's legs.

5.1. Torso Structure

The torso of THOR connects the two legs through their respective hip joints to the upper body through the waist. It houses the majority of each actuator that drives those joints as well as the configurable compliant springs for each SEA [44]. The torso is the only body in the lower half of THOR that interacts with both the left and right legs. Therefore, it must house actuators for both legs without any interference. As discussed in section 4.3, this was one of the major factors driving the placement of the hip linear actuators.

The actuators of THOR all use identical compliant springs for their series elasticity. These springs have the same interfaces to the structure, as seen in Figure 5-1. The compliant springs are located 50 [mm] away from the axis of the actuator, which limits the possible interface locations for a given actuator. The 50 [mm] offset drove the shape of the torso.

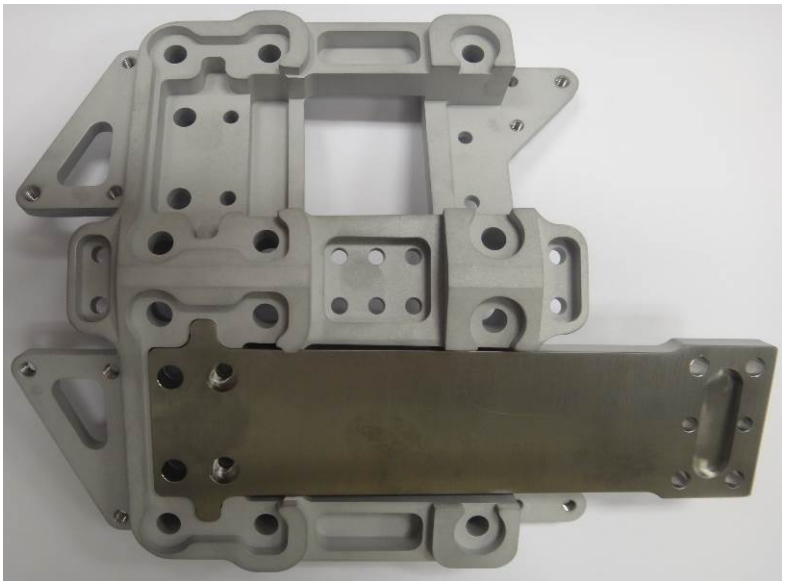

Figure 5-1: Configurable compliant spring interface for the shin with and without a compliant beam

There were four possible locations for each compliant interface to keep the design and manufacture of the torso simple. Placing the interfaces at the four cardinal directions, to the

front, back, inside, or outside of each actuator, would be the fastest to design and easiest to manufacture. The 50 [mm] offset of the compliant beam prevented the interfaces from being located between the actuators. The offset coupled with the deflection of the beams under loading would have forced the hips to be wide to prevent interferences. For the hip, roll torque is more important than yaw torque. Placing the compliant beams either inside or outside of the actuators would be more favorable for roll torque because of the compliant spring deflection direction. Combining these two characteristics, the compliant interfaces were placed to the outside of each actuator.

To place the compliant interfaces on the outside of the actuators, the torso was designed like a box. As shown in Figure 5-2, the left and right sides of the box are slanted to match the nominal angle of the actuators. This box is connected to the pelvis of the robot through three gussets on the front and sides. The back of the box directly bolts into the pelvis.

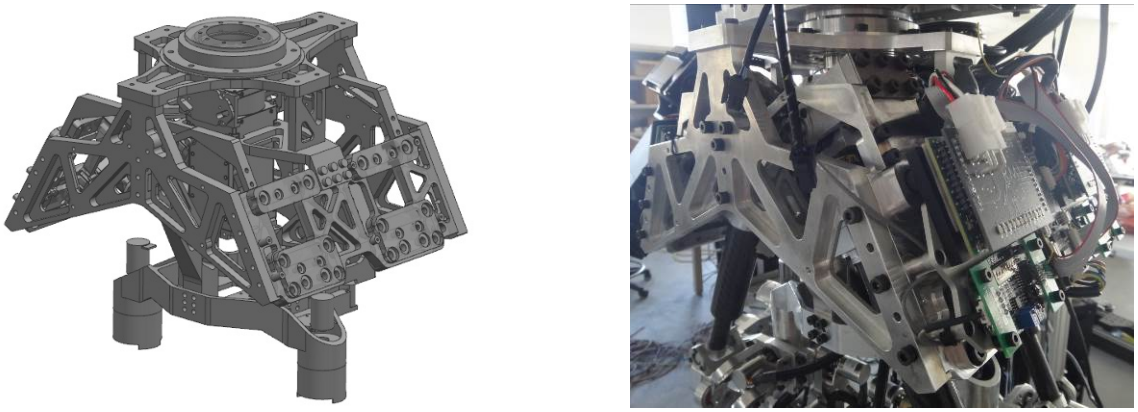

(A) (B)

Figure 5-2: Torso structure around the actuators from (A) the CAD model and (B) THOR

The pelvis shown in Figure 5-3 is the base piece of the torso that connects the two hip joints. Each hip yaw joint has a pair of sealed angular contact bearings to accommodate the vertical loads through the joint. The hip yaw is the only joint that has large axial loads running through it consistently. Even though the bearings are pressed into different pieces, there are locating pins in each part to ensure that the axes align. The space in front of the pelvis is left open to accommodate the thigh during high-kick motions.

There are a few proprioceptive sensors attached to the pelvis. The bottom of the pelvis has a set of locating pegs to align the attitude and heading reference system (AHRS) to the robot. The pelvis serves as the coordinate reference for THOR, so it is important for the inertial sensor to be properly aligned. There is a pair of absolute rotary encoders to measure the yaw angle of each leg. These are the same encoders that are used at each joint throughout the legs. The encoders can be seen on the right and left sides of Figure 5-3. The proprioceptive sensors are discussed further in Appendix A.

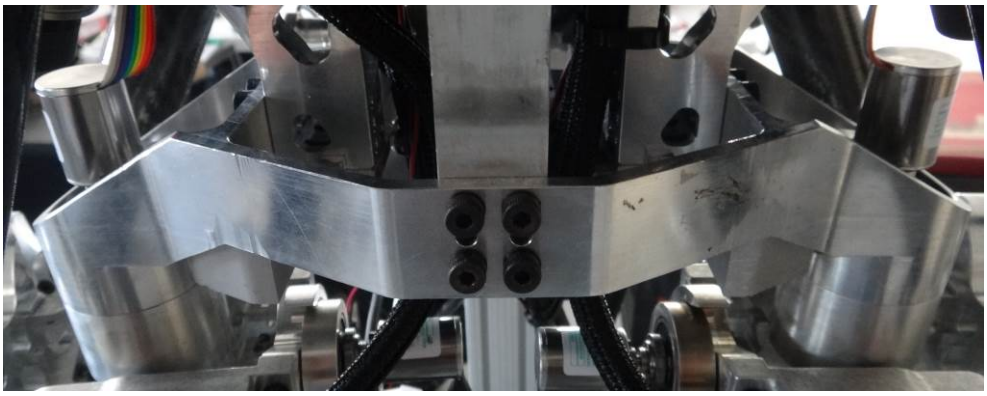

Figure 5-3: Torso pelvis

The actuators for the hip require support electronics to operate. These electronics, shown in Figure 5-4, are mounted on the outside of the torso. Each side of the torso has two motor power supplies, two load cell signal conditioning boards, and one motor controller to support its respective parallel actuators. The motor controller commands both parallel actuators for a hip joint. In addition to the actuator electronics, the torso also houses a smart power distribution circuit for the whole lower body. The power board is mounted to the back of the torso. The motor controller and power distribution board are discussed further in Appendix A.

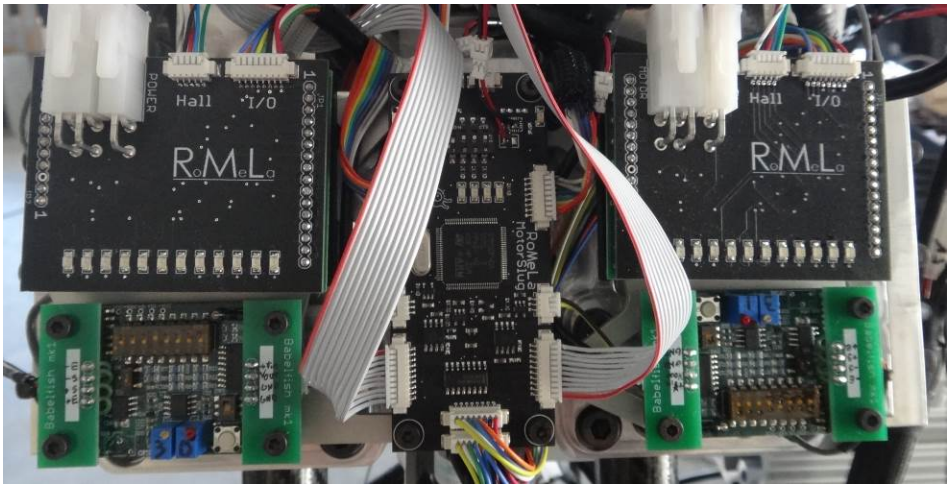

Figure 5-4: Torso actuator electronics

The final component of the torso is the waist yaw actuator and bearing assembly. The torso connects the lower body to the upper body through the waist joint. The waist uses commercial off the shelf (COTS) servo actuators to drive its yaw and pitch DoFs. The yaw actuator is in the center of the torso, between all four hip linear actuators. None of the linear actuators are able to contact the waist actuator, even with the compliant spring deflections. A cross roller bearing is mounted to the torso structure directly above the yaw actuator to prevent any off-axis forces and torques from damaging the servo actuator. The waist joint will be discussed further in Chapter 6.

5.2. Coxa and Hip Cross Gimbal Structure

The coxa is the intermediate body in the middle of the hip joint, which separates the spherical joint into a parallel actuated universal joint and a linkage driven pin joint. A cross gimbal connects the coxa to the torso, making the yaw and roll DoFs into a universal joint. Combined together, the hip cross gimbal and the coxa form the spherical gross gimbal of the hip. Computer generated images of the hip cross gimbal and coxa are shown in Figure 5-5.

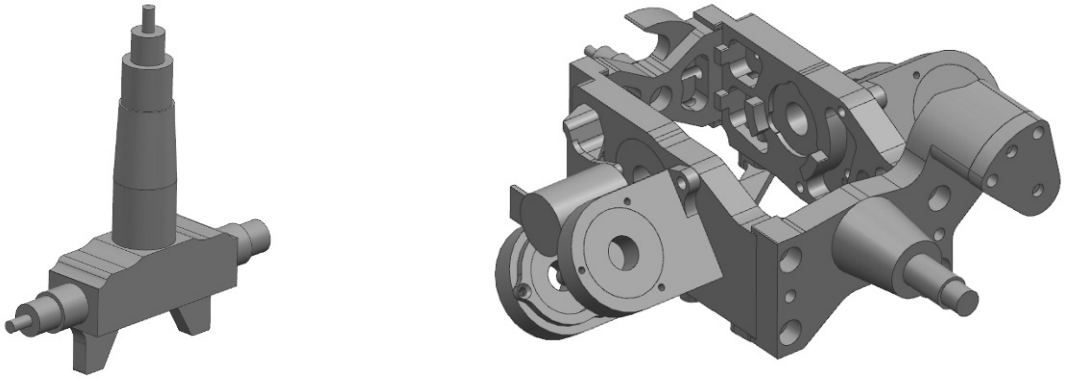

(A) (B)

Figure 5-5: CAD images of the (A) hip cross gimbal and (B) coxa

Several configurations of bearings and shafts were tested for the coxa and hip cross gimbal. Because of the high RoM of the hip, it was important to create a small package that allows for large amounts of unimpeded motion. In order to attach an absolute encoder easily, the cross gimbal could not contain bearings for the roll DoF. If it did, the encoder would need to be mounted in the middle of the gimbal, which would have been challenging for both assembly and maintenance. To interface with the thigh for the pitch DoF, the coxa could not hold the bearings for the same reason. Additionally, placing the pitch DoF bearings in the coxa would increase the size of its bodies, increasing the potential for it to intersect with the torso over the full RoM. A couple of the tested coxa and hip cross gimbal configurations are shown in Figure 5-6.

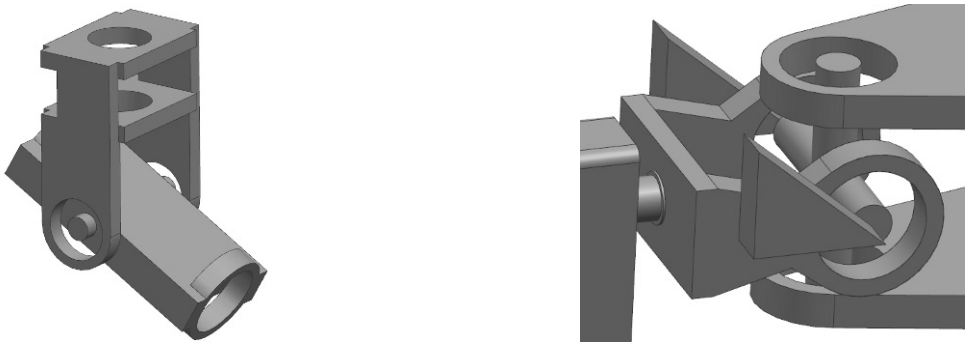

(A) (B)

Figure 5-6: Preliminary coxa and hip cross gimbal designs. The cross gimbal in (A) is similar to its counterpart on SAFFiR.

Similar to the lower universal joints for the hip linear actuators discussed in Section 4.3, the hip cross gimbal places one of its two axes in single support. The single support shaft is designed to fit in the yaw bearing column of the torso to preload the angular contact bearings. The shaft has two different bearing diameter sections. Manufacturing a shaft to tight tolerances over a long length would have been extremely difficult, so the shaft was separated into two different bearing surfaces. This way, the smaller bearing shaft section can be bored before the rest of the cross gimbal is machined. The top and front axes of the cross gimbal have small 3 [mm] posts that fit into the joint absolute encoders. This is a feature on all the shafts that form joint axes.

The coxa, shown in Figure 5-7, is a box structure built around the torso yaw bearing column. The box extends farther to the outside of THOR to avoid interference with the torso over the asymmetric roll RoM. The outside face of the coxa, front right in Figure 5-7, is one of the members of the Hoeken's linkage. Its two bearing shafts rotate in the thigh and the three bearing linkage piece, making the coxa the short lever arm in Figure 4-17.

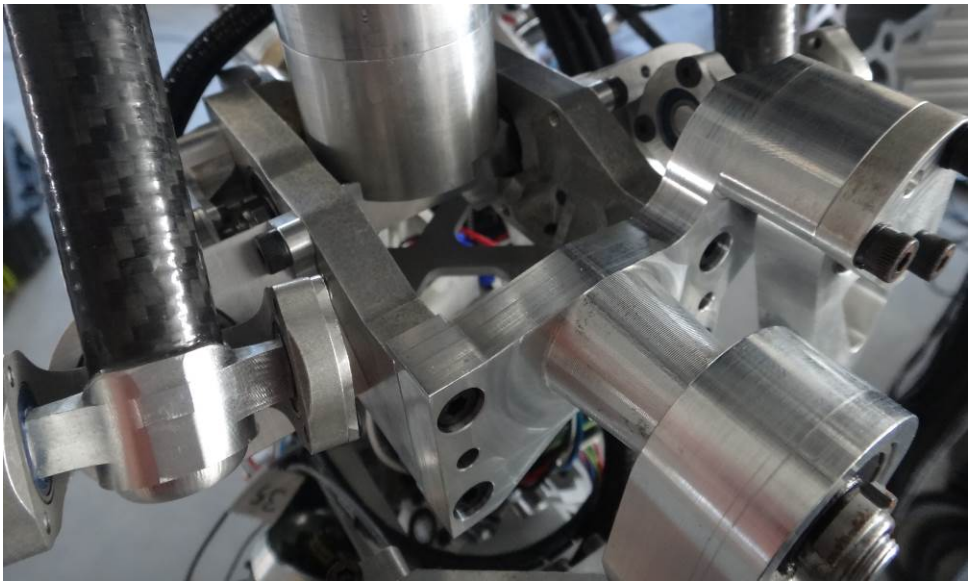

Figure 5-7: The coxa of the left leg

The lower universal joints for the hip actuators bolt onto the front and back of the coxa. They place the joint far enough away from the coxa to avoid interferences over their RoM, but could interfere if the joint needed to rotate significantly more. Because the coxa is an intermediate body, it does not house any support electronics. There is one absolute encoder mounted to the front to measure the hip roll angle, and the inside of the coxa is also the post for the hip pitch absolute encoder.

5.3. Thigh Structure

The thigh houses the actuators and Hoeken's linkages for both the hip and knee pitch DoFs. Similar to the torso, it is an exoskeleton built around the actuators. The top of the thigh surrounds

the coxa and the bottom surrounds the knee. The sides of the thigh do not have a linear shape to avoid interferences over the large hip RoM. Images of the left thigh can be seen in Figure 5-8.

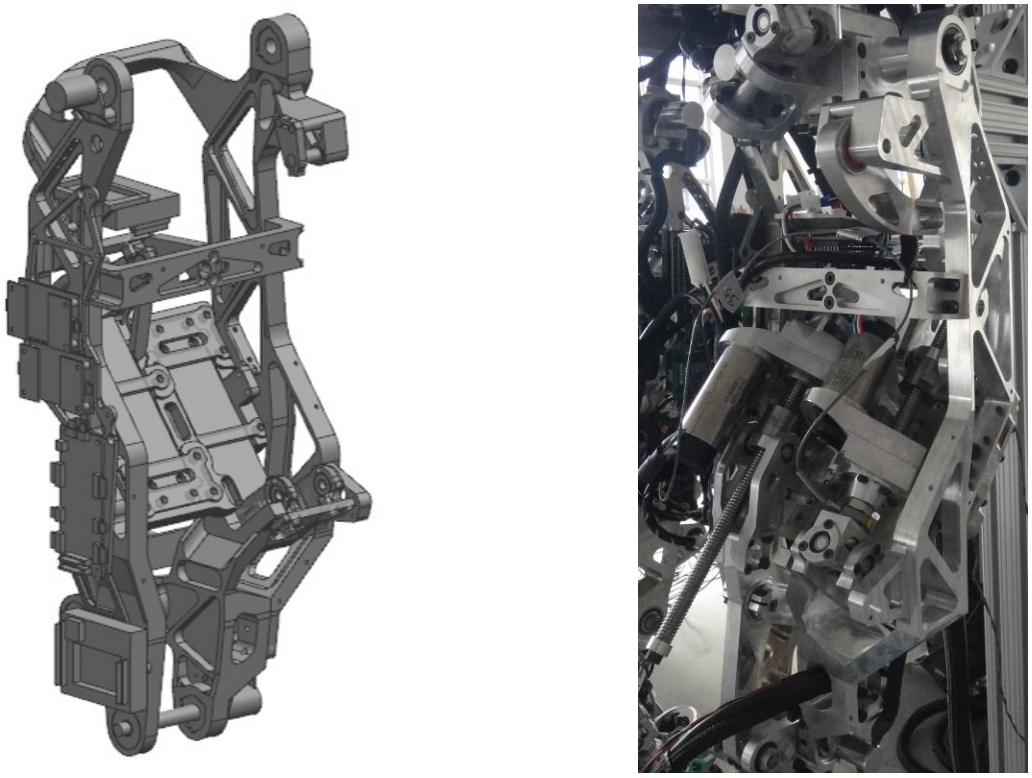

(A) (B)

Figure 5-8: Images of the thigh from (A) the CAD model and (B) THOR

The compliant interfaces for the actuators are mounted to the back of the thigh. Though the actuator axes are not parallel when THOR stands straight up, the two compliant interfaces are parallel. The actuator axes misalign by approximately 2° in their nominal configurations. The compliant interfaces are angled relative to both actuator axes by roughly 1°. This does not impact the performance of either actuator significantly, but it drastically reduces the complexity of manufacture. Both interfaces are machined out of the same piece of aluminum to increase the thigh rigidity and to allow the actuators to be closer to one another.

As discussed in Section 4.4.2, the hip pitch Hoeken's linkage design causes a complicated thigh assembly. In order to reduce its width, each member in the linkage is placed on the robot in a specific order. The thigh is assembled around the coxa while the coxa is suspended from the torso. This also means that the inside and outside members of the thigh cannot be connected before assembly, limiting the ways that the parts could be designed.

The hip pitch Hoeken's linkage only interacts with the outer bone of the thigh. As discussed in Section 4.4.3, the knee Hoeken's linkage has a wider construction that simplifies assembly. This

configuration places the linkage between the inner and outer thigh members, placing bearings in both to put each shaft in double support.

The inside and outside parts of the thigh are designed with a backwards bend in their upper halves. This bend can be seen in Figure 5-9. This shape was designed to avoid interference with the torso and hip yaw and roll actuators during high kick motions. The space in front of the pelvis is also empty to assist with this avoidance. When THOR lifts its leg high, as shown in Figure 5-10, the thigh structure avoids hitting the actuators and torso. The bottom of the bent section provides a convenient mounting surface for the compliant interfaces.

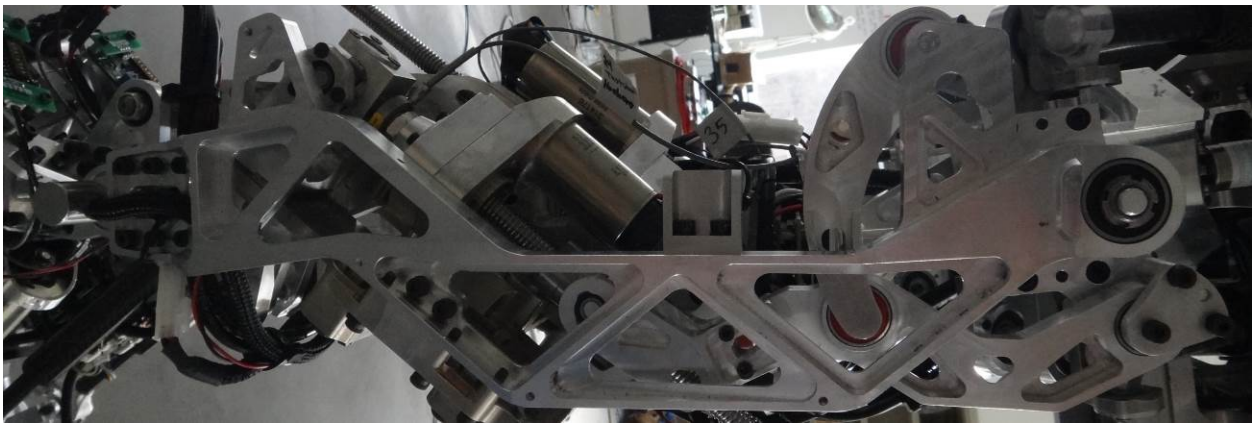

Figure 5-9: Backwards bending shape of the thigh

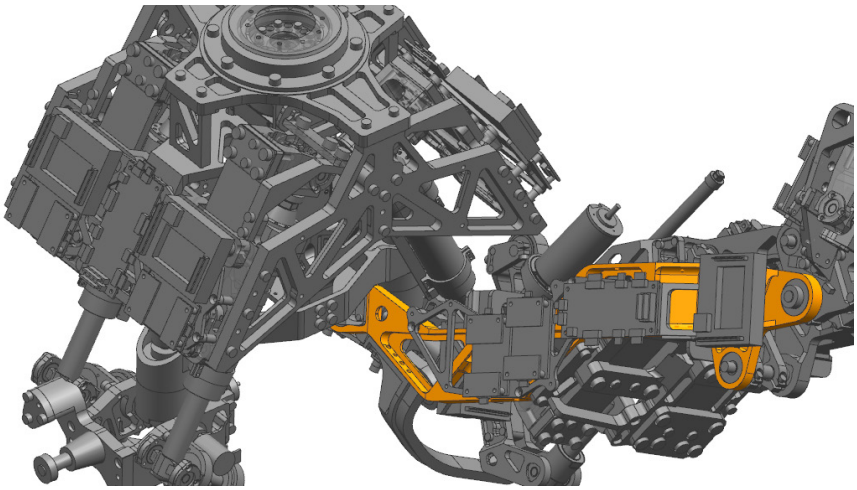

Figure 5-10: CAD rendering of THOR performing a high kick

Like the torso, the thigh houses the support electronics for all of its actuators. The load cell signal conditioning boards, motor controller, and one motor power supply are mounted to the inner thigh. They are in the space between the two legs. The second motor power supply is mounted inside the exoskeleton of the thigh, directly above the knee actuator. This power supply

lies directly beneath the void filled by the coxa during high kicking motions. There are two joint absolute encoders mounted to the thigh for the hip and knee pitch DoFs.

One feature of the thigh that stands out is the protrusion of the actuator ball screws out of the structure. The ball screws from the actuators stick out to both the front and the back, creating large impact and snagging hazards. These actuators cannot be moved without negatively affecting the linkage and joint motions. Carbon fiber covers were designed to protect these ball screws, but they were never manufactured to save time.

5.4. Shin Structure

The shin connects the knee to the ankle and houses the actuators for the ankle joint. It is the only body segment in the leg that mimics the human musculoskeletal structure by having an internal skeleton surrounded by actuators. Because the ankle joint has a symmetric RoM in roll, the shin is identical for the right and left legs. The thigh and coxa for the right leg are mirror images of their counterparts on the left leg. An image of the shin can be seen in Figure 5-11.

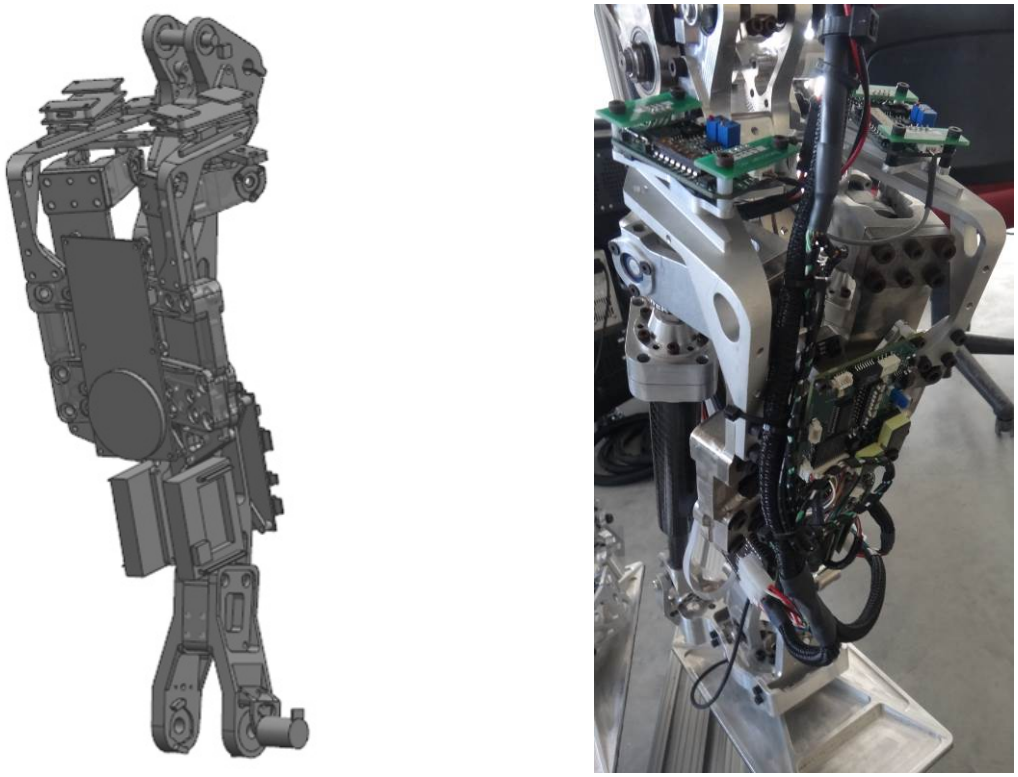

(A) (B)

Figure 5-11: Images of the shin from (A) the CAD model and (B) THOR

The actuators lie on the outside of the shin. Their compliant interfaces are mounted on the wing-shaped part shown in Figure 5-1 that bolts to the front of the shin. In order to fit the shin in a smaller volume, this part contains many non-orthogonal faces. Though this contradicts the

manufacturing-centric design mentality of the rest of the legs, it increased the amount of space between the two shins. When THOR stands with each joint in a nominal configuration, there is only 59 [mm] between the two shins. This space allows the leg to swing inwards when THOR attempts to step, so it is important to have room between the legs.

Similar to the thigh, the shin is shaped to avoid interferences at the far end of the knee RoM. Starting at the knee joint, the shin bone bends forwards and then returns back to the line connecting the joints. This bend, shown in Figure 5-12 is designed to prevent the shin from impacting the thigh when the knee bends to 135°. The bearings on the thigh for the Hoeken's linkage fit into the pocket behind the shin. Figure 4-26 shows how close the shin and thigh come to interference during a large knee bend.

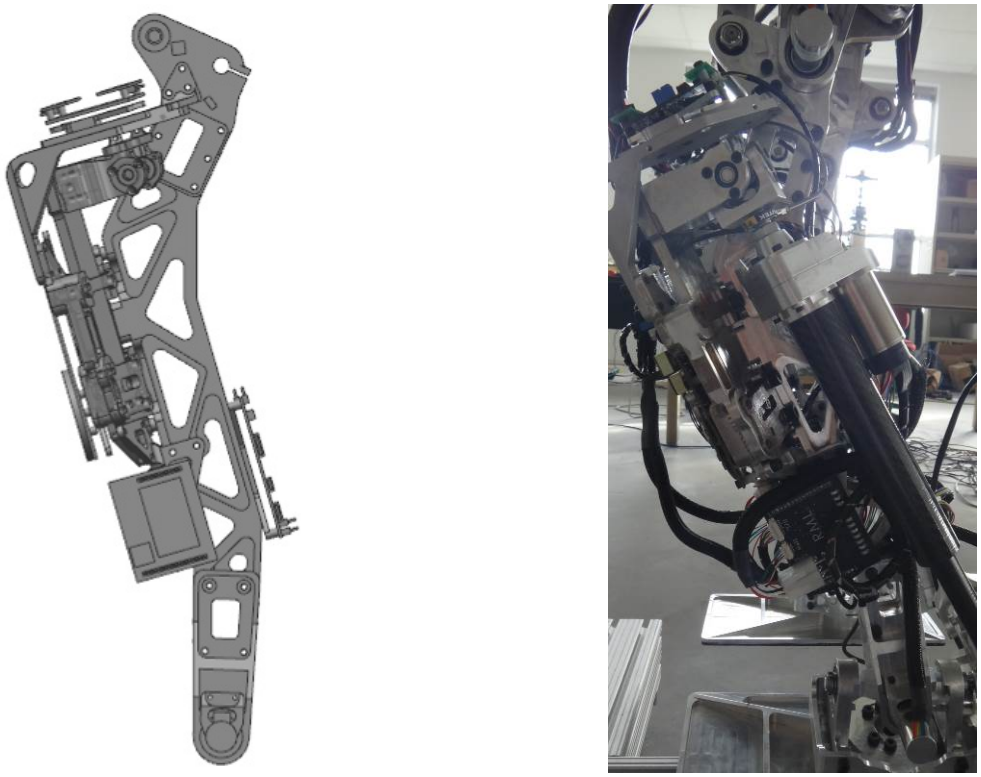

(A) (B)

Figure 5-12: Bend in the shin bone from (A) the CAD model and (B) THOR

Because of the actuator positioning on the shin, the support electronics are scattered to wherever they could fit on the structure. Beyond the support electronics for the two actuators, the shin also holds the signal conditioning circuit for the six-axis force/torque transducer in the foot. The load cell signal conditioning boards are placed on top of the shin, close to the knee joint. The force/torque transducer signal conditioning circuit is mounted to the front of the shin with the motor power supplies directly below it. The most difficult circuit to mount was the motor controller. This is placed between the two actuators on the back of the shin, as seen in Figure

5-13. The actuators move to within 5 [mm] of the board over their RoM, which is close enough to bend some of the wires connecting to the controller. This circuit placement drove the outer dimensions of the motor controller during the design process.

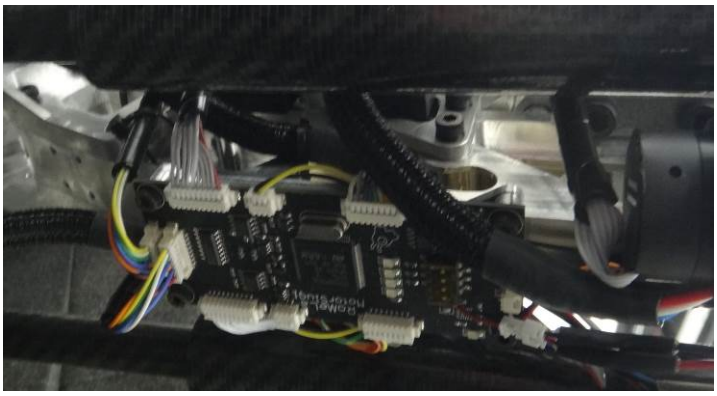

Figure 5-13: Motor controller mounted on the back of the shin

There is an absolute encoder mounted to the shin to measure the ankle pitch angle. The encoder is on the left side of the shin for both legs because of the foot design. This decision will be further discussed in Section 5.5. Because the left and right shins have this sensor on the left side, they are identical instead of mirror images.

5.5. Foot Structure

The foot is the lowest body in the legs. It is an unactuated flat plate that contains a six-axis force/torque transducer to measure the ground reaction forces. An image of the foot is shown in Figure 5-14.

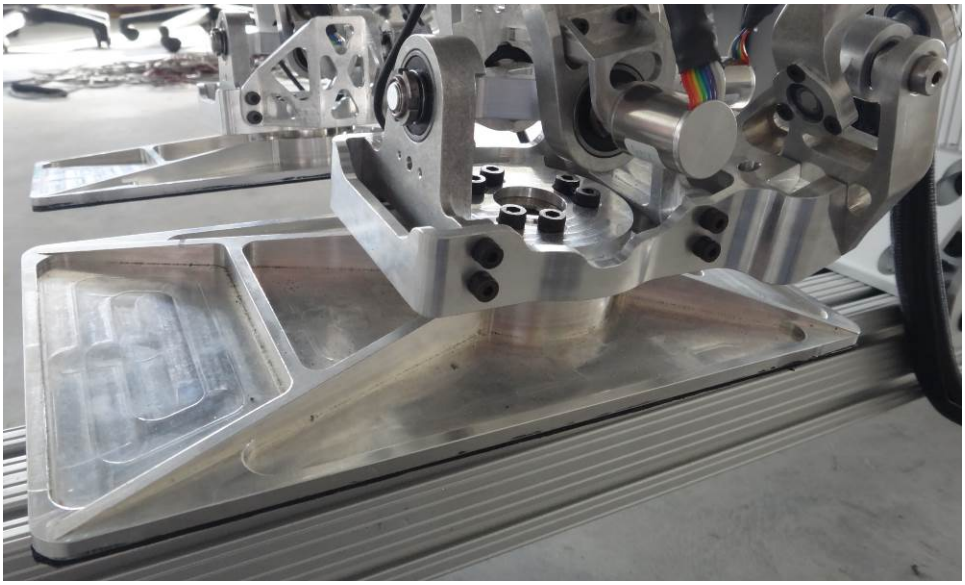

Figure 5-14: The foot of THOR

The foot connects to the shin through a universal joint. The ankle contains a traditional shaped cross gimbal shown in Figure 5-15. The thinner flat sections in the cross gimbal are used as hard stops to limit the RoM in the ankle. The two smaller posts fit into the absolute encoders to measure the ankle pitch and roll.

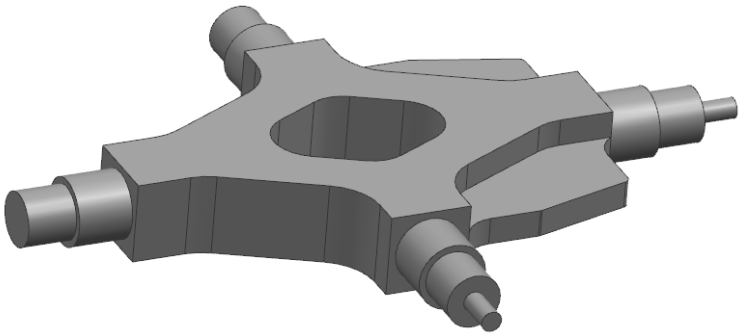

Figure 5-15: CAD model of the ankle cross gimbal

The foot has a pair of proprioceptive sensors. A joint absolute encoder is mounted in the foot to measure the ankle roll angle. The six-axis force/torque transducer is located directly beneath the ankle joint. It has a cable that exits to its side, which caused the shin and feet to be identical for both legs. When the ankle makes a large roll motion, the absolute encoder on the shin for the pitch DoF would have interfered with the cable exiting the sensor if the shins were mirror images of one another. Instead of rotating the sensor, which would have required designing two completely different feet, the shin and foot were left identical for both legs.

The sole of the foot is a flat plate with a rubber bottom. The rubber is glued onto the sole to add grip when balancing on smooth floors. The sole does not have an actuated toe, which could increase the motion capabilities of THOR. The toe would have added extra design complexity and weight to the foot. As discussed in Section 3.1, a toe would not help to complete the DRC tasks. Adding an actuated or passive toe is one area for future improvement to THOR.

5.6. Lower Body Range of Motion

The achievable RoM of the lower body is a function of the combination of the actuator configurations and the structural body designs. Each actuator was configured where the extreme ends of the desired RoM could be reached simultaneously, but designing the support structure with compliant interfaces around the actuators eliminated some of the overall RoM. The hip is a complicated 3 DoF joint that cannot reach its full RoM because of structural interferences [44]. The ankle and knee are both able to reach their desired RoM.

The hip is the most complicated joint in THOR. Isolating the pitch DoF from the yaw and roll DoFs allowed for an actuator configuration that independently allows each hip DoF to reach the ends of its RoM. Interferences between the hip pitch Hoeken's linkage mount on the thigh and the torso compliant interfaces eliminate some of the overall RoM. The amount of RoM limitation

is currently unknown. Figure 5-16 shows the hip at the ends of its RoM in yaw, roll, and pitch. The images do not show the leg rotated to -30° of roll. This pose would have required extending the right leg to at least -30° of roll as well to prevent the two legs from colliding.

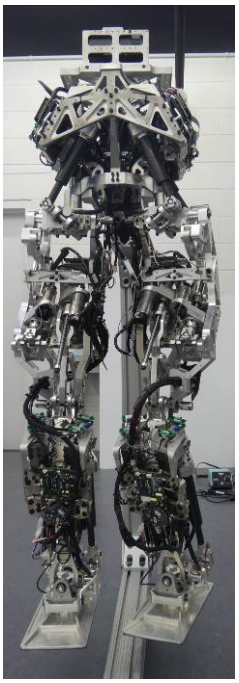

(A)

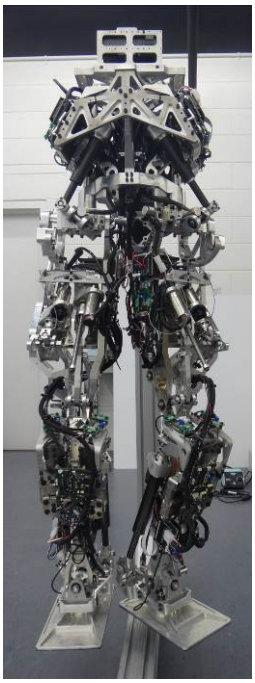

(B)

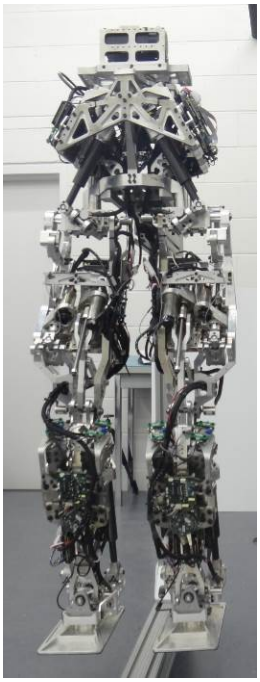

(C)

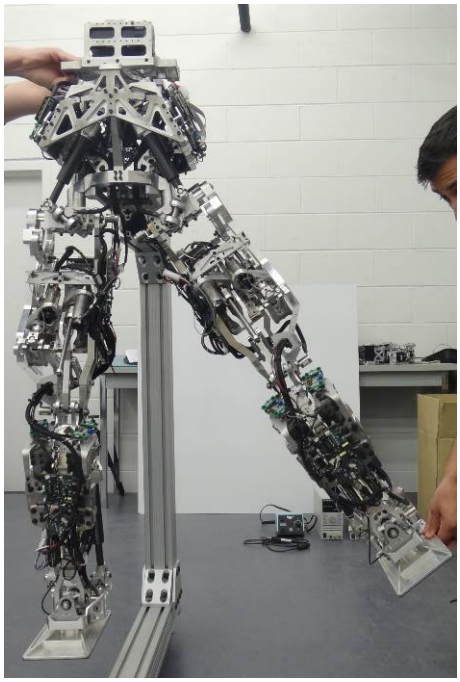

(D)

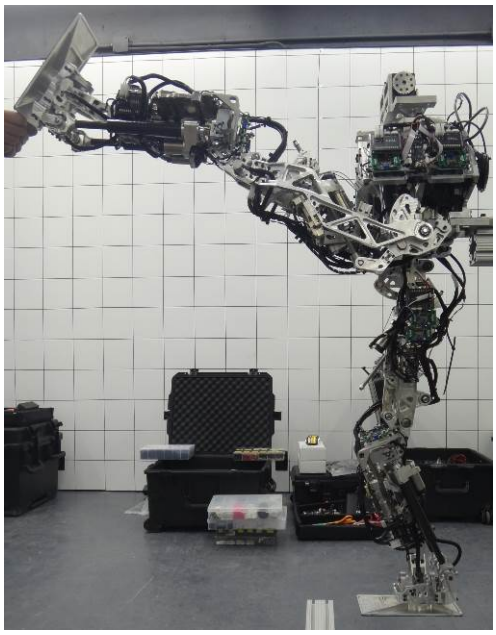

(E)

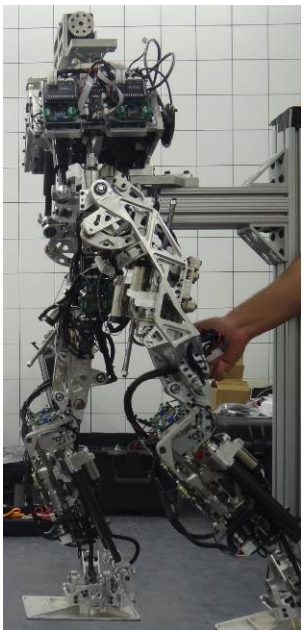

(F)

Figure 5-16: Images of the hip at the ends of its RoM. (A) and (B) show the left hip yaw at approximately -20° and 45° respectively, (C) and (D) show the left hip roll at approximately 0° and 45° respectively, and (E) and (F) show the left hip pitch at approximately -120° and 30° respectively.

The knee is capable of reaching both ends of its desired RoM without any interference. The Hoeken's linkage used in the knee was designed with a 150° range, exceeding the 135° RoM for the knee. The thigh and shin structures were designed to fully accommodate the RoM. Figure 5-17 shows the knee joint at the ends of its RoM.

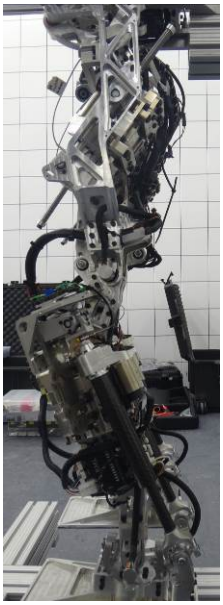

(A)

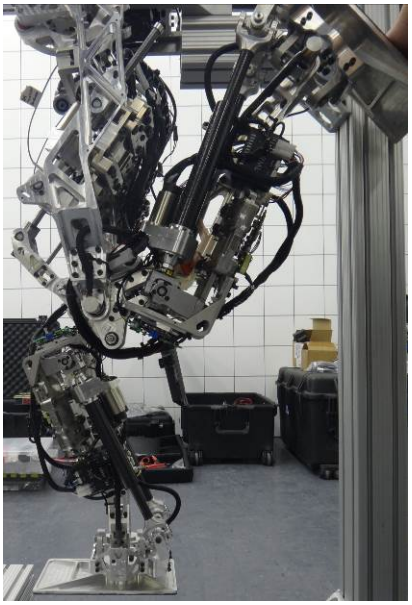

(B)

Figure 5-17: The knee joint bent to approximately (A) 0° and (B) 135°

Even though the parallel actuated ankle joint is more complicated than the knee, it has no limitations over its full RoM space. The parts closest to interfering over the full RoM are the lower actuator universal joints attached to the foot and the bottom of the shin. These two parts come within 3 [mm] of intersection when the ankle is at 35° of pitch and ±30° of roll. Figure 5-18 shows the ankle joint rotated to the pitch and roll RoM limits simultaneously.

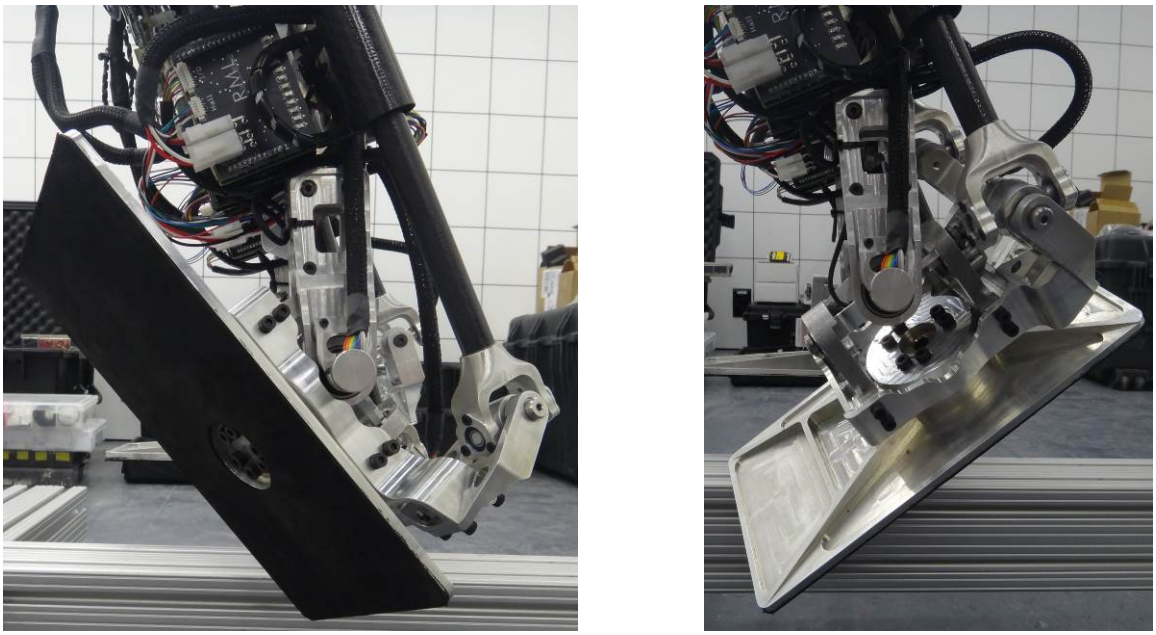

(A) (B)

Figure 5-18: The left ankle joint rotated to approximately (A) -55° of pitch and 30° of roll and (B) 35° of pitch and -30° of roll simultaneously

6. Upper Body Structure

In addition to the lower body discussed in the previous chapter, THOR has a full upper body that is morphologically similar to a human. The upper body joins to the torso through the waist, a 2 DoF joint that moves in both yaw and pitch. The chest is the central structure in the upper body, connecting to the waist, both arms, and the head. There are a number of proprioceptive and perceptions sensors in the upper body, as well as the computers for THOR. This chapter will discuss the parts of the upper body of THOR: the waist, chest, head, arms, and hands.

6.1. Waist Joint

The waist is a 2 DoF joint that connects the torso to the chest. Containing yaw and pitch DoFs, the waist extends the manipulation workspace for THOR without needing to move the lower body. The waist, like the rest of the upper body, uses COTS rotary actuators to drive its DoFs. These actuators, the Robotis Dynamixel-Pro, are available as 20 [W], 100 [W] and 200 [W] versions, all of which are used in THOR. They have internal absolute encoders and are rigid position controlled. Unlike the parallel actuated ankle and hip joints, the waist has one actuator driving each DoF. An image of the waist joint can be seen in Figure 6-1.

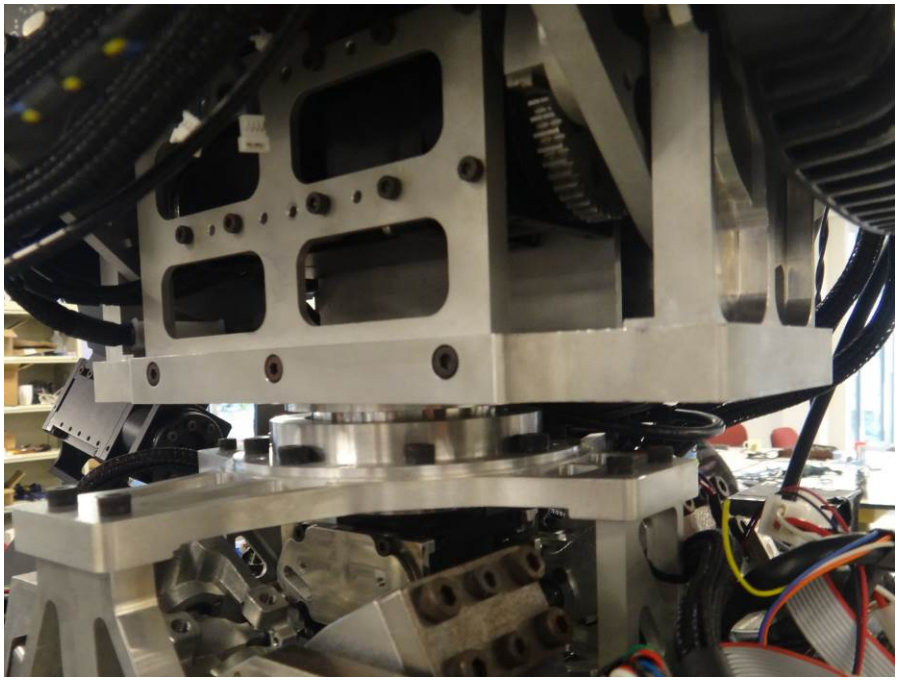

Figure 6-1: Waist joint on THOR

The 200 [W] yaw actuator is located in the center of the torso. It fits between the four hip linear actuators and is not in the path of any compliant deflections. An 80 [mm] diameter cross roller bearing sits above the actuator to transmit non-axial torque loads through the structure of the torso. This bearing also forces the torso structure to carry the weight of the upper body.

The 200 [W] pitch actuator sits directly beneath the chest. It drives the pitch DoF through a gear mounted to the chest. Its 30° RoM is limited by the electronics on the front of the chest and the wires that run behind the waist. The power and data wires that connect the legs to the chest computers are routed behind the waist to avoid snagging over the full waist RoM.

Removing a set of bolts allows the pitch actuator to slide away from the gears, disengaging the gear teeth to allow the upper body to rotate freely. This feature allows THOR to separate at the waist into the upper and lower bodies, making it manageable to pack and transport to the DRC. It is simple to reconnect the two bodies using a small set of basic tools.

6.2. Chest Structure

The chest connects the waist to the two arms and the head. It houses the two perception sensors used to map the ground in front of THOR, both computers for locomotion and perception, and the on-board batteries for untethered operation. Lifting hooks around the shoulder are used to catch THOR during testing and to hoist the robot for maintenance. An image of the chest is shown in Figure 6-2.

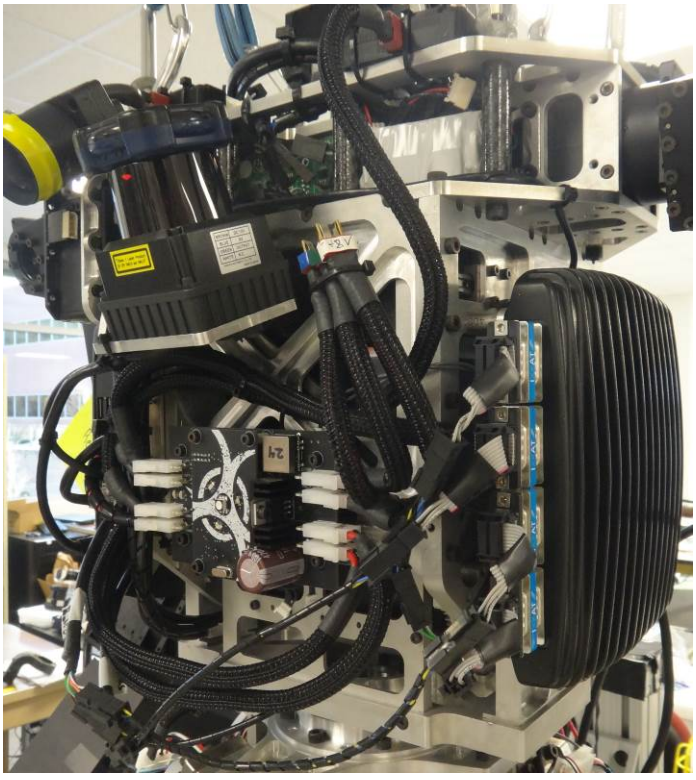

Figure 6-2: The chest of THOR

The chest is an open-backed box with electronics and sensors mounted to its exterior. A pair of fanless, singleboard Intense PC computers with Intel i7 processors sit on either side of the chest. The motion computer on the left side has four CAN channels to communicate with the lower

body motor controllers, the six-axis force/torque transducers, the AHRS, and the power distribution boards. The perception computer on the right side of the chest connects to the cameras and LIDAR sensors to process the information about the world surrounding THOR. The computers are located close enough to the chest that the arms will not hit them while swinging. All of the wires that connect the upper and lower bodies tuck behind the computers to decrease the chance of snagging.

A set of circuit boards are mounted to the chest. A power distribution circuit, similar to the one on the torso, transforms the battery power into the necessary voltages for the upper body actuators, sensors, and computers. This circuit is mounted at the bottom of the chest. There is a USB to RS485 communication board mounted between the shoulders, allowing the computers to talk to the various COTS rotary actuators in the upper body.

The arms and head interface at the top of the chest, each having one actuator that slides into the chest. The shoulder pitch motors slide in from the left and right sides of the chest, with their chassis bolting to the chest structure. The yaw actuator for the head drops into the top of the chest, directly between the two shoulder actuators.

6.2.1. Ground Mapping Sensors

A LIDAR and camera system is mounted to the front of the chest to create a ground map of the area in front of THOR. This information feeds into the footstep planner to direct THOR to safe foot landings. A lighter-weight COTS actuator, the Dynamixel MX-106, rotates the LIDAR in a nodding motion to measure lines of distance information parallel to the front edge of the foot. Even though it generates an excessive amount of torque for the chest, this COTS actuator is the same as in the head, wrists, and hands. The camera above the actuator is pointed downwards to look at the same area in front of the feet. The images from the camera colorize the point cloud generated from the LIDAR to provide helpful information to the operator.

Figure 6-3: Ground mapping sensors on the chest

6.2.2. Power Core

THOR is capable of fully untethered operation in terms of both power and communication. When running with onboard power, it uses a set of four lithium polymer batteries to power the lower body motors, upper body motors, sensors, and electronics. The batteries, shown in Figure 6-4A, fit into the power core, shown in Figure 6-4B. Based on approximate current draws during testing, these batteries hold enough charge to run THOR for at least 45 minutes.

(A) (B)

Figure 6-4: Images of the (A) lithium polymer batteries used for THOR and (B) the power core

The power core slides into the back of the chest for rapid replacement. This process quickly replaces all four batteries for THOR, which reduces the maintenance time between tasks at the DRC. Unlike most parts of THOR, the power core can be replaced with a copy of itself in a matter of seconds. A pair of pins holds the power core in THOR, as shown in Figure 6-5. The power core occupies the entire chest cavity below the shoulders. This location places the heavy weight of the batteries near the center of THOR, which is beneficial for balancing.

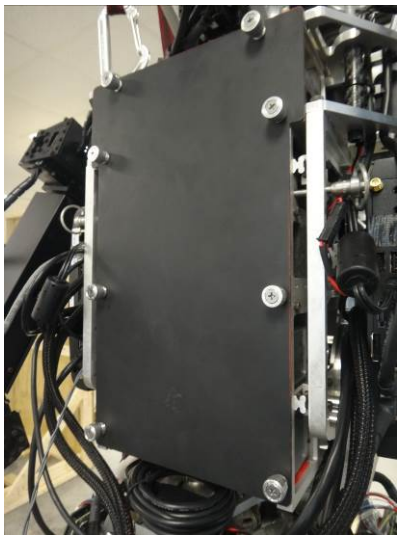

Figure 6-5: Power core inserted into the back of the chest

6.3. Head Structure

The head is used to locate obstacles and other objects of interest around THOR. It has a continuously rotating LIDAR and a camera mounted on top of a 2 DoF neck. The neck yaw actuator is embedded in the chest and the pitch actuator is at the base of the head. An image of the head can be seen in Figure 6-6. The sensors in the head allow for perception that is nearly independent of the body orientation. Additionally, the driving task forces the robots perceive the world around them using sensors that can see above the dashboard of the vehicle, making head sensors a requirement for THOR.

Figure 6-6: THOR head with spinning LIDAR and camera

The LIDAR spins about an axis parallel to its measurement plane. This scanning profile sees the world around the robot with the exception of a 40.0 [mm] diameter cylinder directly in front of the head. This blind spot extends from the head for as far as the LIDAR can measure. Rotating the head through either yaw or pitch allows THOR to see objects in that blind spot. The slip ring installed in the rotation shaft allows the LIDAR to spin continuously.

A vision camera sits above the spinning LIDAR to colorize the point cloud. This camera is higher resolution than its counterpart on the chest, but it is also larger. A second AHRS, identical to the one in the torso, sits directly above the camera. Because the head is kinematically far from the torso, a second AHRS is needed to correct the orientation of the perception data. The AHRS is small and lightweight, so it does not affect the weight distribution of the head significantly.

6.4. Arm Structure

Each arm is a 7 DoF limb with a 3 DoF shoulder, 1 DoF elbow, and 3 DoF wrist. Even though only six actuators are kinematically required to achieve a given end effector orientation and position, the redundancy of the seventh actuator extends the overall manipulation workspace. The arm is built using COTS actuators connected through standard brackets. The THOR arm has a greater-than-human RoM that is limited by the wires connecting the actuators. A picture of the arm is shown in Figure 6-7.

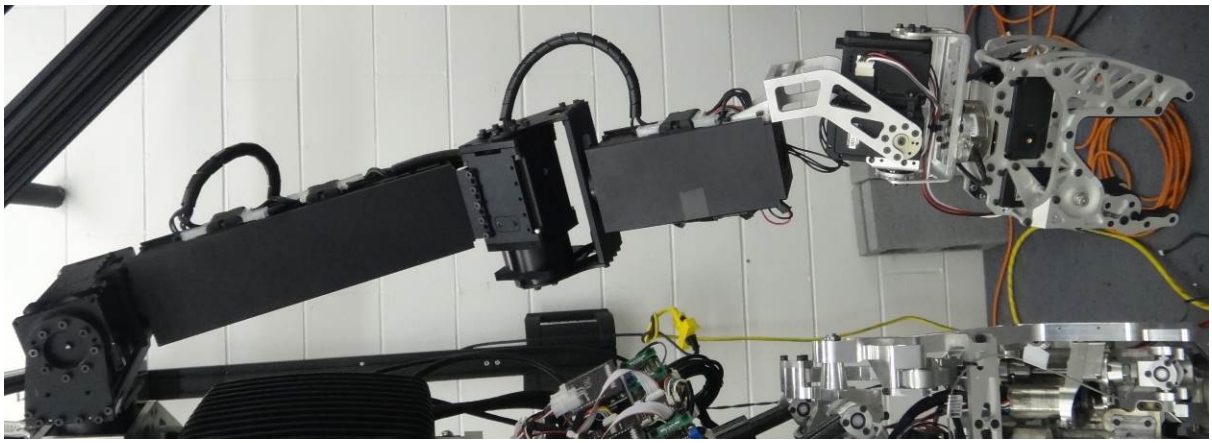

Figure 6-7: The arm of THOR

The wrist has the only custom machined parts on the arm. It uses the same actuators as the chest LIDARs to drive roll and pitch DoFs. Because these actuators are smaller than the other ones used in the arm, the wrist can achieve a human-like RoM. An image of the wrist is shown in Figure 6-8.

Figure 6-8: The wrist on the left arm of THOR

An ATI Mini-45 six-axis force/torque transducer sits at the bottom of the wrist. It is smaller than its counterpart in the feet because it does not need to measure as large of forces and torques. The hands are the second set of bodies that interact with the world. The measurements from the force/torque transducers are used to provide accurate haptic feedback to the remote operator. The signal conditioning and communication board for these sensors mounts below the shoulder.

6.5. Hand Design

The DRC has a wide variety of manipulation targets for its tasks. From operating power tools with triggers to grasping 4”x4” pieces of lumber and aluminum girder sections, nearly every DRC task requires dexterous manipulation. The rules originally stated that if a robot wanted to use multiple end effectors, it would need to swap the manipulators by itself. This task would have been extremely difficult, so THOR needed a single, versatile end effector that could grasp all the objects from the challenge. The THOR end effector is a hand with a pair of dexterous, underactuated fingers and an extended palm for facilitating the manipulation of both small and large objects [47]. An image of the THOR hand is shown in Figure 6-9.

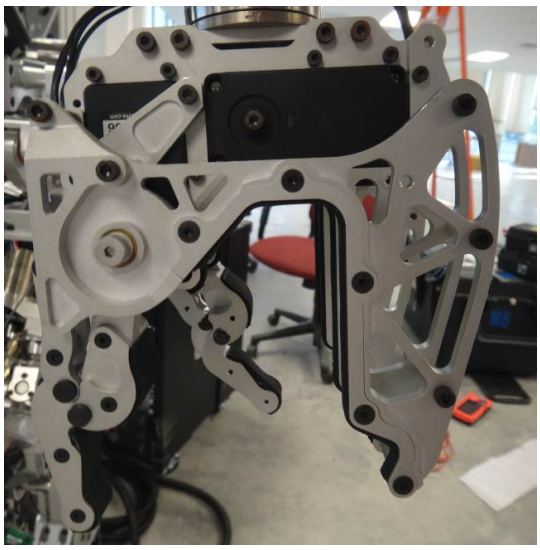

Figure 6-9: Dexterous hand used on THOR

The fingers in the THOR hand are inspired by the linkage from Laliberte [48]. Fundamentally, each finger is an underactuated 2 DoF linkage. A pair of bodies, the proximal phalange shown in blue in Figure 6-10 and the distal phalange shown in green in Figure 6-10, wrap around objects to form a reliable grasp. Initially, both phalanges move as one unit because of a tension spring connecting two of the mechanism links. The distal phalange continues to move after the proximal phalange contacts an object. The proximal and distal phalanges both have nonlinear shapes. The bumps on the proximal and distal phalanges are designed to improve the wrapping ability of the finger [47]. The shapes were determined through numerous iterations to try and improve the hand’s ability to grab and operate the drill trigger. Strips of neoprene rubber are glued to the fingers and palm to improve the grip quality of the hand.

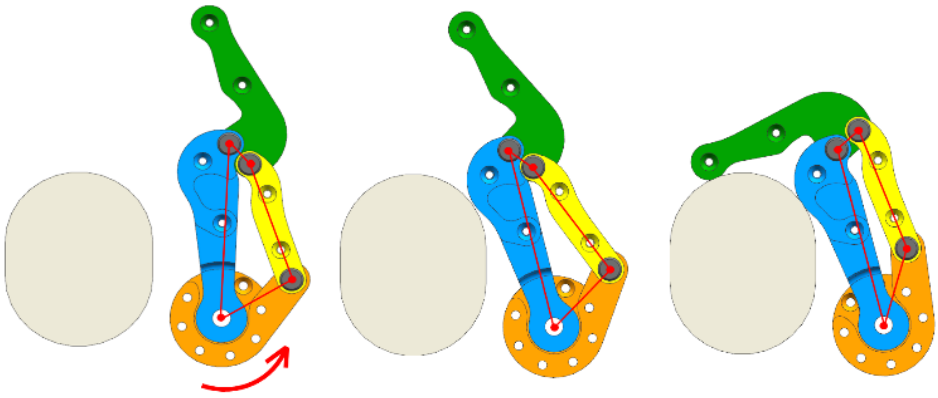

Figure 6-10: Underactuated finger mechanism wrapping around a drill handle-sized object [47]. Image used with permission from M. Rouleau, and Hong, D., "Design of an Underactuated Robotic End-Effector with a Focus on Power Tool Manipulation." Submitted to the *ASME International Design Engineering Technical Conferences & Computers and Information Engineering Conference*, Accepted, 2014.

The extended palm is designed around the various manipulation targets from the DRC. Its shape guides smaller objects to the base of the palm. The fingers are able to wrap around objects situated at the bottom of the hand. THOR needs to press the drill trigger, so it is important that the fingers can wrap around the handle completely. The extended palm has notches away from the base to help grasp larger objects like the 4"x4" piece of lumber. Some examples of the THOR hand grasping DRC objects are shown in Figure 6-11.

Figure 6-11: THOR hand grasping a 4"x4" piece of lumber, a battery operated power drill, and an aluminum truss section from the debris task [47]. Images used with permission from M. Rouleau, and Hong, D., "Design of an Underactuated Robotic End-Effector with a Focus on Power Tool Manipulation." Submitted to the *ASME International Design Engineering Technical Conferences & Computers and Information Engineering Conference*, Accepted, 2014.

7. Conclusions

The goal of this study was to design and build a full-sized humanoid robot with human-like motion capabilities for disaster response scenarios. The DARPA Robotics Challenge provided a unique avenue to evaluate the abilities of THOR by basing tasks around first-responder activities. An investigation of past humanoid systems showed that a number of capable platforms had been developed, but none able to complete the DARPA Robotics Challenge. For a humanoid robot to perform disaster response tasks, especially in a human-designed environment, it must have a similar, if not greater, range of motion and set of limb lengths compared to the average person.

Creating a humanoid robot around a vague set of tasks presented a big challenge. In order to determine the desired range of motion, a test subject attempted representative tasks to see how a similar sized human moved to complete relevant challenges. The tests determined a goal for the range of motion for each degree of freedom in the THOR lower body. Combined with limb measurements of the test subject, a set of design requirements was determined experimentally. Having a similar range of motion and body size to the test subject would allow THOR to complete the DARPA Robotics Challenge tasks. The upper body design would have a greater range of motion than the test subject, enabling it to complete the challenge.

Designed around custom linear series elastic actuators, the lower body of THOR is able to achieve the majority of its desired range of motion. The largest challenge in designing THOR was configuring the actuators in places that would allow the joint to reach its full range of motion without physical interferences between parts of the actuators and parts of the simplified structure. The ankle joint uses a pair of actuators to cooperatively control both the pitch and roll degrees of freedom. The knee uses an inverted straight-line mechanism to drive its pitch degree of freedom through a large range of motion. Because of its complexity and disparity in desired range of motion, the hip joint is designed like a hybrid of the ankle and knee, incorporating parallel actuators and an inverted straight-line mechanism to drive its three degrees of freedom. Each actuator configuration was evaluated against the achievable range of motion, maximum joint torques over the full range of motion, minimum actuator stroke, maximum actuator fixed length, and actuator universal joint rotation required.

The lower body of THOR has an intuitive, yet intricate, structure built around the actuators. The main driving factor in the lower body structural design was the placement of the configurable compliant springs around the actuators. The other driving factor was the leg range of motion, forcing both the thigh and shin to have bends incorporated into their structure to avoid intersecting other structural bodies. Driven by COTS actuators, the upper body has a simpler design than the lower body. The upper body incorporates the onboard computers, perception sensors, batteries, and flexible arms with dexterous hands.

7.1. Future Work

This study presented the design of a high range of motion humanoid robot with the mechanical capability of a similar sized human. Some initial testing not included in this study has shown that THOR is a very capable platform, balancing in mild, rocking conditions. However, there are a number of areas for further work on THOR before it is ready to engage in a full-blown disaster response scenario. These areas are outlined below.

The hip joint has a reduced range of motion compared to what was desired, as stated in Section 5.6. This is from the hip Hoeken's linkage mount on the thigh interfering with the torso compliant interface mounts. Their interference prevents THOR from simultaneously reaching the ends of the range of motion for all three hip degrees of freedom. Even though this portion of the hip range of motion is inaccessible to average humans, it would be useful for THOR.

The foot of THOR is a flat, rectangular plate. While this foot design is acceptable for laboratory testing and the DARPA Robotics Challenge, it does not necessarily possess the flexibility to tackle disaster scenarios. Humans have a jointed, flexible foot that conforms to the terrain. Additionally, toes assist with locomotion, balance, and reach. THOR would benefit from a redesigned foot that incorporates mechanisms to assist with its walking and balancing.

THOR has a number of sensitive components throughout its body that are exposed to the elements. From circuit boards to actuator ball screws, these components would not function well in rain and dust. A set of protective covers would provide some shielding to many of these components, as well as prevent operators from getting fingers snagged in pinch points.

The upper body currently uses COTS actuators to drive each degree of freedom above the waist. The COTS actuators communicate through RS-485 while the lower body and several sensors use CAN, causing the need for additional electronics and communication protocol software. The units tested for THOR have been unreliable, often breaking in a number of ways and requiring extensive servicing to replace. Finally, these actuators are not torque controllable, unlike their counterparts in the lower body. This means that the upper body uses a completely different control strategy from the lower body. Designing new series elastic actuators for the upper body would unify the communication and control software while creating a safer working environment around THOR.

Bibliography

[1] Kato, I., Ohteru, S., Kobayashi, H., Shirai, K., and Uchiyama, A., "Information-Power Machine with Senses and Limbs." *Proc. CISM-IFToMM Symposium on Theory and Practice of Robots and Manipulatiors*, pp. 12-24, 1973.

[2] Lim, H., and Takanishi, A., "Biped Walking Robots Created at Waseda University: WL and WABIAN Family." *Philisophical Transactions of the Royal Society A*, Vol. 365, pp. 49-64, 2006.

[3] Hirai, K., Hirose, M., Haikawa, Y., and Takenaka, T., "The Development of Honda Humanoid Robot." *Proceedings of the IEEE International Conference on Robotics and Automation*, pp. 1321-1326, 1998.

[4] Hirose, M., and Ogawa, K., "Honda Humanoid Robots Development." *Philosophical Transactions of the Royal Society A*, Vol. 365, No. 1850, pp. 11-19, 2007.

[5] Kaneko, K., Harada, K., Kanehiro, F., Miyamori, G., and Akachi, K., "Humanoid Robot HRP-3." *Proceedings of the IEEE/RJS International Conference on Intelligent Robots and Systems*, pp. 2471-2478, 2008.

[6] Park, I., Kim, J., Lee, J., and Oh, J. "Mechanical Design of Humanoid Robot Platform KHR-3 (KAIST Humanoid Robot – 3: HUBO)." *Proceedings of the IEEE-RAS International Conference on Humanoid Robots*, pp. 321-326, 2005.

[7] Ogura, Y., Aikawa, H., Shimomura, K., Kondo, H., Morishima, A., Lim, H., and Takanishi, A., "Development of a New Humanoid Robot WABIAN-2" *Proceedings of the IEEE International Conference on Robotics and Automation*, pp. 76-81, 2006.

[8] Tellez, R., Ferro, F., Garcia, S., Gomez, E., Jorge, E., Mora, D., Pinyol, D., Oliver, J., Torres, O., Velazquez, J., and Faconti, D., "Reem-B: An Autonomous Lightweight Human-Size Humanoid Robot." *Proceedings of the IEEE-RAS International Conference on Humanoid Robots*, pp. 462-468, 2008.

[9] Han, J., "Bipedal Walking for a Full Size Humanoid Robot Utilizing Sinusoidal Feet Trajectories and Its Energy Consumption." Doctorate of Philosophy dissertation, Virginia Tech Department of Mechanical Engineering, 2012.

[10] Pratt, G., "Low Impedance Walking Robots." *Integrative and Comparative Biology*, Vol. 42, Iss. 1, pp. 174-181, 2002.

[11] Pratt, J., and Pratt, G., "Exploiting Natural Dynamics in the Control of a Planar Bipedal Walking Robot." *Proceedings of the Allerton Conference on Communication, Control, and Computing*, 1998.

[12] Paluska, D., "Design of a Humanoid Biped for Walking Research." Master's thesis, Massachusetts Institute of Technology Department of Mechanical Engineering, 2000.

[13] Pratt, J., and Krupp, B., "Design of a Bipedal Walking Robot." *Proceedings of SPIE Unmanned Systems Technology X*, Vol. 6962, 2008.

[14] Lohmeier, S., Buschmann, T., and Ulbrich, H., "Humanoid Robot LOLA." *Proceedings of the IEEE Conference on Robotics and Automation*, pp. 775-780, 2009.

[15] Lohmeier, S., Buschmann, T., Ulbrich, H., and Pfeiffer, F., "Modular Joint Design for Performance Enhanced Humanoid Robot LOLA." *Proceedings of the IEEE International Conference on Robotics and Automation*, pp. 88-93, 2006.

[16] Kaneko, K., Kanehiro, F., Morisawa, M., Akachi, K., Miyamori, G., Hayashi, A., and Kanehira, N., "Humanoid Robot HRP-4 – Humanoid Robotics Platform with Lightweight and Slim Body." *Proceedings of the IEEE/RJS International Conference on Intelligent Robots and Systems*, pp. 4400-4407, 2011.

[17] Nelson, G., Saunders, A., Neville, N., Swilling, B., Bondaryk, J., Billings, D., Lee, C., Playter, R., and Raibert, M., "PETMAN: A Humanoid Robot for Testing Chemical Protective Clothing." *Journal of the Robotics Society of Japan*, Vol. 30, No. 4, pp. 372-377, 2012.

[18] Lahr, D., Orekhov, V., Lee, B., and Hong, D., "Development of a Parallely Actuated Humanoid, SAFFiR." *Proceedings of the ASME International Design Engineering Technical Conferences & Computers and Information in Engineering Conference*, 2013.

[19] Otani, T., Iizuka, A., Takamoto, D., Motohashi, H., Kishi, T., Kryczka, P., Endo, N., Jamone, L., Hashimoto, K., Takashima, T., Lim, H., and Takanishi, A., "New shank Mechanism for Humanoid Robot Mimicking Human-like Walking in Horizontal and Fontal Plane." *Proceedings of the IEEE International Conference on Robotics and Automation*, pp. 667-672, 2013.

[20] Hobbelen, D., Boer, T., and Wisse, M., "System Overview of Bipedal Robots Flame and TUlip, Tailor-made for Limit Cycle Walking." *Proceedings of the IEEE/RSJ International Conference on Intelligent Robots and Systems*, pp. 2486-2491, 2008.

[21] Oort, G., Reinink, R., and Stramigioli, S., "New Ankle Actuation Mechanism for a Humanoid Robot." *Preprints of the IFAC World Congress*, pp. 8082-8088, 2011.

[22] Pratt, G., and Williamson, M., "Series Elastic Actuators." *Proceedings of the IEEE International Conference on Intelligent Robots and Systems*, Vol. 1, pp. 399-406, 1995.

[23] Pratt, J., Krupp, B., and Morse, C., "Series Elastic Actuators for High fidelity Force Control." *Industrial Robot: An International Journal*, Vol. 29, No. 3, pp. 234-241, 2002.

[24] Pratt, J., and Krupp, B., "Series Elastic Actuators for Legged Robots." *Proceedings of the SPIE Unmanned Ground Vehicle Technology VI*, Vol. 5422, pp. 135-144, 2004.

[25] Robinson, D., Pratt, J., Paluska, D., and Pratt, G., "Series Elastic Actuator Development for a Biomimetic Walking Robot." *Proceedings of the IEEE/ASME International Conference on Advanced Intelligent Mechatronics*, pp. 561-568, 1999.

[26] Pratt, G., Willisson, P., Bolton, C., and Hofman, A., "Late Motor Processing in Low-Impedance Robots: Impedance Control of Series Elastic Actuators." *Proceedings of the 2004 American Control Conference*, Vol. 4, pp. 3245-3251, 2004.

[27] Van Ham, R., Sugar, T., Vanderborght, B., Hollander, K., and Lefeber, D., "Compliant Actuator Designs." *IEEE Robotics and Automation Magazine*, pp. 81-94, Sep. 2009.

[28] Hurst, J., Chestnutt, J., and Rizzi, A., "The Actuator with Mechanically Adjustable Series Compliance." *IEEE Transactions on Robotics*, Vol. 26, No. 4, pp. 597-606, 2010.

[29] Taylor, M., "A Compact Series Elastic Actuator for Bipedal Robots with Human-Like Dynamic Performance." Master's Thesis, Carnegie Mellon University Robotics Institute, 2011.

[30] Paine, N., Oh, S., and Sentis, L., "Design and Control Considerations for High-Performance Series Elastic Actuators." *IEEE/ASME Transactions on Mechatronics*, Vol. PP, Iss. 99, pp. 1-12, 2013.

[31] Lee, B., Orekhov, V., Lahr, D., and Hong, D., "Design and Measurement Error Analysis of a Low-Friction, Lightweight Linear Series Elastic Actuator." *Proceedings of the ASME International Design Engineering Technical Conferences & Computers and Information Engineering Conference*, 2013.

[32] Orekhov, V., Lahr, D., Lee, B., and Hong, D., "Configurable Compliance for Series Elastic Actuators." *Proceedings of the ASME International Design Engineering Technical Conferences & Computers and Information Engineering Conference*, 2013.

[33] "Initial Task Descriptions." www.theroboticschallenge.org, 2013.

[34] "DRC Trials Task Description." www.theroboticschallenge.org, 2013.

[35] Fujiwara, K., Kanehiro, F., Kajita, S., Yokoi, K., Saito, H., Harada, K., Kaneko, K., and Hirukawa, H., "The First Himan-size Humanoid That Can Fall Over Safely and Stand-up Again." *Proceedings of the IEEE/RSJ International Conference on Intelligent Robots and Systems*, pp. 1920-1926, 2003.

[36] Hirukawa, H., Kajita, S., Kanehiro, F., Kaneko, K., and Isozumi, T. "The Human-size Himanoid Robot That Can Walk, Lie Down and Get Up." *The International Journal of Robotics Research*, Vol. 24, No. 9, pp. 755-769, 205.

[37] Fujiwara, K., Kanehiro, F., Kajita, S., Kaneko, K., Yokoi, K., and Hirukawa, H., "UKEMI: Falling Motion Control to Minimize Damage to Biped Humanoid Robot." *Proceedings of the IEEE/RSJ International Conference on Intelligent Robots and Systems*, pp. 2521-2526, 2002.

[38] Chengalur, S., Rodgers, S., and Bernard, T. *Kodak's Ergonomic Design for People at Work*. Hoboken: Wiley, 1986.

[39] Robbins, D., "Anthropometric Specifications for Mid-Sized Male Dummy, Volume 2." Final Report, the University of Michigan Transportation Research Institute, 1983.

[40] "WKC-7761-P: How to Evaluate Disability Under Wisconsin's Worker's Compensation Law." www.dwd.wisconsin.gov, 2006.

[41] Tennant, J., Jensen, R., and Potter, R., "GM-ATD 502 Anthropomorphic Dummy – Development and Evaluation." *SAE Technical Paper 740590*, 1974.

[42] Knabe, C., Lee, B., Orekhov, V., and Hong, D., "Design of a Compact, Lightweight, Electromechanical Linear Series Elastic Actuator." Submitted to the *ASME International Design Engineering Technical Conferences & Computers and Information Engineering Conference*, Accepted, 2014.

[43] Lahr, D., and Hong, D., "Statics Analysis of Clemen's Linkage for Robotic Applications." *Proceedings of the ASME International Design Engineering Technical Conferences & computers and Information Engineering Conference*, 2013.

[44] Lee, B., Knabe, C., Orekhov, V., and Hong, D., "Design of a Human-Like Range of Motion Hip Joint for Humanoid Robots." Submitted to the *ASME International Design Engineering Technical Conferences & Computers and Information Engineering Conference*, Accepted, 2014.

[45] Knabe, C., Lee, B., and Hong, D., "An Inverted Straight Line Mechanism for Augmenting Joint Range of Motion in a Humanoid Robot." Submitted to the *ASME International Design Engineering Technical Conferences & Computers and Information Engineering Conference*, Accepted, 2014.

[46] Norton, R., *Design of Machinery*, 4th ed. Boston: McGraw Hill, 2008.

[47] Rouleau, M., and Hong, D., "Design of an Underactuated Robotic End-Effector with a Focus on Power Tool Manipulation." Submitted to the *ASME International Design Engineering Technical Conferences & Computers and Information Engineering Conference*, Accepted, 2014.

[48] Laliberte, T., Birglen, L., and Gosselin, C., "Underactuation in Robotic Grasping Hands." *Machine Intelligence & Robotic Control*, Vol. 4, No. 3, pp. 1-11, 2002.

Appendix A. Sensors and Electronics

THOR uses a wide variety of sensors and electronics to assist with its balancing, walking, and localization. The sensors provide information about the current robot state and the world around THOR. A number of custom-designed circuits control the lower body actuators, intelligently distribute power to various components, and translate sensor readings to usable communication messages. This appendix will discuss the proprioceptive and perception sensors and custom-designed circuits used in THOR.

A1. Proprioceptive Sensors

The proprioceptive sensors provide feedback about the current state of THOR. This state information is used in the walking controller. The majority of the proprioceptive sensors are mounted to the lower body because the COTS actuators in the upper body contain integrated absolute encoders.

A1.1. Absolute Encoders

The Gurley Precision Instruments A19 is an optical, rotary absolute encoder placed on each joint axis in the lower body. At 19 [mm] in diameter, the A19 is one of the smallest optical encoders available. The encoders have a 15-bit resolution and their signals feed directly into the local motor controllers. An image of the A19 encoders is shown in Figure A-1.

Figure A-1: Gurley Precision Instruments A19 absolute encoder

A1.2. Uni-directional Load Cell

The Futek LCM-200 is a compact uni-directional tension/compression load cell that is integrated into each linear SEA [42]. The load cell is threaded into the end of the bearing housing and the upper universal joint. It is axially aligned with the ball screw axis to accurately measure the force output of each actuator. The THOR SEA load cells are calibrated to measure in excess of 2200 [N], but the sensor can be recalibrated to measure over 4400 [N]. The Futek LCM-200 can be seen in the left of Figure A-2. Each LCM-200 is paired with signal amplification circuit that is shown in the right of Figure A-2. The load cell and amplification board are calibrated together by Futek at their factory.

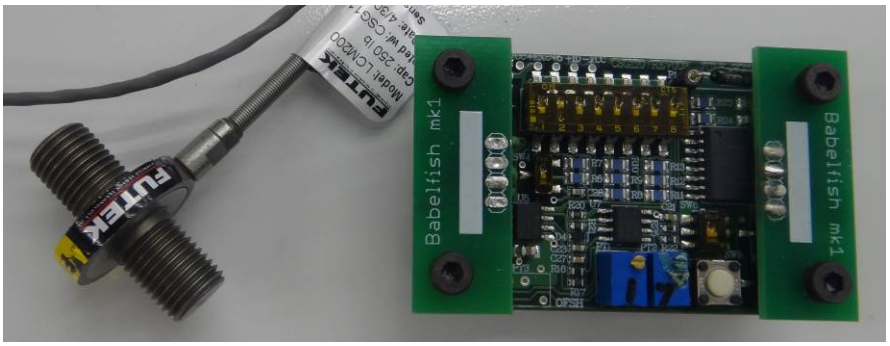

Figure A-2: The Futek LCM-200 load cell and its signal amplification circuit

A1.3. Six-Axis Force/Torque Transducers

The ATI Mini-45 and Mini-58 are compact six-axis force/torque transducers. Located at the end of the wrist, the Mini-45 measures interactions between the hands and the outside world. It is calibrated to measure up to 580 [N] of force and 10 [Nm] of torque. The Mini-45 has a diameter of 45 [mm] and a weight of 0.092 [kg]. Located in the foot, the Mini-58 measures the contact between THOR and the ground. It is calibrated to measure up to 3,400 [N] of force and 60 [Nm] of torque. The Mini-58 is a larger sensor with a diameter of 58 [mm] and a mass of 0.499 [kg]. To reduce both height and weight, it is mounted without the tool adapter plate attached. The Mini-58 and Mini-45 are shown in the top of Figure A-3.

Figure A-3: From the top left: the Mini-58 transducer, the Mini-45 transducer, and the sensor interface board

Each transducer is paired with a sensor interface board that reads the strain gage measurements, converts those readings into forces and torques, and translates the data to CAN messages. The circular board on the right side of the interface board amplifies the measurements from the transducer and converts them into digital signals. Because the analog-to-digital converter is far from the transducer, the measurements are susceptible to noise. Therefore, it was important to

get the interface boards as close to the transducers as possible. The boards for the foot Mini-58s are mounted to the front of the shin. The wrist Mini-45 interface boards are mounted to the upper segment of the arm because they are too large to fit on the forearm. The rest of the force/torque interface board transforms the digital strain gage measurements into forces and torques and then converts those into CAN messages to feed into the motion computer.

A1.4. Attitude and Heading Reference System

The AHRS measures the body orientation and acceleration for both the torso and the head. THOR uses an Analog Devices ADIS16480 as its AHRS. The AHRS measures the orientation and acceleration to 16 bit accuracy. Each sensor is mounted on a custom circuit that converts the readings into CAN messages for the motion computer. An image of the mounted AHRS is shown in Figure A-4.

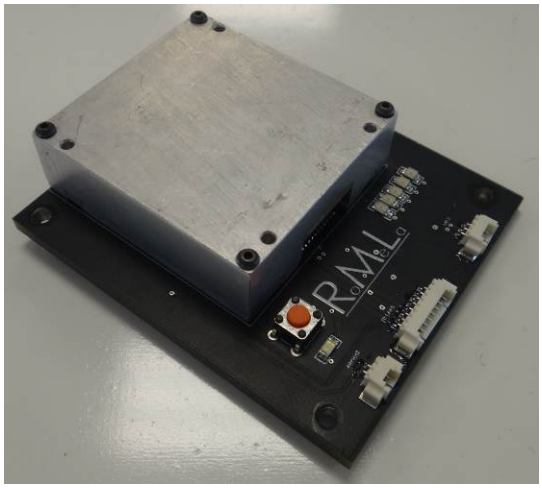

Figure A-4: The AHRS mounted on its interface board

A2. Perception Sensors

THOR uses a number of perception sensors to see the world around it. The DRC has a large number of tasks, each with its own specialized perception targets. Additionally, based on the setup of the DRC, the communication link between THOR and the operator would be limited, so using fewer sensors was important. All of the perception sensors are mounted to the upper body, but future iterations of THOR could include cameras on the shins.

A2.1. LIDAR

The Hokuyo UTM-30LX-EW is a compact LIDAR sensor with a 30 [m] range. It outputs a line of distances for a 270° fan of laser scans. The sensor updates at a rate of 40 [Hz], which is faster than either camera that it pairs with. This is necessary to provide a point cloud of distance data for the cameras to colorize. An image of the UTM-30LX-EW is shown in Figure A-5.

Figure A-5: Hokuyo UTM-30LX-EW LIDAR

Each LIDAR only outputs distances for a fan of points in front of it. Because of this, the sensors are mounted to an actuator to scan the regions around THOR. The ground mapping LIDAR on the chest rotates in a nodding direction, producing lines of data parallel to the leading edge of the foot. The scan is limited to only the region in front of the feet, making the chest LIDAR not very useful for detecting obstacles. The head LIDAR continuously rotates about an axis point forward from the head. This scan pattern creates a blind spot directly in front of the head, but allows THOR to see the rest of the world.

A2.2. Chest Camera

The Point Grey Firefly MV is a small USB color camera. At 44x34x24 [mm] without the lens, it is small enough to fit at several places on THOR. The first iteration of THOR has only one camera mounted on the chest to colorize the ground scans from the LIDAR. The Firefly is small enough to fit on both the wrists and shins. This would provide better images of manipulation targets and the ground to the operator. An image of the Firefly MV is in Figure A-6.

Figure A-6: Firefly MV camera with a lens

A2.3. Head Camera

The Allied Vision Technologies Prosilica GT is a higher-resolution Gig-E ethernet color camera. Sitting atop the head, it colorizes the head LIDAR scans of images of obstacles and objects of

interest. These objects are often farther away than the ground, so the camera needed to have a higher resolution than the chest cameras. Its adjustable lens is glued in place to preserve the image calibration settings. The Prosilica GT is shown in Figure A-7.

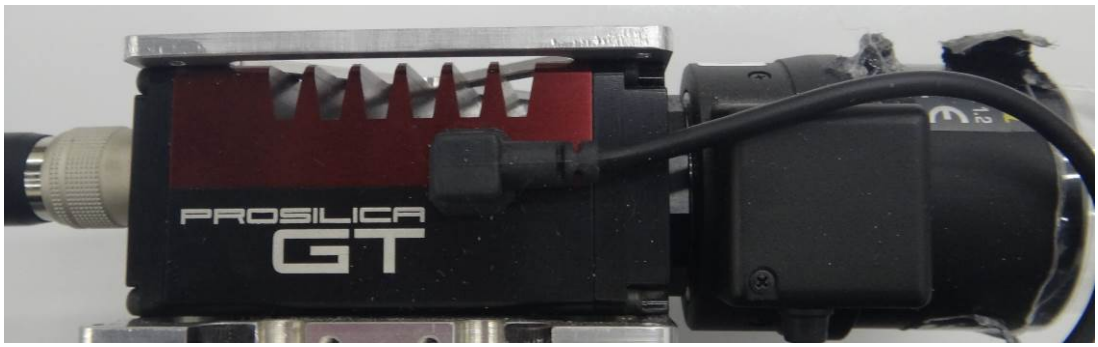

Figure A-7: Prosilica GT camera with lens

A3. Custom Electronics

THOR uses a number of custom designed circuits to control motors, intelligently distribute power, and interface with COTS sensors. For the motor controller and power distribution board, COTS solutions were not capable enough to perform all the necessary functions. These custom boards are designed both to provide the needed functionality and to fit within the mechanical constraints of the robot. This section will only discuss the motor controller and power distribution board.

A3.1. Motor Controller

Testing on SAFFiR showed the need for local, joint-level motor controllers. The motor controllers passed information back to the motion computers and waited for the computers to solve the inverse kinematics and statics of the joint. This control loop took too much time to compute to be reliable for THOR. The solution is to move the joint level inverse kinematics and statics computation away from the motion computer and down to the motor controllers.

The Motor Slug is a dual-axis motor controller to control joints in the lower body. The lower body design of THOR splits the joints into three pairs of actuators: the parallel hip yaw and roll actuators, the thigh Hoeken's linkages, and the parallel ankle actuators. Each pair of actuators is tied to a single motor controller that solves the inverse kinematics and statics associated with each joint-level command. The Hoeken's linkage motor controller uses look-up tables to calculate the actuator displacements and forces for the joint angles and torques.

The motor controller was designed to fit between the two ankle actuators on the back of the shin. As stated in Section 5.4, the shin does not have many locations to mount electronics. Therefore, it was necessary to design the motor controller to fit between the two actuators, occupying a space that no other component could. Including connectors and a couple millimeters of wiring, the motor controller is 47 [mm] wide. An image of the motor controller is shown in Figure A-8.

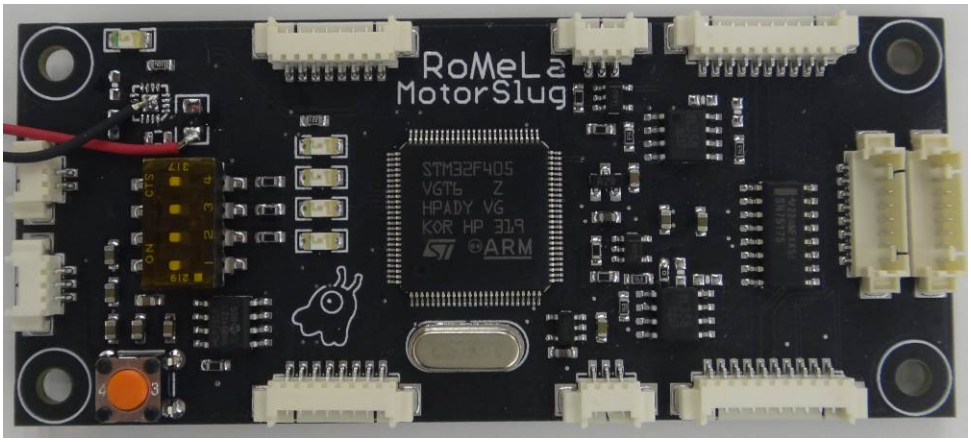

Figure A-8: Custom dual-axis motor controller

A3.2. Power Distribution Board

The second custom designed circuit on THOR is the power distribution board on both the upper and lower bodies. These boards incorporate filtering and monitoring circuitry to intelligently distribute power throughout THOR. The power boards also provide visual feedback to the operators about battery status and current draw. It connects to an external emergency stop button to let the operators disable the robot quickly and safely. An image of the upper body power distribution board is in Figure A-9.

Figure A-9: Power distribution board on the upper body

Appendix B. Photo Credits

Figures 3-1 through 3-7 are used with the permission of DARPA.
http://www.darpa.mil/NewsEvents/Usage.aspx
Email attached

Figure 4-17 is used with permission from the author of [45], C. Knabe.
Email attached

Figures 6-10 and 6-11 are used with permission from the author of [47], M. Rouleau.
Email attached

Bryce Lee

From: Allen, Robert (contr-tto) <Robert.Allen.ctr@darpa.mil>
Sent: Tuesday, February 11, 2014 4:25 PM
To: 'leebryce@vt.edu'
Cc: TheRoboticsChallenge; ekrotkov@Griffin-Technologies.com; michael.revill@navy.mil; Pratt, Gill; Spangenberg Jones, Johanna [USA] (spangenbergjones_johanna@bah.com); Kilbride, Timothy (contr-diro)
Subject: RE: [Media Inquiry] Image usage for a Master's Thesis

Hi Bryce,

The documents that you referenced have been approved for public release and you are welcome to use the images in those documents in your thesis. DARPA should be credited for the images as indicated in DARPA's Usage Policy http://www.darpa.mil/NewsEvents/Usage.aspx

Regards,
Bob

Bob Allen
Contractor support to DARPA
robert.allen.ctr@darpa.mil
Phone: (571) 218-4527 / Fax: (703) 248-1921

-----Original Message-----
From: brantrevill@gmail.com [mailto:brantrevill@gmail.com] On Behalf Of leebryce@vt.edu
Sent: Monday, February 10, 2014 9:15 AM
To: TheRoboticsChallenge; Allen, Robert (contr-tto); ekrotkov@Griffin-Technologies.com; michael.revill@navy.mil
Subject: [Media Inquiry] Image usage for a Master's Thesis

Bryce Lee (leebryce@vt.edu) sent a message using the contact form at http://theroboticschallenge.org/contactus.

Hello,
My name is Bryce Lee, a Master's student in Virginia Tech's Robotics and Mechanisms Lab. I am in the process of writing a thesis based on the design of THOR, the original entrant to the DRC for team THOR. I am looking to get permission to use images from two older rules releases from DARPA because they more-accurately represent our knowledge of the trial layout during the design process. These two documents are the "DRC Trials Initial Task Descriptions DISTAR Case 21473" dated 7/10/2013 and the "DRC Trials Task Description Release 3 DISTAR 21990" dated 10/18/2013. I would be happy to further discuss which particular images from each document that I would like to use in my thesis. If you do grant me permission, what name should be placed in the photo credits?
Thank You,
Bryce Lee

Bryce Lee

From: Coleman Knabe <csknabe@gmail.com>
Sent: Wednesday, April 09, 2014 8:41 AM
To: Bryce Lee
Subject: Re: permission to use image in master's thesis

You have my permission to use the figure.

On Apr 9, 2014 8:36 AM, "Bryce Lee" <bryce.kt.lee@gmail.com> wrote:

Coleman,

I am looking to get formal permission to use an image from your Hoeken's linkage IDETC paper #35123 in my thesis. The image is Figure 8 from your paper. In order to use the image, I would need a simple email reply stating that I may "use the image with permission".

Thanks,

Bryce

1

Bryce Lee

From: Mike Rouleau <mrouleau@vt.edu>
Sent: Wednesday, February 19, 2014 12:40 PM
To: Bryce Lee
Subject: Re: permission to use images in master's thesis

You may use the images with permission.

On Tue, Feb 18, 2014 at 7:06 PM, Bryce Lee <bryce.kt.lee@gmail.com> wrote:

Mike,

I am looking to get formal permission to use a couple of images from your IDETC paper in my thesis. The images are Figures 3 and 10 from your paper. In order to use the images, I would need a simple email reply stating that I may "use the image with permission".

Thanks,

Bryce

1